TECHNISCHE UNIVERSITÄT MÜNCHEN

Wissenschaftszentrum Weihenstephan
für Ernährung, Landnutzung und Umwelt

Lehrstuhl für Entwicklungsgenetik

Axonal wiring defects and critical period plasticity in the postnatal motor system

Michaela Sabine Helmbrecht

Vollständiger Abdruck der von der Fakultät Wissenschaftszentrum Weihenstephan für Ernährung, Landnutzung und Umwelt der Technischen Universität München zur Erlangung des akademischen Grades eines

Doktors der Naturwissenschaften

genehmigten Dissertation.

Vorsitzender:		Univ.-Prof. Dr. E. Grill
Prüfer der Dissertation:	1.	Univ.-Prof. Dr. W. Wurst
	2.	Univ.-Prof. Dr. H. Luksch

Die Dissertation wurde am 08.04.2015 bei der Technischen Universität München eingereicht und durch die Fakultät Wissenschaftszentrum Weihenstephan für Ernährung, Landnutzung und Umwelt am 25.06.2015 angenommen.

Für meine Eltern

TABLE OF CONTENTS

I. SUMMARY

I.1. Abstract

The proper functionality of each neuronal network depends on the correct interplay of progressive and regressive events during development. In the progressive phase, axon outgrowth and pathfinding are under the tight spatiotemporal control of guidance molecules like class 3 semaphorins (Semas) and their neuropilin (Npn) receptors in order to allow for the precise wiring of neuronal connections. Later, regressive events such as naturally occurring cell death or axon pruning facilitate the maturation of the newly established networks and even in the postnatal stage connectivity can still be refined by plastic adaptations. However, in adult animals this remarkable adaptive potential of the nervous system gradually declines and consequently neuronal degeneration or injury lead to permanent damage. In order to develop new therapeutic strategies that promote neuronal regeneration, it is therefore necessary to first understand the naturally occurring mechanisms of circuit maturation and postnatal plasticity. To address this goal we used models of specific embryonic axon miswiring for the investigation of postnatal consequences and to analyze mechanisms that allow for their compensation.

In a first approach, we explored the consequences of embryonic axon wiring deficits on the postnatal animal. Miswiring of central and peripheral neuronal tracts that is caused by a deficient Sema3A-Npn1 signaling is particularly well investigated during embryonic development. Thus, loss of the Npn1 receptor from all motor neurons in *Olig2-Cre^{+};Npn1^{cond}* mutants has been shown to result in severe axon defasciculation, pathfinding deficits, and a reduced length of developing motor projections. In contrast, a defective binding site for Sema3A in the Npn1 receptor, as engineered in mutants of the *Npn1^{Sema-}* mouse line, causes a precocious ingrowth of motor projections into the forelimb tissue and wiring defects that affect both, motor and sensory axons. Interestingly, behavioral, anatomical, and morphological investigations in postnatal animals revealed that of both mouse lines only *Olig2-Cre^{+};Npn1$^{cond-/-}$* mice display permanent postnatal deficits in motor coordination, forepaw posturing, and bone structure as well as atrophy of forelimb extensor muscles. We therefore investigated the underlying reasons that allow *Npn1^{Sema-}* animals to compensate for developmental axon miswiring, while *Olig2-Cre^{+};Npn1^{cond}* mutants exhibit permanent postnatal

defects. To address this question, I used genetic motor neuron markers and retrograde tracing of brachial nerves to visualize the motor axons of specific peripheral nerves and analyze their projection patterns. The morphological analysis of the brachial nerves revealed a specific loss of motor axons in the radial nerve of *Olig2-Cre*$^{+}$*;Npn1*$^{cond-/-}$ mice. Furthermore, a direct correlation between the reduction of motor axons and the degree of postural impairment became evident. These observations were corroborated by retrograde tracings from brachial nerves, which revealed that in *Olig2-Cre*$^{+}$*;Npn1*^{cond} mutants a reduced number of spinal motor neurons innervate the radial nerve. In contrast, *Npn1*$^{Sema-}$ mutants displayed no abnormalities concerning the composition and motor innervation of the radial nerve. These results suggest that loss of Sema3A-Npn1 signaling is not the only cause for the anatomical deficits in *Olig2-Cre*$^{+}$*;Npn1*$^{cond-/-}$ mice: additional, yet unknown binding partners for Npn1 may be involved, which result in the differences of developmental wiring deficits and allow for compensation in *Npn1*$^{Sema-}$ mutants.

In a second approach, I analyzed the postnatal plastic potential of spinal motor circuits after embryonic axon miswiring. For this purpose I used animals in which the loss of the guidance molecule Sema3F causes very specific wiring deficits of motor neurons from the medial aspect of the lateral motor column (LMCm). These anatomical deficits in the wiring of brachial nerves are not compensated during circuit maturation and persist until adulthood. Additionally, *Sema3F* mutants show behavioral impairments in motor coordination and a disorganization of the LMCm motor pool on the neuroanatomical level. Interestingly, housing the animals in an enriched environment from birth allows for the compensation of these deficits during postnatal development. Nevertheless, it remained unclear which underlying mechanisms allow for this amazing compensation of locomotor defects and reorganization of the motor pool. Using behavioral, functional and neuroanatomical studies I first analyzed if the observed plasticity was limited to a specific time frame during postnatal development. Indeed, a delayed start of enriched environment housing starting at 4 weeks after birth does not induce improvements in motor performance or reorganization of neuroanatomy. This suggests a critical period for adaptive plasticity in the spinal motor system. A closer analysis of mechanisms that influence critical period plasticity revealed that within the critical period activity-dependent mechanisms induce the formation of excitatory synapses on LMCm neurons. Since inhibitory synapses and perineuronal nets have been shown to be involved in critical period regulation we used these factors to investigate if housing conditions have an influence on the timing of the critical period. However, both criteria were not affected by

changes in the housing conditions, suggesting that regulation of the critical period is not involved in the observed adaptive changes in the spinal motor system of *Sema3F* mice.

Thus, using the embryonic axon miswiring of *Sema3F* mutants as a model we established a new, non-injury based system for the investigation of adaptive plasticity in the spinal cord. This model will allow for the discrimination of changes that are caused by plastic adaptations without the secondary effects that are caused by inflammation or scar formation after spinal cord injury and thereby provide new insights into the mechanisms of postnatal plasticity that might help to develop new therapies for neuronal regeneration.

I.2. Zusammenfassung

Die Funktionalität eines jeden neuronalen Netzwerks ist vom korrekten Zusammenspiel progressiver und regressiver Ereignisse in der Entwicklung abhängig. Während der progressiven Phase stehen Wachstum und Wegfindung der Axone unter der strikten Kontrolle von Wegfindungsmolekülen wie den Semaphorinen der Klasse 3 (Sema3) und ihren Neuropilin-Rezeptoren (Npn), um die korrekte Bildung des Nervensystems zu gewährleisten. Die so entstandenen neuronalen Netzwerke können anschließend durch regressive Ereignisse wie dem Zurechtstutzen von Axonen oder natürlich stattfindenden Zelltod weiter maturieren und sogar nach der Geburt können die Netzwerke durch plastisches Anpassungsvermögen weiter verfeinert werden. Dieses erstaunliche plastische Potential des Nervensystems verringert sich in adulten Tieren stetig, sodass neuronale Degeneration oder Verletzungen zu permanenten Schäden führen können. Um neue therapeutische Strategien zur Regeneration des Nervensystems zu entwickeln, ist es daher notwendig die natürlichen Prozesse der Reifung neuronaler Netzwerke und ihrer postnatalen Plastizität zu verstehen. Daher verwendete ich Modelle spezifischer, embryonaler Vernetzungsfehler, um in zwei unterschiedlichen Ansätzen die Konsequenzen in postnatalen Tieren zu analysieren und Mechanismen zu untersuchen, die es ermöglichen diese zu kompensieren.

Im ersten Ansatz analysierte ich die postnatalen Auswirkungen von embryonalen Defekten des Axonenwachstums. Während der Embryonalentwicklung sind Vernetzungfehler von zentralen und peripheren Nervenbahnen, die durch eine fehlerhafte Interaktion von Sema3A und seinem Rezeptor Npn1 ausgelöst werden, besonders gut untersucht. So verursacht ein spezifischer Verlust des Npn1 Rezeptors in den Motorneuronen von *Olig2-Cre^{+};Npn1^{cond}* Mutanten schwere Defizite in der Faszikulierung und Wegfindung von Motoraxonen und eine reduzierte Länge dieser Nervenfasern. Im Gegensatz dazu hat eine fehlerhafte Sema3A Bindungsstelle des Npn1 Rezeptors, wie sie bei der Mauslinie *Npn1^{Sema-}* vorliegt, ein vorzeitiges Einwachsen der motorischen Projektionen in das sich entwickelnde Vorderbein zur Folge und führt zu Vernetzungsstörungen sowohl von motorischen als auch von sensorischen Axonen. Anatomische und morphologische Untersuchungen sowie Verhaltenstests von postnatalen Tieren beider Mauslinien zeigten interessanterweise, dass nur *Olig2-Cre^{+};Npn1$^{cond-/-}$* Mäuse permanente postnatale Störungen in Motorkoordination, Haltung der Vorderbeine und Knochenstruktur aufweisen, die mit einer Atrophie der Extensormuskeln in den Vorderbeinen einhergehen. Daher untersuchten wir die zugrundeliegenden Ursachen, die es *Npn1^{Sema-}* Mäusen ermöglichen die embryonalen Fehler ihrer Axonenvernetzung zu

kompensieren, während *Olig2-Cre^{+};Npn1^{cond}* Mutanten bleibende postnatale Schäden zeigen. Zu diesem Zweck untersuchte ich die morphologische Zusammensetzung spezifischer peripherer Nerven und deren Projektionsmuster mit Hilfe eines genetischen Markers für Motorneuronen und der retrograden Markierung von brachialen Nervenbahnen. Die Analyse der brachialen Nerven zeigte einen spezifischen Verlust von Motoraxonen im Radialisnerv von *Olig2-Cre^{+};Npn1$^{cond-/-}$* Mäusen. Des Weiteren ließ sich eine direkte Korrelation zwischen der Reduktion der Anzahl an Motoraxonen und dem Ausmaß der Haltungsschäden erkennen. Diese Erkenntnisse wurden durch die retrograden Markierungen der brachialen Nerven bestätigt, die eine verringerte Anzahl an spinalen Motorneuronen, die den Radialisnerv innervieren, zeigte. Im Gegensatz dazu ließen *Npn1^{Sema-}* Mutanten keine Abweichungen bezüglich der Zusammensetzung oder Innervierung des Radialisnervs erkennen. Diese Ergebnisse weisen darauf hin, dass der Verlust der Sema3A-Npn1 Bindung nicht der einzige Grund für die anatomischen Defizite in *Olig2-Cre^{+};Npn1$^{cond-/-}$* Mäusen sein kann: zusätzliche, noch nicht identifizierte Bindungspartner des Npn1 Rezeptors könnten die Unterschiede in der Entwicklung des peripheren Nervensystems verursachen und dafür sorgen, dass *Npn1^{Sema-}* Mutanten die embryonalen Defekte kompensieren können.

Im zweiten Ansatz untersuchte ich das postnatale plastische Potential spinaler Netzwerke, in denen embryonale Fehlverschaltungen vorliegen. Zu diesem Zweck nutzte ich *Sema3F* knockout Mäuse, welche sehr spezielle Verschaltungsdefizite der Motorneuronen aus dem medialen Teil der lateralen Motorsäulen (LMCm) aufweisen. Diese anatomischen Fehlverknüpfungen der brachialen Nerven werden während der Reifung des Netzwerks nicht kompensiert und bleiben bis ins Erwachsenenalter erhalten. Außerdem zeigen *Sema3F* Mutanten Verhaltensdefizite in der Motorkoordination sowie eine neuroanatomische Desorganisation der Motorneuronenpopulation im LMCm. Interessanterweise bewirkt eine Haltung der Mäuse in einer aufgewerteten Umgebung (enriched environment) von Geburt an, einen Ausgleich dieser Defizite während der postnatalen Entwicklung. Dennoch bleibt es unklar welche Mechanismen dieser erstaunlichen Kompensationsfähigkeit auf der Ebene von Verhalten und Neuroanatomie zugrunde liegen. Durch die Analyse des Verhaltens und funktioneller sowie neuroanatomischer Studien untersuchte ich zunächst, ob die beobachtete Plastizität auf einen bestimmten Zeitraum während der postnatalen Entwicklung beschränkt ist. Tatsächlich bewirkt ein verspäteter Beginn der enriched environment Haltung 4 Wochen nach Geburt keine Verbesserung der motorischen Leistung oder Reorganisation der Neuroanatomie. Dies weist auf eine kritische Periode für adaptive Plastizität im spinalen

Motorsystem hin. Eine genauere Untersuchung von Mechanismen, die die Plastizität in der kritischen Periode beeinflussen, zeigte, dass Aktivität in diesem Zeitraum die Bildung anregender Synapsen an LMCm Neuronen induziert. Da hemmende Synapsen und perineurale Netze bereits mit der Regulation der kritischen Periode in Verbindung gebracht wurden, benutzten wir diese Faktoren, um herauszufinden ob Haltungsbedingungen einen Einfluss auf die Steuerung der kritischen Periode haben. Beide Kriterien zeigten allerdings keine Auswirkungen durch veränderte Haltungsbedingungen, woraus gefolgert werden kann, dass die Regulation der kritischen Periode für die beschriebenen, adaptiven Veränderungen im motorischen System der *Sema3F* Mäuse keine Rolle spielt.

Unsere Daten zeigen, dass wir durch die Nutzung der embryonalen Vernetzungsfehler in *Sema3F* Mutanten als Modell, ein von Verletzungen unabhängiges System für die Untersuchung von adaptiver Plastizität im Rückenmark entwickeln konnten. Dieses Modell ermöglicht die Unterscheidung von Effekten, die durch plastische Anpassungen entstehen, und solchen, die durch Entzündungsreaktionen oder Narbenbildung als sekundäre Folgen von Rückenmarksverletzungen hervorgerufen werden. Daher erlaubt uns dieses System neue Erkenntnisse über die zugrundeliegenden Mechanismen der postnatalen Plastizität zu gewinnen, die dabei helfen können neue Therapien für die neuronale Regeneration zu entwickeln.

II. INTRODUCTION

All motor behaviors, ranging from simple and standardized reflex actions to very skilled movements such as ballet dancing or playing the violin, depend on the proper function of distinct muscles that are controlled by motor neuron activity. In order to allow for this huge repertoire of movements, the activity of motor neurons, in turn, needs to be strictly controlled by motor circuits of the central nervous system (CNS). These circuits are formed with enormous precision during embryonic development. Later, neuronal connectivity is refined by axon pruning and naturally occurring cell death during processes of circuit maturation and even after birth the nervous system can be modified by plasticity in order to fulfill the demands of their environment. Together, these highly complex mechanisms make sure that motor functions are properly controlled but flexible enough to meet the everyday challenges of postnatal life.

II.1. Neuronal circuits controlling motor behavior

Neuronal circuits that control motor behavior are organized in multiple layers. Thus, the activity of spinal motor neurons, which exert direct control over their target muscles in the periphery, is regulated by intraspinal neuronal circuits, which in turn interact with supraspinal centers in brain-stem and higher brain areas (Arber, 2012). Due to the high complexity of these circuits and their interactions, understanding voluntary locomotion is a very challenging task and the underlying mechanisms have been studied for years.

II.1.1. Motor control by descending neuronal tracts

In the brain, the main areas that control motor behavior are the basal ganglia, the cerebellum, and the cerebral cortex. The basal ganglia are mainly involved in the basic control of movements and pathological deficits in this brain region can lead to severe movement disorders like Parkinson's Disease or Huntington's Disease (Graybiel *et al.*, 1994; Grillner *et al.*, 2005). In contrast, the cerebral cortex and the cerebellum are responsible for the fine-tuning of voluntary movements (Arber, 2012). All these centers of motor control exert their regulating function on spinal motor circuits via descending pathways.

The best described descending pathway is the corticospinal tract (CST), which arises from layer five pyramidal neurons in the primary motor, premotor and somatosensory cortices (Miller, 1987). Most of the axons cross to the opposite side at the caudal end of the brain stem and descend directly to their target areas in the spinal cord. Here, they terminate in the intermediate zone of the grey matter and also some direct connections to motor neurons in the ventral horn have been described (Lemon, 2008) (Figure 1A). The importance of cortical input on motor behavior is demonstrated by lesion studies, which revealed that the severity of specific movement impairments is directly related with the size of the lesion area in the cortex (Whishaw *et al.*, 1991). Furthermore, a comparative study across different species has shown a direct relationship of the development of the CST and motor control abilities (Heffner & Masterton, 1983). Thus, while rodents do not reveal any direct connections of CST axons with spinal motor neurons, monosynaptic projections gain more and more influence from non-human primates to humans (Lemon, 2008). The monosynaptic connections allow for a very direct control of motor behavior, however, this system always works in parallel with indirect corticospinal pathways, which can be of considerable importance and mediate their regulating functions via segmental interneurons or propriospinal neurons.

In contrast to the cerebral cortex, the basal ganglia and the cerebellum are not directly connected to the spinal cord (Figure 1B). Hence, the basal ganglia control the initiation and termination of movements by signaling via the thalamus to the motor cortex. Additionally, they can mediate their function by their connection to the reticulospinal tract, which connects the centers of the reticular formation with spinal motor neurons and interneurons of the ventro-medial intermediate zone of the spinal cord gray matter (Peterson *et al.*, 1979; Lemon, 2008). The third important brain region that controls motor behavior is the cerebellum. It coordinates the fine-tuning of motor behaviors by the implementation of sensory feedback that is sent to the motor cortex (via thalamus) or to the red nucleus. The latter is the origin of the rubrospinal tract that projects mostly to the dorsal and lateral intermediate zone of the spinal cord gray matter (ten Donkelaar, 1988). But also some direct connections to spinal motor neurons have been described that are thought to have a role in motor control of the distal forelimb (Kuchler *et al.*, 2002).

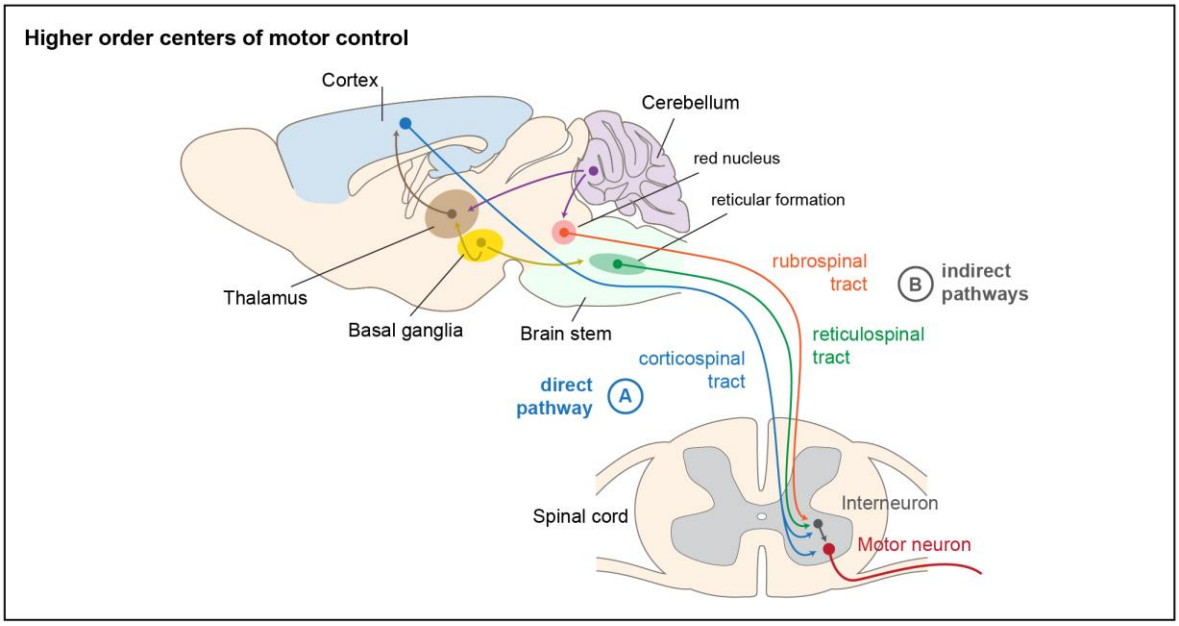

Figure 1: Higher order centers of motor control and their descending pathways

Motor behavior is controlled by specific brain centers like the motor cortex, the cerebellum, or the basal ganglia. **(A)** The motor cortex can exert its influence on motor control directly via the corticospinal tract on motor neurons of the ventral horn. **(B)** In contrast, the cerebellum and the basal ganglia use indirect pathways. Thus, the cerebellum mediates its regulatory function either through the rubrospinal tract that originates in the red nucleus and projects mostly towards interneurons of the intermediate zone of the spinal cord gray matter, or it uses a pathway via the thalamus and motor cortex. The latter pathway may also be activated during the mediation of motor control from the basal ganglia. Alternatively, they may induce motor behavior through reticulospinal tract, which has its basis in reticular formation of the brain stem.

II.1.2. Modification of motor neuron activity by intraspinal circuits

Despite the considerable impact of higher order centers on motor control, most of them rely on the modification of intraspinal circuits that exert the final input on executing spinal motor neurons. Furthermore, it has been shown that also without higher order control movement can be initiated by spinal motor circuitry alone. The simplest form of such an independently working motor circuit is the monosynaptic reflex arc (Chen *et al.*, 2003). It consists of a sensory neuron that receives proprioceptive information of stretch-sensitive muscle spindles and makes an excitatory monosynaptic connection to an α-motor neuron in the spinal cord. In contrast, a polysynaptic reflex needs one or more interneurons to integrate the sensory

information and activate the motor efferents (Figure 2A). Other studies with decorticate cats or cats after complete spinal cord transection have shown that also more complex movements can be elicited on a treadmill independently from higher order inputs (Bjursten *et al.*, 1976; Barbeau & Rossignol, 1987). However, for a long time it was not clear whether these movements were caused by a complex chain of reflexes or if they are controlled by the spinal cord itself. Then, already 100 years ago, Graham Brown proposed the model of a simple neuronal circuit within the spinal cord, which are now generally known as central pattern generators (CPGs) (Figure 2B) (Brown, 1914). These local neuronal circuits consist of a network of interneurons and motor neurons and are capable of generating rhythmic motor patterns that govern repetitive movements independently from extrinsic information on phasic timing. Nevertheless, the activity of CPGs can be modulated by sensory or higher order input in order to correct for environmental differences and sculpture muscle activities within the movement cycle (reviewed in Marder & Bucher, 2001).

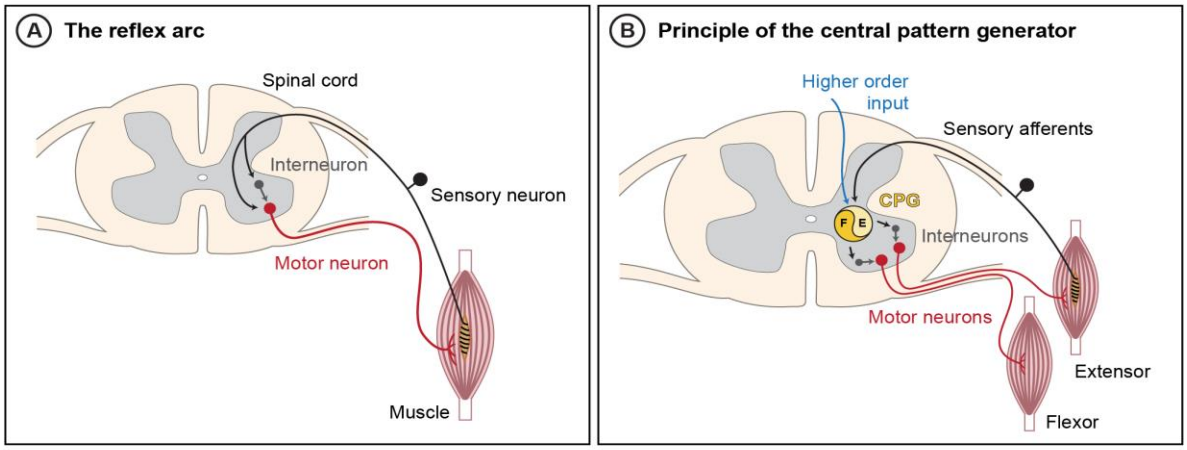

Figure 2: Reflex arcs vs. central pattern generator

(A) Reflexes may be mediated either in a monosynaptic or a polysynaptic manner. In monosynaptic reflexes the proprioceptive information of the muscle spindle is directly conducted by class Ia sensory afferents towards α-motor neurons that induce the contraction of a specific muscle. In contrast, in polysynaptic reflexes the sensory information is transmitted to the executing motor neurons via at least one interneuron. In more complex withdrawal reflexes the activation of a cascade of interneurons may be necessary to assure the appropriate activation or inactivation of contralateral muscle groups. **(B)** The central pattern generator (CPG) is a circuit of interneurons within the spinal cord, which may induce rhythmic motor activity of extensor (E) and flexor (F) muscles in the absence of sensory input. Muscle activities can be modulated by sensory or higher order input in order to adapt the movement according to environmental circumstances.

II.2. Development of the spinal motor circuitry

II.2.1. Generation of motor neurons

During development of the spinal cord, the graded expression of sonic hedgehog (Shh) from notochord and floorplate leads to the establishment of 5 distinct progenitor domains in the subventricular zone of the ventral spinal cord (p0-p2, pMN, and p3). These regions are spatially restricted by the expression of mutually repressive homeodomain transcription factors and give later rise to specific subsets of neurons (reviewed in Jessell, 2000). Hence, the pMN domain is defined by the expression of Pax6, Nkx6.1/6.2 and Olig2, and gives rise to some of the first postmitotic cells in the ventral spinal cord, the motor neurons, and later due to a transcriptional switch also to oligodendrocytes (Jessell, 2000; Lee & Pfaff, 2001).

After their generation, newborn motor neurons migrate laterally towards their assigned position within the spinal cord. Here, motor neuron subtypes group according to their innervation targets and form distinct columns along the rostro-caudal axis of the spinal cord (Tsuchida *et al.*, 1994; Bonanomi & Pfaff, 2010). Motor neurons that innervate the trunk musculature reside within the medial motor columns at all spinal levels, while limb innervating motor neurons form the lateral motor columns (LMCs) at brachial and lumbar levels of the spinal cord. In the LMC, motor neurons can be assigned to two distinct divisions, the medial and the lateral LMC, which can be recognized according to their ventral or dorsal axon target zones, respectively (Eisen, 1999; Jessell, 2000; Landmesser, 2001; Bonanomi & Pfaff, 2010). Thus, already the organization of motor neurons in the spinal cord is strictly controlled in order to facilitate the outgrowth of their axons along their assigned trajectories.

II.2.2. Molecules governing motor axon pathfinding

In order to assure that each motor neuron projects towards the appropriate target area in the periphery, axon pathfinding is strictly controlled by the action of axon guidance molecules. These environmental cues are of attractive or repulsive nature and can mediate their function either by direct contact or over long distances via chemotactic mechanisms (Figure 3) (Huber *et al.*, 2003). During the last decades, a variety of different ligand-receptor pairs have been identified that influence the axon trajectory by the regulation of growth cone dynamics and motility. Among them are the Netrin-DCC, the Slit-Robo and the Ephrin-Eph system (Keino-Masu *et al.*, 1996; Brose *et al.*, 1999; Huber *et al.*, 2003; Kao *et al.*, 2012). Furthermore, the

secreted class 3 semaphorins and their receptors, the neuropilins, have been shown to play an important role in the pathfinding of LMC neurons (Kolodkin *et al.*, 1997).

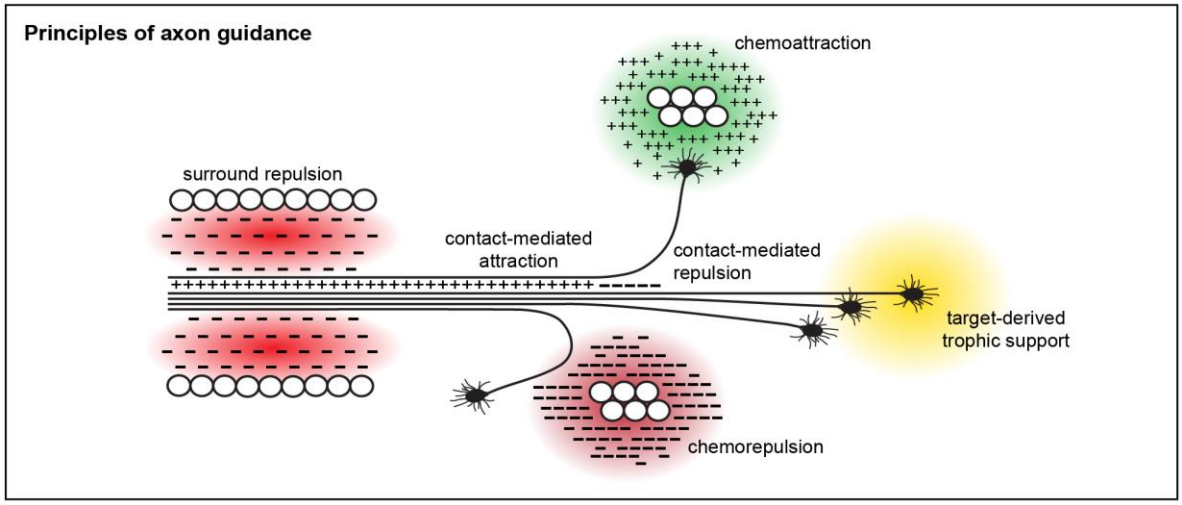

Figure 3: Principles of axon guidance

During development secreted molecules or direct contact may mediate attractive or repulsive effects on the neuronal projections that control axon outgrowth, fasciculation and steering (adapted from Huber *et al.*, 2003).

II.2.3. Semaphorin-neuropilin signaling

Semaphorins (Semas) belong to a large family of axon guidance molecules that is defined by a conserved sequence of approximately 500 amino acids – the N-terminal Sema domain. Up to now, 8 classes of semaphorins have been described (class 1-7 and class V), which are classified by their protein sequence and structural similarities (Semaphorin Nomenclature Committee, 1999) (Figure 4A). Class 1 and 2 are restricted to invertebrates and class V is only expressed in viruses. The remaining five classes (3-7) are expressed in vertebrates, whereof class 3 is the largest subfamily and consists of seven family members of secreted proteins (Sema3A-G) (O'Malley *et al.*, 2014). Functionally, semaphorins are involved in various different processes like the integrity of the immune system, tumor formation, or the development of the cardiovascular system (reviewed in Nasarre *et al.*, 2014; Vadasz & Toubi, 2014; Epstein *et al.*, 2015). However, originally they were identified for their role in nervous system development and the formation of axon trajectories (Kolodkin *et al.*, 1992; Luo *et al.*, 1993). Thus, in the

murine spinal cord, Sema3A and Sema3F have been shown to be of special importance for motor axon guidance, since they mediate the timing of axon outgrowth, axon fasciculation and are involved in the dorso-ventral guidance decision (Huber *et al.*, 2005).

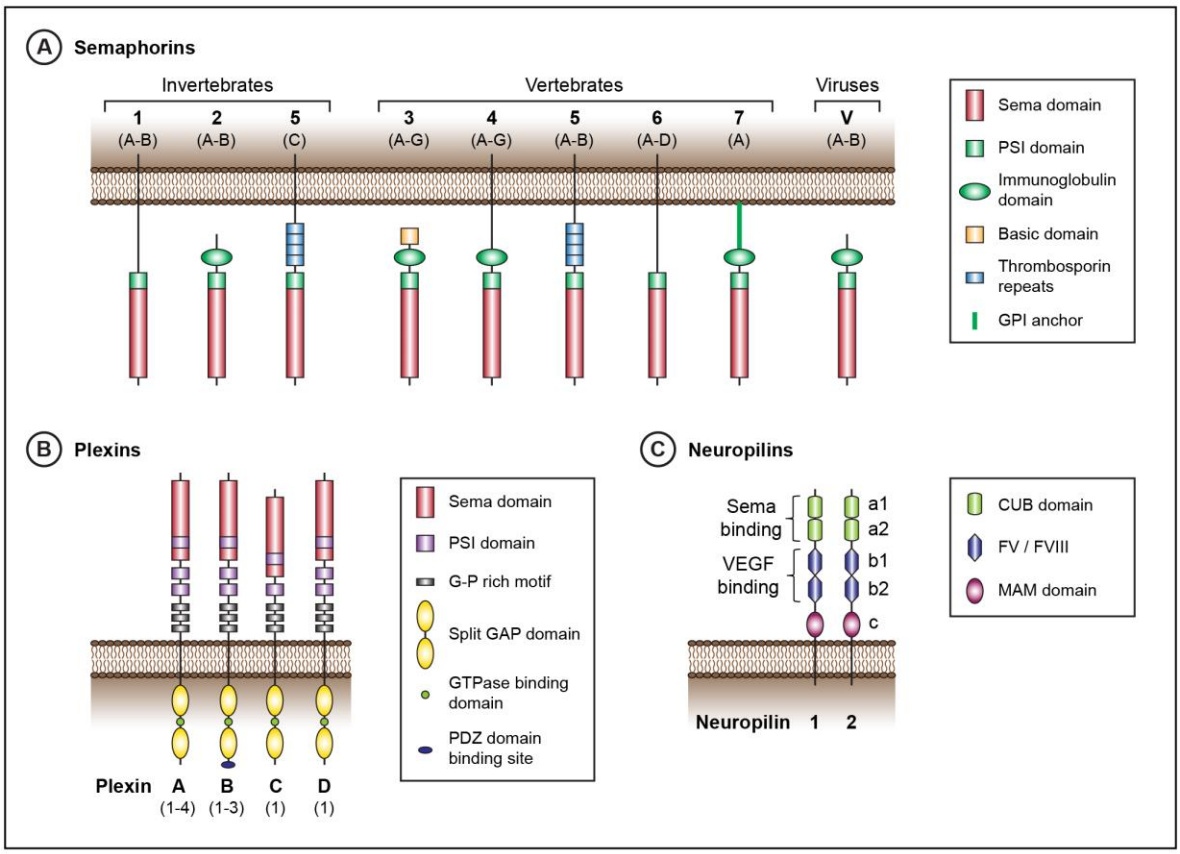

Figure 4: Semaphorins and their receptors

(A) Overview of the semaphorin family of membrane-linked or secreted axon guidance molecules. All semaphorins share structural similarity by a common sema domain at their amino-terminal that is linked to a PSI domain. The carboxyl-terminal end, in contrast, varies among the classes. **(B)** Sema signaling is mediated by plexins. **(C)** Some semaphorins, like class 3 Semas, cannot interact directly with plexins. Instead, they bind to one of two neuropilin receptors that form complexes with one of the four PlexinA family members, which mediate the signal transduction (adapted by permission from Macmillan Publishers Ltd: Neufeld & Kessler, 2008).

Signaling of semaphorins is conveyed by specific signal-transducing receptors, the plexins, which are a large family of transmembrane proteins that are grouped into four classes (A1-4, B1-3, C1 and D1) (Tamagnone *et al.*, 1999) (Figure 4B). The subfamily A is of particular

importance for the signaling of the secreted class 3 Semas. However, while most semaphorins (class 4-7) can bind directly to plexins via a divergent sema domain on the receptor (Gherardi *et al.*, 2004), class 3 Semas need co-receptors, such as the neuropilins, that mediate the binding (Figure 4C). The neuropilins are type 1 transmembrane proteins that only have a very small cytoplasmic domain and are not able to transduce Sema3 signaling. Consequently, the formation of a Neuropilin-PlexinA receptor complex is necessary in order to allow for a functional signal transduction (Kolodkin *et al.*, 1997).

Semaphorins are not the only ligands of the neuropilin receptors: the extracellular domain of neuropilin 1 (Npn1) can bind a number of structurally very different proteins such as transforming growth factor beta1 (TGF-β1), vesicular endothelial growth factor (VEGF), or the cell adhesion and pathfinding molecule L1 (Castellani, 2002; Gu *et al.*, 2003; Glinka & Prud'homme, 2008). Thus, a full knockout of Npn1 is embryonically lethal between embryonic day (E) 10.5 and E12.5, due to defects in heart development and vasculature (Kawasaki *et al.*, 1999). Furthermore, during development of the nervous system Npn1 is of particular importance e.g. for the branching of basket cells in the cerebellum and in the guidance of pioneering axons from the cingulate cortex (Piper *et al.*, 2009; Cioni *et al.*, 2013). Also the development of the peripheral nervous system depends on a functional Npn1 receptor (Kitsukawa *et al.*, 1997). In order to identify the function of individual ligands for Npn1, the mouse line *Npn1*$^{Sema-}$ has been generated, in which an exchange of 7 amino acids in the sema binding site of the Npn1 receptor causes a dysfunctional semaphorin binding. By the use of this model system, Huber and colleagues determined that at E10.5 the interaction of this ligand-receptor pair prevents a precocious ingrowth of axons, since the repulsive ligand Sema3A is expressed in the entire limb mesenchyme. Later, a change in the Sema3A expression pattern clears a distinct path for the outgrowing axons and guides their way through the developing limb. During this phase, Sema3A-Npn1 signaling is playing an important role in the fasciculation and pathfinding of sensory and motor axons. (Gu *et al.*, 2003; Huber *et al.*, 2005; Kolodkin & Tessier-Lavigne, 2011). The importance of a functional Sema3A-Npn1 signaling in axon fasciculation and pathfinding has been further described by a study of Huettl at al. that shows that the conditional removal of Npn1 from sensory neurons affects the fasciculation of both, motor and sensory fibers. In contrast, a depletion of the receptor selectively from motor neurons does not affect sensory axon fasciculation, while motor axons are severely defasciculated. Additionally, these motor axons have shorter projections and display dorsal-ventral pathfinding errors (Huettl *et al.*, 2011).

In addition to Sema3A-Npn1 signaling, also the interaction of the receptor Npn2 with its ligand Sema3F is of crucial importance for the development of the CNS. Thus, it has been shown to mediate the formation of the retinocollicular map, pathfinding and fasciculation of olfactory sensory neuron projections and the development of the limbic system (Sahay *et al.*, 2003; Cloutier *et al.*, 2004; Claudepierre *et al.*, 2008). Also during the development of peripheral projections it plays an important role. Here, Npn2, which is selectively expressed on motor neurons of the medial division of the LMC (LMCm), is repelled by Sema3F in the dorsal limb mesenchyme and thereby mediates the growth of LMCm motor axons towards a ventral trajectory. Consequently, loss of the repulsive interaction of Sema3F or its receptor Npn2 leads to misguidance of LMCm axons towards dorsal target areas (Huber *et al.*, 2005).

In conclusion, these examples show the specific significance of both signaling complexes for PNS development. Thus, Sema3A-Npn1 signaling is involved in various processes during axon outgrowth and pathfinding of all sensory and motor neurons in the brachial spinal cord, while the interaction of the receptor Npn2 with its ligand Sema3F has a very distinct role in the dorsal-ventral trajectory decision of LMCm neurons.

II.3. Circuit maturation during late embryonic and early postnatal development

During development, billions of neurons have to extend their axons and establish the appropriate connections in order to allow for the correct functioning of the nervous system. To make sure that each neuron finds its designated target zone, pathfinding of their extending projections is therefore mediated in a stepwise manner by a complex system of attractive or repellent guidance cues. Nevertheless, since in each of these steps errors in axon pathfinding might occur, this system alone is not sufficient to allow for the observed accuracy that underlies the establishment of neuronal circuits. Hence, in order to avoid the formation of malfunctioning neuronal circuits, connections are formed in abundance during embryonic development and then, through a variety of processes, connectivity is refined and only correctly established synapses are maintained.

II.3.1. Naturally occurring cell death and the neurotrophic hypothesis

When we think of the development of an organism, we usually first notice progressive processes like cell division, maturation and specification, which are necessary to form a complex organism. However, regressive events like the death of a well-defined group of cells are equally important, since they are crucial for the formation of specific structures, such as the digits of the hand, and deficits in the genetic programs underlying programmed cell death result in developmental abnormalities (reviewed in Baehrecke, 2002). Likewise, in the nervous system progressive events like neurogenesis, axon outgrowth and synapse formation form the basis of all neuronal circuits. At the same time regressive events are of significant importance in order to refine the neuronal patterns and establish a mature circuitry. Hence, waves of cell death have been described throughout the development of the nervous system. During the establishment of the spinal motor circuits motor neurons are generated in abundance and are reduced by about 50% during late embryonic and early postnatal development (Hamburger & Levi-Montalcini, 1949; Hamburger, 1975; Sendtner *et al.*, 2000). Classical experiments in the chicken embryo by Viktor Hamburger showed that the extent of motor neuron death is depending on the size of the target field, since the number of dying LMC neurons increased after removal of their target limb (Hamburger, 1958). This finding was later supported by studies with his colleague Margaret Hollyday, who found that programmed cell death of LMC motor neurons can be reduced by the extension of the peripheral target area (Hollyday & Hamburger, 1976). These results together with the discovery of the nerve growth factor (NGF) in 1956 gave rise to the idea that programmed cell death is not a fixed process, but regulated by target-derived factors, which provide trophic support - the neurotrophic hypothesis (Figure 5A) (Cohen & Levi-Montalcini, 1956; Purves *et al.*, 1988). Accordingly, the competition for survival factors in the periphery displays a mechanism that facilitates the quantitative regulation of target innervation (Gould & Enomoto, 2009).

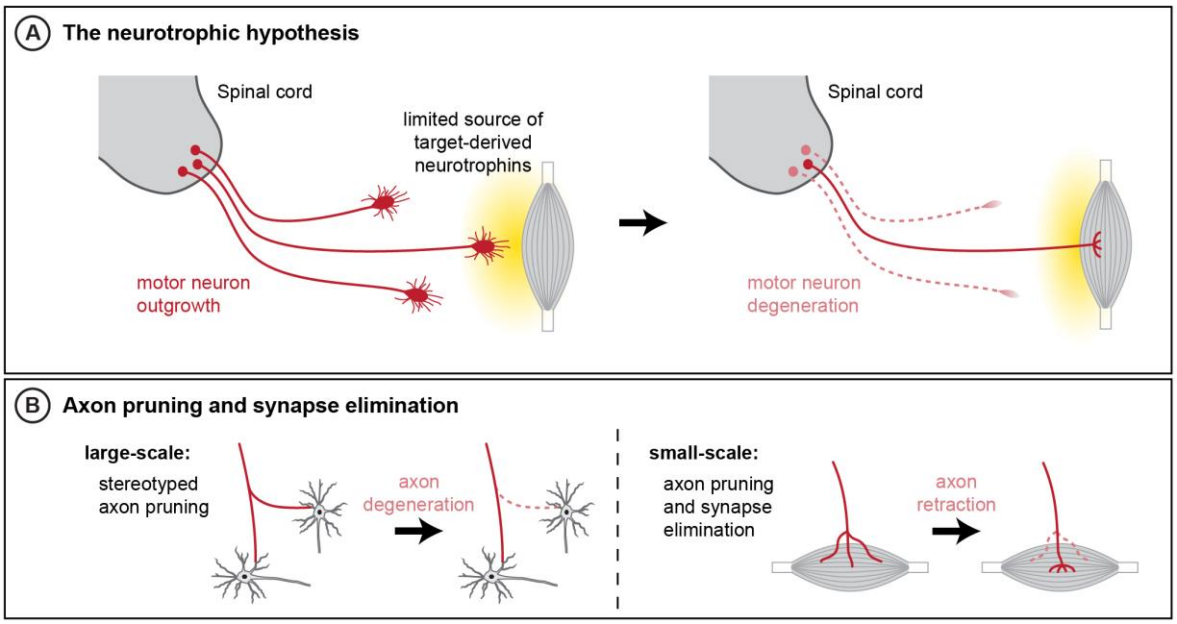

Figure 5: Regressive events during circuit maturation

(A) During development, neuronal connectivity is established in excess. Neurons extend their axons towards their target zones, where only a limited supply of trophic factors is available. Consequently, neurons that receive insufficient neurotrophic support will die by programmed cell death. **(B)** Axons can be pruned during circuit maturation in large- or small-scale events. Large-scale events cause the degeneration of whole axon branches that innervate inappropriate targets. In small-scale events of axon pruning only the axon terminals within the same target zone are affected. Here, competition causes the retraction of weak synaptic connections, while the strongest synapse will be strengthened and maintained ((B) adapted from Vanderhaeghen & Cheng, 2010).

II.3.2. Synapse elimination and axon pruning

Not all neurons that undergo regressive events during circuit maturation are completely eliminated by programmed cell death. Thus, axon pruning only affects the peripheral connections of a neuron, while its cell body remains intact. Generally, these processes of axon elimination can be divided in two groups depending on the extent to which the axon is affected. In large-scale events of axon pruning major axon branches or a significant length of the primary axon are eliminated, while small-scale events only remove supernumerary synapses and the most distal advancements of an axon (Figure 5B).

The elimination of axons in large-scale events is mainly governed by degeneration. Layer five neurons of the neocortex for example first extend their primary axons along the corticospinal

tract which initially grow past all target areas. Then, the axon forms several collaterals to a large number of layer five target areas and later, when cortical areas are organized according to their subsequent functions, exuberant projections or the distal part of the primary axon degenerate. Hence, neurons in visual areas will eliminate their entire caudal axon in the corticospinal tract, while neurons of the motor areas will lose their connections to the superior colliculus, but keep their collateral branches to centers of motor control, including the spinal gray matter (Luo & O'Leary, 2005). In contrast, small-scale events of axon elimination typically occur due to retraction of selective branches that form an axon arbor or specific axon segments and their terminal endings (Bernstein & Lichtman, 1999). A good example for such a small-scale event is the reduction of axon terminals at the neuromuscular junction (NMJ) (Vanderhaeghen & Cheng, 2010). A developing NMJ is initially innervated by several different motor neurons, which then compete with each other for the maintenance of their synapses. This process of competition is modulated by activity-based mechanisms that are responsible for changes in synaptic structure and strength. Thereby, most synapses are weakened and finally eliminated until the connectivity of each muscle fiber is reduced to a mononeuronal innervation pattern. The remaining synapse is strengthened and will be maintained throughout life (Luo & O'Leary, 2005).

Both strategies are highly effective and allow for the refinement of neuronal connectivity. Consequently, these events display basic mechanisms of early plastic adaptations that allow for the proper function of the nervous system.

II.4. Postnatal plasticity of neuronal circuits

Neuronal networks are established during embryonic development and for a long time they have been considered as hard-wired after birth because injury or disease leads to permanent damage. However, since the studies of Hubel and Wiesel more than 50 years ago it has become clear that also during postnatal life neuronal networks can be shaped by experience. They showed that in cats monocular visual deprivation within the first postnatal weeks causes anatomical rearrangements in the visual cortex that are known as ocular dominance plasticity (Wiesel & Hubel, 1963a; b). During this process the closure of one eye leads to a dramatic decrease in the activity of the corresponding cortical area. Due to the competition of both eyes for control of receptive fields in the cortex this in turn causes a shift in the cortical organization towards the non-deprived eye. Furthermore, they found evidence for the

existence of a sensitive period in the fourth and fifth postnatal week in which these adaptive changes can take place, since only during this time period the procedure is capable of causing the described ocular dominance shift (Hubel & Wiesel, 1970). These pioneering studies revealed a new principle for the regulation of postnatal neuronal plasticity – the critical period.

II.4.1. Critical periods in postnatal adaptive plasticity

According to Takao K. Hensch "A critical period is an extreme form of a more general sensitivity, when neuronal properties are particularly susceptible to modification by experience" (Hensch, 2004). Such critical periods have been studied for decades and were identified for a large variety of sensory and motor systems, like the organization of the visual and auditory cortex or synapse elimination at the neuromuscular junctions (Hubel & Wiesel, 1970; Walsh & Lichtman, 2003; Barkat *et al.*, 2011). Nevertheless, in order to investigate factors that modulate the regulation of critical period plasticity (Figure 6) the visual cortex still serves as the primary model. Onset and termination of the critical period have been shown to depend on certain inhibitory thresholds, since an early reduction of intracortical inhibition causes a delayed start, and increased inhibition leads to a precocious closure of the critical period (Fagiolini & Hensch, 2000; Berardi *et al.*, 2003). Furthermore, there is evidence for a strong link between intracortical inhibition and the expression of brain-derived neurotrophic factor (BDNF). Thus, the genetic overexpression of BDNF induces an accelerated maturation of GABA-mediated cortical circuits and consequently causes a shift in the timing of the critical period for ocular dominance plasticity (Huang *et al.*, 1999).

Next to these functional aspects, also structural features seem to play a crucial role in the regulation of critical periods. Hence, it has been shown that the termination of critical periods is highly dependent on the formation of specialized networks of extracellular matrix that limit the connectivity of neurons - the perineuronal nets (PNNs). These nets form a structure that is similar to cartilage and wrap neurons in a mesh-like structure with open holes for synaptic contacts (Wang & Fawcett, 2012). Thereby, they stabilize the existing connectivity of a mature neuronal circuit and protect the neurons from plastic changes. The importance of PNNs in the regulation of critical period plasticity was further corroborated by studies, which showed that the destruction of these networks of extracellular matrix lead to the opening of critical period plasticity in the mature visual cortex and after spinal cord injury (Bradbury *et al.*, 2002;

Pizzorusso *et al.*, 2002). Hence, the formation of PNNs can be directly linked to the closure of critical periods and thereby regulate adaptive plasticity in postnatal neuronal circuits.

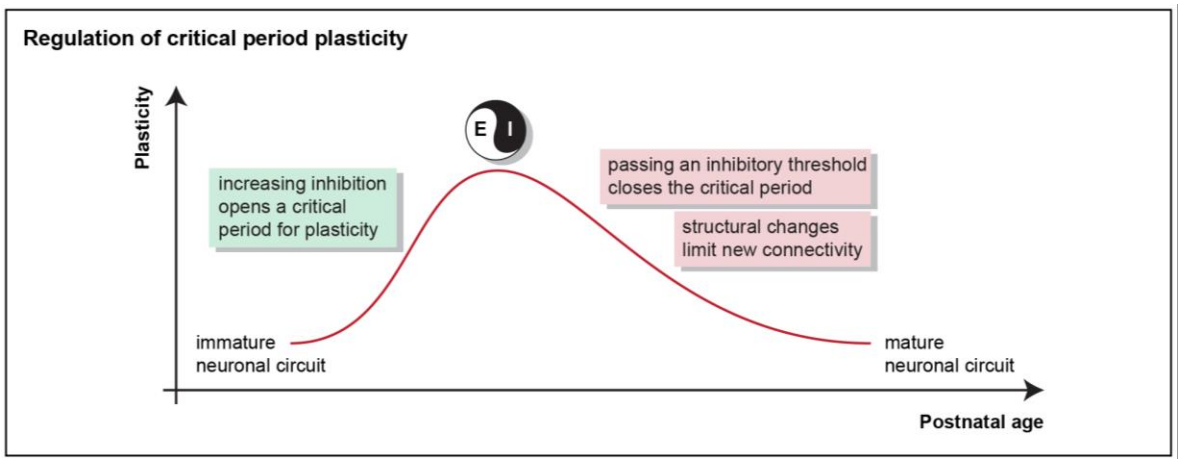

Figure 6: Critical period regulation during postnatal adaptive plasticity

Adaptive changes in the postnatal nervous system are usually restricted to well-defined periods of time of increased plastic potential – the critical periods. These critical periods are highly sensitive to the balance of excitation (E) and inhibition (I). Hence, during the maturation of neuronal circuits critical periods are opened by the increase of inhibition, and surpassing a specific inhibitory threshold causes their termination. Furthermore, also structural changes, like the development of perineuronal nets, can cause critical period closure.

II.4.2. Modulation of adaptive plasticity by activity-based mechanisms

Interestingly, the formation of PNNs can be attenuated by housing the animals in an enriched environment, which causes the extension of the critical period for adaptive plasticity in the visual cortex (Foscarin *et al.*, 2011). Such an enriched environment (EE) typically consists of a combination of inanimate and social stimuli, which facilitate the stimulation of distinct cognitive, sensory or motor functions (Rosenzweig *et al.*, 1978). Next to its impact on the critical period in the visual cortex, EE housing has also been shown to have various effects on postnatal development and plasticity of neuronal circuits (van Praag *et al.*, 2000; Bengoetxea *et al.*, 2012). In this respect, it causes changes of the dendrite structure in the auditory cortex and accelerates the development of the visual cortex (Sale *et al.*, 2004; Bose *et al.*, 2010). Moreover, the effects of dark-rearing on visual cortex maturation can be prevented by EE housing and the recovery of sensory and motor functions after severe spinal cord injury are improved

(Bartoletti *et al.*, 2004; Berrocal *et al.*, 2007). But what are the molecular principles that mediate the beneficial effects of EE housing?

Beside its effects on the expression of neurotrophic factors such as BDNF and on the survival and dendritic sprouting of neurons (van Praag *et al.*, 2000; Pham *et al.*, 2002), enriched environment housing has also been shown to affect activity-dependent mechanisms by increasing the expression of synapse proteins and inducing changes in the expression of subunits of the glutamate receptors (Naka *et al.*, 2005; Nithianantharajah & Hannan, 2006). Especially N-methyl-D-aspartate (NMDA) receptors have been recognized for their modulatory function in experience-dependent plasticity, since they are both transmitter- and voltage-dependent and mediate plasticity-related intracellular signaling via the regulation of Ca^{2+} influx (Berardi *et al.*, 2003). Interestingly, NMDA receptors have been shown to be expressed during a restricted period of time in the developing ventral horn and to be functionally implicated in activity-dependent plasticity during the maturation of spinal motor circuits (Nelson *et al.*, 1990; Kalb *et al.*, 1992). Furthermore, blocking of NMDA receptors prevented the effects of dark-rearing on the organization of the visual cortex (Bear, 1996), which further corroborates its importance in the mediation of experience-induced postnatal plasticity.

All-in-all, a multitude of molecular and functional experiments in different model systems has broadened the knowledge on adaptive plasticity in postnatal neuronal circuits. Nevertheless, further investigations are necessary, in order to fully understand how plastic changes in the nervous system are governed and which factors contribute to experience-dependent adaptations during postnatal development.

II.5. Aim of the thesis

The establishment of a functional nervous system is controlled by a complex set of mechanisms that regulate the accurate formation of neuronal connectivity and allow for circuit maturation and experience-dependent adaptations. These mechanisms make sure that each neuronal circuit is shaped with precision and meets the challenges of its environment. In adult animals, however, the adaptive potential of the nervous system is limited and consequently, neuronal degeneration or injury leads to permanent damage. In order to develop new therapeutic strategies that promote neuronal regeneration, the understanding of naturally occurring compensation and plasticity processes in the nervous system is of crucial importance.

In this thesis, I aimed to gain new insights into the postnatal aspects of neuronal circuit development by the investigation of two questions: (1) What are the consequences of embryonic axon miswiring for the postnatal development? (2) How can adaptive plasticity be induced in the postnatal animal in order to compensate for embryonic deficits? To address these questions, we used the murine motor system as a model and investigated both aspects in two different approaches that are explained in the following.

II.5.1. Determination of postnatal consequences of a deficient Sema3A-Npn1 signaling

Npn1 deficient animals reveal severe but specific and well described axon guidance deficits. Hence, in *Olig2-Cre;Npn1^{cond}* mice the specific ablation of the entire Npn1 receptor from all motor neurons causes defasciculation of motor axons, pathfinding errors and reduced length of developing motor projections (Huettl *et al.*, 2011). In contrast, disruption of the semaphorin binding site in the Npn1 receptor of *Npn1^{Sema-}* mutants causes a precocious ingrowth of motor axons. Furthermore, the deficits in axon fasciculation and pathfinding are not restricted to motor axons, but also sensory axons are affected (Huber *et al.*, 2005). What do these embryonic deficits mean for the postnatal animal? Using behavioral, anatomical, and morphological analyses, a former study in our lab revealed that only *Olig2-Cre^{+};Npn1^{cond}* mutants display postnatal deficits in forelimb posturing and severe dysfunctions in skilled motor behavior, while *Npn1^{Sema-}* mutants do not show such deficits. The postural abnormalities in *Olig2-Cre^{+};Npn1^{cond}* mutants were accompanied by muscle atrophy in the extensors of the forelimb and result in bone malformations in adult animals (Soellner, 2012; Helmbrecht *et al.*,

2015a). Thus, previous work has described the developmental and postnatal phenotype of both mouse lines extensively. Which are the underlying reasons for the abnormal phenotype in forelimb posturing of *Olig2-Cre*$^{+}$*;Npn1*$^{cond-/-}$ mice and the difference to *Npn1*$^{Sema-}$ mutants?

In order to investigate if alterations in forelimb motor innervation are responsible for the anatomical differences of both mouse lines, it was necessary to compare the two mouse lines in detail and specifically assess individual nerves that innervate particular forelimb muscles using different methodological approaches.

Parts of this section are published in (Helmbrecht *et al.*, 2015a).

II.5.2. Analysis of postnatal adaptive plasticity in the spinal motor system of *Sema3F* mutants

The classic approach for the investigation of experience-dependent plasticity in the postnatal motor circuitry uses spinal cord injury as a model system. However, injury models show poor reproducibility even within the same lab. Furthermore, injury-induced processes like scar formation, vascularization and inflammation make it hard to distinguish between the consequences of these secondary effects and experience-dependent plastic adaptations. Hence, we aimed to apply a non-injury based model for the analysis of spinal cord plasticity. In this respect, the very specific axon guidance deficits of *Sema3F* mutants displayed an excellent model, since their deficits only affect the pathfinding of LMCm motor neurons, while axon fasciculation and timing of axon outgrowth are not affected (Huber *et al.*, 2005). In a former study from our lab these guidance deficits have been found to be still evident in postnatal animals and to be accompanied by neuroanatomical reorganization of the LMCm. Furthermore, mutant animals display deficits in skilled motor tasks, while general locomotion was not affected. The study also revealed evidence for postnatal adaptive plasticity in these animals that became evident on a behavioral and neuroanatomical level and were induced by challenging the mice in an enriched environment starting at birth (Soellner, 2012; Helmbrecht *et al.*, 2015b (accepted)).

Nevertheless, it remained unclear if the described plastic adaptations were restricted to a specific critical period during early postnatal life, and what caused the plastic changes on the molecular level. To that end, I first analyzed the constraints of the critical period for plastic changes in the spinal motor system. By the use of behavioral, functional, and neuroanatomical

studies I investigated the effects of a delayed exposure to an enriched environment on *Sema3F* mutants. Subsequently, the molecular mechanisms underlying postnatal plasticity were dissected by analyzing the formation of perineuronal nets and staining for excitatory and inhibitory synapses on ventrally projecting motor neurons.

Results from this section are published in (Helmbrecht *et al.*, 2015b (accepted)).

III. MATERIAL AND METHODS

III.1. Animal husbandry

III.1.1. Ethics statement

Mice were handled according to the federal guidelines for the use and care of laboratory animals, approved by the Helmholtz-Zentrum München Institutional Animal Care and Use Committee. All experimental procedures were approved by and conducted in adherence to the guidelines of the Regierung von Oberbayern.

III.1.2. Animal housing

In normal housing conditions, mice were housed in groups of 3 animals per cage under standard laboratory conditions in IVCs.

For the investigation of the effects of environmental enrichment on postnatal development two additional housing conditions were used. One group was housed in an enriched environment (EE) starting at birth. The second group received an enriched environment starting at 4 weeks and animals were kept in normal housing conditions before.

For EE conditions, mice were housed in larger cages (37 cm x 21 cm x 18 cm) in groups of 5 animals per cage. These cages also contained a Mouse Low Profile Wireless Running WheelR and a custom-made mini step ladder. Furthermore, a metal shelter and wood-wool (5 g) were provided as nesting material.

III.1.3. Mouse lines

The following mouse lines on a C57BL/6 background were used: *Hb9::eGFP* (Wichterle et al., 2002), *Npn1*^{cond} (Gu et al., 2003), *Npn1*$^{Sema-}$ (Gu et al., 2003), *Olig2-Cre* (Dessaud et al., 2007), *Sema3F* (Sahay et al., 2003)

III.1.4. Genotyping

DNA isolation from mouse tails

Instruments

Eppendorf Thermomixer 5436	Eppendorf, Hamburg, Germany
Eppendorf centrifuge 5417R	Eppendorf, Hamburg, Germany

Chemicals

Ethanol absolut for analysis	Merck KGaA, Darmstadt, Germany
Ethylenediaminetetraacetic acid (EDTA)	Sigma-Aldrich, Steinheim, Germany
Proteinase K (100 mg)	Invitrogen, Darmstadt, Germany
Tris-Hydroxy-Methyl-Amino-Methan (Tris)	Carl Roth, Karlsruhe, Germany
Trizma Hydrochloride (HCl)	Sigma-Aldrich, Steinheim, Germany
Sodium chloride (NaCl)	Carl Roth, Karlsruhe, Germany
Sodium dodecylsulfate (SDS) 10%	Invitrogen, Darmstadt, Germany
Sodium hydroxid (NaOH)	Merck KGaA, Darmstadt, Germany

Buffers

Regular prep buffer	10 mM Tris pH8.0
	10 mM NaCl
	10 mM EDTA pH8.0
	0.5% SDS
	filled up with MilliQ-H_2O to 50 ml
1x TE buffer	10 mM Tris-HCl, pH8.0
	1 mM EDTA

1-2 mm of tail tissue was used for genotyping and DNA was isolated by digestion with 100 µl of 50 mM NaOH at 95°C for 30 min. Then, 30 µl of 1 M Tris pH7.0 was added to stabilize the DNA. Subsequently, 1-2 µl of this DNA solution was directly used for PCR.

For genotyping of *Sema3F* mice the DNA had to be purified for PCR. Thus, tails were digested in a shaker overnight at 60°C in 500 µl regular prep buffer with 20 µl Proteinase K (10 mg/ml). The next day 250 µl 5 M NaCl was added and the samples were vigorously shaken for 10 min. After 10 min on ice the samples were centrifuged at low speed (6000 rpm) for 10 min at room temperature. Then, 700 µl of the supernatant were transferred into a new tube and 100 µl 100% EtOH was added and mixed by inverting the tube several times. Afterwards, the samples were centrifuged at high speed (13000 rpm) at 4°C for 25 min. The pelleted DNA was washed in 70% EtOH and centrifuged at high speed (13000 rpm) for 10 min at 4°C. After brief drying, the DNA pellet was resuspended in 50 µl of 1x TE and subsequently used for PCR.

Polymerase chain reaction

Instruments

Labcycler Gradient	SensoQuest, Goettingen, Germany
Mastercycler EP Gradient 5341	Eppendorf, Hamburg, Germany

Buffers and Solutions

Desoxynucleotides (dNTPs)	Fermentas, St.Leon-Rot, Germany
Oligonucleotides	Metabion, Martinsried, Germany
MilliQ-H_2O	Millipore, Schwalbach, Germany
10x Coral Load PCR buffer (CL buffer)	Qiagen, Hilden, Germany
$MgCl_2$ (25 mM)	Qiagen, Hilden, Germany
Q-Solution	Qiagen, Hilden, Germany
Taq DNA Polymerase	Qiagen, Hilden, Germany

10x PCR buffer	Invitrogen, Darmstadt, Germany
5x Betaine	Sigma-Aldrich, Steinheim, Germany
$MgCl_2$ (50 mM)	Invitrogen, Darmstadt, Germany
Taq DNA Polymerase	Invitrogen, Darmstadt, Germany

Primers and amplification parameters

Cre allele

Cre Forward: GTG TCC AAT TTA CTG ACC GTA CAC

Cre Reverse: GAC GAT GAA GCA TGT TTA GCT GG

Reaction batch: 1 µl of DNA

19 µl Mastermix (2 µl 10x CL buffer, 0.2 µl dNTPs, 0.1 µl Primer Cre Forward, 0.1 µl Primer Cre Reverse, 0.25 µl Taq DNA Polymerase (Qiagen), 16.35 µl H_2O)

Amplification parameters: Preheating: T=95°C for 5 min. 30 cycles of Denaturation (T=95°C for 1 min), Annealing (T=59.5°C for 1 min), Extension (T=72°C for 30 s). End: T=72°C for 15 min.

GFP allele

872: AAG TTC ATC TGC ACC ACC G

1416: TCC TTG AAG ATG TGT CG

Reaction batch: 1 µl of DNA

24 µl Mastermix (2.5 µl 10x PCR buffer (Invitrogen), 0.75 µl $MgCl_2$, 5 µl 5x Betaine, 0.25 µl dNTPs, 0.25 µl Primer 872, 0.25 µl Primer 1416, 0.2 µl Taq DNA Polymerase (Invitrogen), 14.8 µl H_2O)

Amplification parameters: Preheating: T=95°C for 3 min. 35 Cycles of Denaturation (T=95°C for 30 s), Annealing (T=60°C for 1 min), Extension (T=72°C for 1 min). End: T=72°C for 15 min.

Npn-1 allele 5'SacI Ex2: AGG CCA ATC AAA GTC CTG AAA GAC AGT CCC

3'SacI: AAA CCC CCT CAA TTG ATG TTA ACA CAG CCC

Reaction batch: 1 µl of DNA

24 µl Mastermix (2.5 µl 10x CL buffer, 4 µl $MgCl_2$, 1 µl dNTPs, 0.028 µl Primer 5'SacI Ex2, 0.028 µl Primer 3'SacI, 0.25 µl Taq DNA Polymerase (Qiagen), 16.19 µl H_2O)

Amplification parameters: Preheating: T=95°C for 3 min. 35 Cycles of Denaturation (T=95°C for 45 s), Annealing (T=63°C for 45 s), Extension (T=72°C for 45 s). End: T=72°C for 5 min.

Sema3F allele Sema3F 3-1: GAA TGC CCG GGT AAA CAC CA

Sema3F 3-2B: TCG AAG CGT ACC CTG GCT CT

Sema3F3-3A: AAG GAG CGC ACA GAG GAC CA

Reaction batch: 1 µl of DNA

24 µl Mastermix (2.5 µl 10x CL buffer, 5 µl Q-Solution, 0.25 µl dNTPs, 0.1 µl Primer Sema3F 3-1, 0.1 µl Primer Sema3F 3-2B, 0.1 µl Primer Sema3F 3-3A, 0.25 µl Taq DNA Polymerase (Qiagen), 15.7 µl H_2O)

Amplification parameters: Preheating: T=94°C for 5 min, 30 Cycles of Denaturation (T=94°C for 1 min), Annealing (T=60°C for 1 min), Extension (T=72°C for 1 min). End: T=72°C for 10 min.

Agarose gel electrophoresis

Instruments

PowerPac Basic Power Supply	Bio-Rad, Munich, Germany
PerfectBlue Gel System Midi S	PEQLAB Biotechnologie, Erlangen, Germany

Chemicals

Agarose	Biozym, Oldendorf, Germany
EDTA	Sigma-Aldrich, Steinheim, Germany
Midori Green Advance	Nippon Genetics Europe, Dueren, Germany
GeneRuler 1 kB DNA ladder	Fermentas, St.Leon-Rot, Germany
Tris-Acetat	Carl Roth, Karlsruhe, Germany

Buffers

1x TAE buffer	40 mM Tris-Acetat 1 mM EDTA, pH 8.0

The size of the amplification products was determined by gel electrophoresis on a 2% agarose gel in 1x TAE buffer with 0.05 µl/ml Midori Green.

III.2. Behavioral analysis

III.2.1. Experimental design

Material	
Individually ventilated cages (IVC)	Biozone Global, Kent, UK
Mini step ladder (10 cm x 5 cm x 5 cm, 19 rungs of 5 mm diameter each)	HMGU Craft services, Munich, Germany
Wood-wool	Abedd, Vienna, Austria
Mouse Low Profile Wireless Running Wheel^{R}	Med Associates Inc, St. Albans, USA

To analyze the effect of EE on motor behavior mice of three different housing groups (normal housing, EE starting at birth and EE starting at 4 weeks) were tested on the horizontal ladder. Behavioral analysis was performed as repetitive testing at the ages of 4, 8 and 12 weeks after birth.

III.2.2. The ladder rung walking test

Material	
Horizontal ladder (74 cm length, 17 cm high walls of plexiglass, 146 metal rungs of 1 mm diameter)	HMGU Craft services, Munich, Germany

Animals were placed on a vertical ladder with irregularly spaced bars and plexiglass walls on both sides. Upon voluntary crossing of the ladder, the time and the number of errors in fore- and hindlimb placement (missing or slipping off) were determined and averaged over 3 consecutive runs.

III.3. Electromyography

III.3.1. Anesthesia

Components	
Ketamine 10%	Bela-Pharm GmbH & Co. KG, Vechta, Germany
Xylazine 2%	CP-pharma GmbH, Burgdorf, Germany

Animals were anesthetized by i.p. injection of Ketamine (0.1 mg/g) and Xylazine (0.01 mg/g). If necessary, anesthesia was supplemented during the experiment. The animals were euthanized before recovering from anesthesia.

III.3.2. EMG recordings

Instruments	
Generation of the Pulse	
Digidata 1440A Digitizer	Molecular devices, Sunnyvale, USA
Isoflex- Flexible stimulus isolator	A.M.P.I, Jerusalem, Israel
Master-8 pulse generator	A.M.P.I, Jerusalem, Israel
Signal detection	
Teflon-insulated multi-stranded stainless steel fine wire	A-M Systems Inc., Sequim, USA
Amplifier P511 DC	Astromed GmbH, Rodgau, Germany
Data analysis	
AxoScope software	Molecular devices, Sunnyvale, USA

The skin covering the *biceps brachii* and *triceps brachii* was opened with a small incision and the muscles were exposed. Then, Teflon isolated fine wire was thread into the end of an injection needle and inserted unilaterally into these muscles in order to detect bipolar EMG signals as

described previously (Pearson *et al.*, 2005). An additional electrode was inserted into the animal's body for grounding. With another small incision the brachial plexus was exposed to gain access to the musculocutaneous nerve. The nerve was stimulated with single bipolar electric pulses (100 μs duration) using custom made stimulation electrodes with 2 hooks (stainless steel, 0.2 mm in diameter with 1 mm in between) and stimulation intensity was increased from 0 to 0.1 mA in 0.05 intervals. EMG signals were detected using the AxoScope software.

III.4. Neuroanatomical analysis

III.4.1. Anesthesia

Components	
Ketamine 10%	Bela-Pharm GmbH & Co. KG, Vechta, Germany
Xylazine 2%	CP-pharma GmbH, Burgdorf, Germany
Meloxicam (Mobic 15 mg/1.5 ml)	Boehringer Ingelheim, Biberach, Germany

Animals were anesthetized by i.p. injection of Ketamine (0.1 mg/g) and Xylazine (0.01 mg/g). Meloxicam (2 μg/g) was added as analgesic.

III.4.2. Retrograde labeling of motor neurons

Material	
Cholera toxin B subunit (CTB) Alexa488- or Alexa555-conjugated (1 mg/ml)	Molecular Probes, Darmstadt, Germany
Borosilicate glass capillaries	World Precision Instruments, Sarasota, Florida, USA

Hamilton syringe (10 µl)	Hamilton GmbH, Höchst, Germany
HistoacrylR	B. Braun AG, Melsungen, Germany
Paraformaldehyde (PFA)	Sigma-Aldrich, Steinheim, Germany

Animals were anesthetized and the skin of the forearm was opened by small incisions to reveal the underlying muscles.

For retrograde labeling of forelimb motor pools CTB conjugates were injected into forelimb muscles (biceps, dorsal or ventral muscles of the lower forelimb) by pressure injection using a 10 µl Hamilton syringe or fine pointed glass capillaries. The injected volume was dependent on the age of the animals.

Age	Volume	Injector	Incubation time
P7	1 µl	glass capillary	2 days
P14	2 µl	glass capillary	3 days
P21	3 µl	Hamilton syringe	3 days
P28	4 µl	Hamilton syringe	3 days
Adult	5 µl	Hamilton syringe	3 days

For retrograde labeling of specific nerves, pectoral muscles were opened to expose the forelimb plexus and 1 µl of the CTB conjugate was injected directly into the nerve using fine pointed glass capillaries.

After injection, the skin was closed with the tissue adhesive Histoacryl^{R} and animals were sacrificed after 2-3 days by transcardial perfusion (5 min 1x PBS, 10 min 4% PFA in PBS).

III.4.3. Preparation of spinal cord tissue

Material	
D (+)-Saccharose (Sucrose)	Merck KGaA, Darmstadt, Germany
Paraformaldehyd (PFA)	Sigma-Aldrich, Steinheim, Germany
Sliding microtome SM2010 R	Leica GmbH, Wetzlar, Germany

The spinal cord was dissected from the spinal column starting at the cervical vertebra C2. The tissue was post-fixed overnight in 4% PFA and incubated in 30% sucrose in PBS for cryoprotection. For analysis 40 μm coronal sections were prepared using a sliding microtome.

III.4.4. Reconstruction of spinal motor pools

Material

Fluorescent microscope Axiovert 200	Zeiss, Jena, Germany
Camera AxioCam HR	Zeiss, Jena, Germany
Image capturing software AxiovisionX.X	Zeiss, Jena, Germany
Reconstruct™ software	(http://synapses.clm.utexas.edu)

Every second section of the spinal cord was used for the reconstruction of the labeled forelimb motor pools. Pictures of the retrogradely labeled motor neurons were taken with a fluorescent microscope and the images of the sections were aligned by the use of 4 optical reference points (the dorsal and ventral edges of the gray commissure, the central canal and the lateral edge of the ventral horn). The motor neurons were then labeled and analyzed with the Reconstruct™ software (Fiala, 2005).

III.4.5. Determination of a scatter index for the expansion of dorsal and ventral motor pools

The physiologically increased diameter of spinal sections at the level of the cervical enlargement was corrected for by post-section alignment. A reference curve was defined for all sections using 5 points on the lateral edge of the spinal cord grey matter. For each individual section the intercept point between the reference curve and the perpendicular to the main (mid-sagittal) symmetry axis through the central canal was calculated. Each section was then separately readjusted after spline interpolation of these intersection points.

A scatter index (SI) as the quantitative readout for the spreading of medial and lateral motor pools was calculated by determining the area of an ellipse fitted to the samples using a method similar to Principal Component Analysis: The covariance matrix of the X- and Y-Coordinates

of the motor neuron traces was computed for both motor pools. Its 2 eigenvectors are perpendicular and represent the major and minor axes of an ellipse centered at the data mean, with width adjusted to the directional standard deviations (in other words the optimal fit of a bivariate correlated Gaussian distribution). By multiplying the product of the 2 eigenvalues with π, we determined the area of the ellipse and thus a single, comparable value - the scatter index $\left[SI = \pi \cdot \prod_{i=1,2} eig_i \left(\mathrm{cov}[x; y] \right) \right]$ is obtained for each motor pool. The values were multiplied by the factor 1000 to reduce decimals.

III.4.6. Immunohistochemistry

Antibodies and Agglutinins

Primary

Rabbit anti-GFP (1:2000)	Life Technologies, Darmstadt, Germany
Goat anti-Hsp-27(1:250)	Santa Cruz Biotechnology, Santa Cruz, USA
Rat anti-MBP (1:250)	Biozol Diagnostica, Eching, Germany
Mouse anti-myosin MY32 (1:400)	Sigma-Aldrich, Steinheim, Germany
Mouse anti-neurofilament 2H3 (1:50)	DSHB, Iowa,USA
Rabbit anti-neurofilament 200 (1:250)	Sigma-Aldrich, Steinheim, Germany
Mouse anti-synaptophysin (1:100)	Sigma-Aldrich, Steinheim, Germany
Rabbit anti-TrkA (1:8000)	kindly provided by L.F. Reichardt
Goat anti-TrkC (1:250)	R&D Systems, Minneapolis, USA
Rabbit anti-vGAT (1:1000)	Synaptic Systems GmbH, Goettingen, Germany
Rabbit anti-vGlut1 (1:1000)	Synaptic Systems GmbH, Goettingen, Germany

Tetramethylrhodamin α-bungarotoxin (1:500)	Life Technologies, Darmstadt, Germany
Wisteria Floribuda Agglutinin (1:250) WFA, biotinylated L-1516	Sigma-Aldrich, Steinheim, Germany
Secondary	
Donkey anti-goat Ax647 (1:250)	Life Technologies, Darmstadt, Germany
Donkey anti-mouse Ax488 (1:250)	Life Technologies, Darmstadt, Germany
Donkey anti-mouse Ax546 (1:250)	Life Technologies, Darmstadt, Germany
Donkey anti-mouse Ax647 (1:250)	Life Technologies, Darmstadt, Germany
Donkey anti-rabbit Ax488 (1:250)	Life Technologies, Darmstadt, Germany
Donkey anti-rabbit Ax546 (1:250)	Life Technologies, Darmstadt, Germany
Donkey anti-rabbit Ax647 (1:250)	Life Technologies, Darmstadt, Germany
Donkey anti-rat Cy3 (1:250)	Jackson IR, Suffolk, UK
Streptavidin Ax488	Life Technologies, Darmstadt, Germany

Buffers

Blocking solution	10% normal horse serum in PBS-T
PBS-T	0.1% TritonX-100 in 1x PBS

Material	
BSA	Sigma-Aldrich, Steinheim, Germany
D (+)-Saccharose (Sucrose)	Merck KGaA, Darmstadt, Germany
Glass cover slips	Carl Roth, Karlsruhe, Germany
Horse serum, heat inactivated	Life Technologies, Darmstadt, Germany
Mowiol mounting medium	Calbiochem, Darmstadt, Germany
Paraformaldehyd (PFA)	Sigma-Aldrich, Steinheim, Germany
Slides SuperFrost Plus	Thermo Fisher Scientific, Bonn, Germany
Slides SuperFrost Plus Gold	Thermo Fisher Scientific, Bonn, Germany
TritonX-100	Sigma-Aldrich, Steinheim, Germany

Tissue sections were washed in PBS (3x 5 min) at room temperature (RT) and afterwards blocked in blocking solution for 30 min. Then, sections were incubated in blocking solution containing the primary antibodies in a humidified chamber overnight at 4°C. The next day, sections were washed in PBS-T (3x 5 min, RT) and secondary antibody was applied in blocking solution for 60 min at room temperature. Afterwards, sections were washed in PBS (3x 5 min) and mounted in Mowiol.

III.4.7. Analysis of neuromuscular junctions

Forelimb muscles were dissected from perfused, adult animals and fixed overnight in 4% PFA. After cryoprotection in 30% sucrose, muscles were cut at 80 µm using a cryostat and stained free floating. After washing in PBS (3x 15 min) the tissue was permeabilized in PBS containing 2% TritonX-100 for 30 min and blocked in blocking solution (4% BSA and 1% TritonX-100 in PBS) for another 30 min. Then sections were incubated with the primary antibodies (mouse anti-synaptophysin (1:100) and mouse anti-neurofilament 2H3 (1:50) overnight at 4°C. The next day, sections were washed (4x 15 min) in PBS and rhodamin-labeled α-bungarotoxin (1:500) was applied in blocking buffer for 30 min. Afterwards, sections

were incubated with the secondary antibody in blocking buffer (donkey anti-mouse Ax488, 1:250) for 2 h. After the final washing steps in PBS (3x 15 min) sections were mounted in Mowiol and analyzed using a confocal microscope. For the analysis the surface areas of at least 100 neuromuscular junctions were measured for each animal.

III.4.8. Nerve fiber analysis

Material

Definiens Enterprise Image Intelligence Suite software	Definiens, Munich, Germany
Laser scanning microscope LSM510 META	Carl Zeiss Microscopy, Jena, Germany

Nerves were dissected just distally from the plexus and fixed in 4% PFA overnight at 4°C. After dehydration in 30% sucrose nerves were cross sectioned at 12 µm and stained with antibodies against myelin basic protein (rat anti-MBP), neurofilament (mouse anti-neurofilament 2H3) and Hb9-GFP (rabbit anti-GFP). Cross sections were captured with a confocal laser scanning microscope.

The individual pictures were then analyzed with Definiens Enterprise Image Intelligence Suite software. The region of interest was defined and the size of nerve cross section was determined. Motor and sensory fibers were counted automatically using the softwares algorithm-based rule sets to identify and further refine pixel clusters referred to as image objects. Thus, single axon fibers and their surrounding myelin sheath were identified from background structures based on their staining intensity, size, shape and neighborhood. For each nerve the mean of at least 4 cross sections was used for analysis.

III.4.9. Analysis of excitatory and inhibitory synapses

Ventral muscles of the lower forelimb were retrogradely labeled with CTB-Ax555 as described above. Consecutive spinal cord sections were stained for vGAT and vGlut1 and motor neurons were captured using a confocal laser scanning microscope (LSM510 Meta, Zeiss). At the central level of each motor neuron the area of the cell body was measured using ImageJ software. In this area, additionally, the number and size of labeled synapses was measured.

III.5. Statistical evaluation

Results were calculated as means ± SEM and tested for normal distribution using GraphPad Prism 5.0 software. If data values followed normal distribution, differences of statistical significance were determined with the Student's *t*-test. For data with significant differences in their variances the Welch's correction was applied. If data values were not normally distributed the Mann-Whitney test was used. Analysis of significant differences between more than two groups was performed using the one-way ANOVA. P-values below 0.05 were considered as statistically significant. * $p < 0.05$, ** $p < 0.01$, *** $p < 0.001$.

IV. RESULTS

IV.1. Loss of Npn1 from motor neurons causes postnatal deficits independent from Sema3A signaling

Sema3A-Npn1 signaling plays an essential role in the development of the peripheral nervous system. Accordingly, the specific ablation of Npn1 from motor neurons leads to severe deficits in motor axon fasciculation. In these mutants also the dorsal-ventral pathfinding of motor axons is affected and the most advanced defasciculated motor projections hardly reach the distal forelimb (Huettl *et al.*, 2011). In a former study by Huber et al., (2005) *Npn1*$^{Sema-}$ mice were investigated, in which the semaphorin binding site of the Npn1 receptor is mutated in the entire organism: also here motor axons were defasciculated within the plexus even though individual nerve branches were still found in a roughly correct position distal to the plexus. Nevertheless, retrograde tracing from the ventral forelimb musculature also revealed dorsal-ventral pathfinding deficits of Npn1 expressing motor neurons. Additionally, these mice displayed deficits in sensory axon fasciculation and a precocious ingrowth of both, motor and sensory axons, into the limb (Huber *et al.*, 2005). Interestingly, these defects are maintained in late embryonic stages where deficits became also evident in the sciatic and intercostal nerves (Haupt *et al.*, 2010).

In this respect, the importance of Sema3A-Npn1 signaling for the embryonic development of the peripheral nervous system has been investigated intensively, however, the resulting consequences on postnatal development did not receive the same attention. Therefore, in a previous study from our lab, Heidi Soellner investigated postnatal *Olig2-Cre;Npn1*^{cond} mice, where the axon guidance receptor Npn1 is specifically deleted from all motor neurons. She found that these animals display an atypical forelimb posturing already at birth that is accompanied by muscular atrophy of extensor muscles in the affected forelimbs and a dysfunctional innervation of the forelimb by the *N. radial.* Furthermore, these animals suffer from bone malformation as a consequence of permanent biomechanical misuse. Interestingly, *Npn1*$^{Sema-}$ mutants, which show similar axon pathfinding deficits and defasciculation of motor axons in the embryonic state, are not equally affected after birth and reveal none of the anatomical impairments (Soellner, 2012; Helmbrecht *et al.*, 2015a). Thus, the dissertation described the postnatal phenotype of *Olig2-Cre*$^{+}$*;Npn1*^{cond} mutants in detail, however, in order

to fully understand the underlying reasons for their severe posturing deficit further examination of the mouse line remained necessary. For this reason, we investigated the forelimb innervation of *Olig2-Cre;Npn1*^{cond} mice by analysis of motor and sensory axons in dorsally and ventrally projecting forelimb nerves and retrograde tracings of motor neurons from these nerves in the brachial plexus. Moreover, since *Npn1*$^{Sema-}$ mutants do not show any phenotypic alterations even though also in these animals axonal pathfinding is affected in the embryonic stage, I compared both mouse lines in order to investigate to which extent embryonic deficits in the nervous system can be compensated.

IV.1.1. Postnatal weight development is affected in *Olig2-Cre*$^{+}$*;Npn1*^{cond} and *Npn1*$^{Sema-}$ mutants

Previous results from our lab show that starting at postnatal day four, *Olig2-Cre*$^{+}$*;Npn1*^{cond} mutants reveal growth retardation and a decreased weight when compared to control littermates (Soellner, 2012; Helmbrecht *et al.*, 2015a). In order to assess the differences in postnatal development between *Olig2-Cre*$^{+}$*;Npn1*^{cond} and *Npn1*$^{Sema-}$ mutants, I first investigated if this parameter of general health is affected differentially in both mouse lines. Interestingly, I found that also *Npn1*$^{Sema-}$ mutants show deficits in weight development within the first 3 postnatal weeks. Here, mutants are significantly lighter starting already 3 days after birth and this defect becomes even more pronounced during postnatal development (Figure 7).

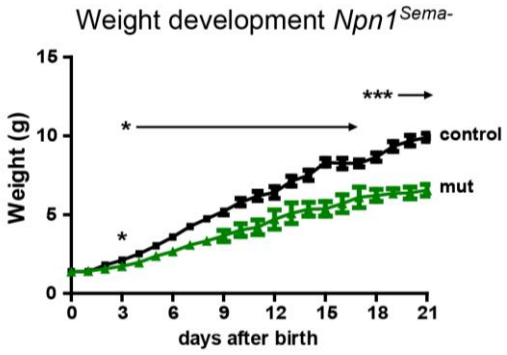

Figure 7: Postnatal weight development of *Npn1*$^{Sema-}$ animals

Starting at day 3 after birth, *Npn1*$^{Sema-}$mutants show a significantly decreased weight compared to wt littermates (2.11 ± 0.06 g, n = 7 vs. 1.73 ± 0.13 g, n = 4, $p < 0.02$). With increasing age this effect becomes stronger (P18: 8.66 ± 0.26 g, n = 10 vs. 6.23 ± 0.38 g, n = 4, $p < 0.001$).

Thus, our results show that weight development is affected in both mouse lines and can therefore not explain the phenotypic differences between *Olig2-Cre^{+};Npn1^{cond}* and *Npn1^{Sema-}* mutants. Hence, a more detailed analysis of anatomical factors is needed in order to assess this question.

IV.1.2. *Olig2-Cre^{+};Npn1^{cond}* mutants reveal a loss of motor axons in the *N. radial* that causes alterations in nerve composition

Dysfunctional Sema3A-Npn1 signaling causes severe deficits in motor axon pathfinding and fasciculation during embryonic development. Furthermore, *Olig2-Cre^{+};Npn1^{cond}* mutants show an abnormal functionality of muscle innervation in the *N. radial* that might be responsible for the atrophy of forelimb extensors and cause the posturing phenotype in these animals. In contrast, *Npn1^{Sema-}* mutants did not show the same defects. Therefore, we analyzed the composition of the brachial nerves in postnatal animals of both lines in order to reveal if differences in the peripheral nervous system are responsible for these differences.

Previous data from ultra-structural analysis of the brachial nerves showed that in *Olig2-Cre^{+};Npn1^{cond}* mutants the *N. radial* contains a decreased number of large diameter axons, while nerves from *Npn1^{Sema-}* mutants were not affected (Soellner, 2012; Helmbrecht *et al.*, 2015a). This reduction may be caused by two different mechanisms: (1) The decreased number of large diameter neurons is a result of the loss of motor axons that did not reach their target muscle and died due to a lack of trophic support (Hollyday & Hamburger, 1976; Gould & Enomoto, 2009); or (2) The number of motor axons is still unchanged, however, these axons have a reduced diameter due to alterations in the neurofilament network (Perrot *et al.*, 2008).

IV.1.2.1. Expression of Hb9::GFP during postnatal development

In order to investigate which of the two mechanisms is responsible for the described effect, I crossed both mouse lines with a line that expresses the genetic marker *Hb9::eGFP*. In these animals motor neurons and their axons are labeled by the expression of GFP (Wichterle *et al.*, 2002), which allows for the discrimination between sensory and motor axons within the same nerve. However, since Hb9 is expressed in motor neurons only during embryonic development, I first needed to establish that GFP expression is maintained in postnatal motor

neurons. For this reason, I quantified the number of GFP-labeled motor neurons in the brachial spinal cord of both mouse lines. Additionally, I used an alternative marker to count motor neurons independently of *Hb9::eGFP* expression. For this purpose the 27-kDa heat shock protein was used, since it shows a constitutive expression pattern in almost all motor neurons of the ventral horn (Plumier *et al.*, 1997). Upon quantification of both markers (Figure 8A) no significant differences were found between the total number of motor neurons in the brachial spinal cord of mutant and control animals or between the two mouse lines (Figure 8B and C). Furthermore, the number of Hsp-27 positive cells is slightly lower compared to the numbers of GFP expressing motor neurons. Since most but not all motor neurons express Hsp27, this suggests that the expression pattern of *Hb9::GFP* is not affected in the postnatal spinal cord of *Olig2-Cre*$^{+}$*;Npn1*^{cond} and *Npn1*$^{Sema-}$mutants.

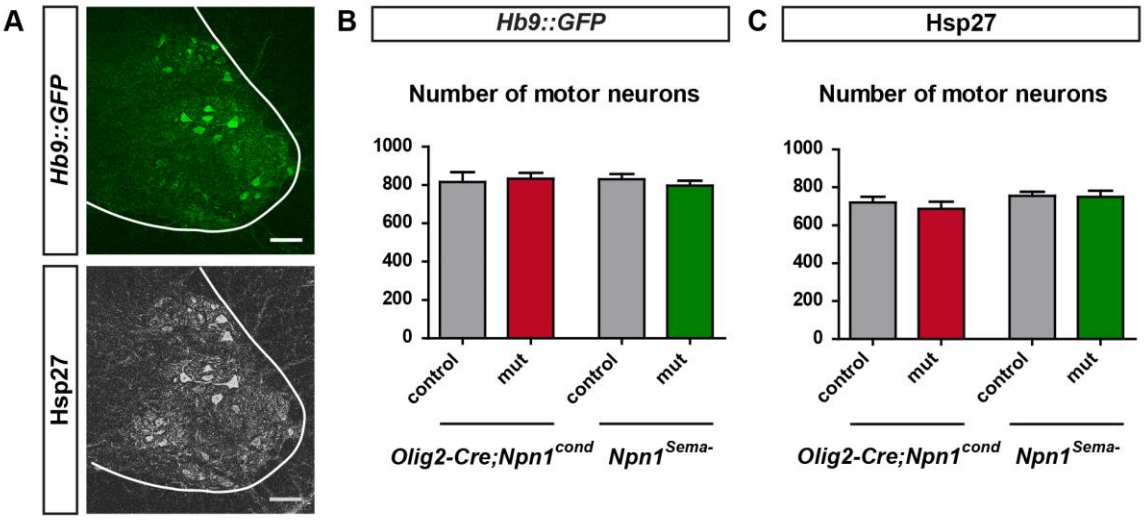

Figure 8: Total number of motor neurons in Npn1 deficient animals

(A) Motor neurons of the brachial spinal cord labeled by the expression of *Hb9::GFP* and *Hsp27*. **(B)** At the age of 6 weeks, the total number of GFP^{+} motor neurons in the spinal cord of *Olig2-Cre;Npn1*^{cond} and *Npn1*$^{Sema-}$ mice is not significantly different between groups (*Olig2-Cre;Npn1*^{cond}: 816.6 ± 51.03, n = 5 vs. 834.0 ± 28.92, n = 3, p = 0.82; *Npn1*$^{Sema-}$: 830.8 ± 26.85, n = 4 vs. 796.8 ± 26.55, n = 4, p = 0.40). **(C)** The total number of Hsp27^{+} motor neurons shows no significant alterations between controls and mutants of the investigated lines (*Olig2-Cre;Npn1*^{cond}: 720.0 ± 31.56, n = 5 vs. 687.0 ± 36.86, n = 3, p = 0.53; *Npn1*$^{Sema-}$: 754.8 ± 21.29, n = 5 vs. 749.8 ± 31.32, n = 5, p = 0.90).

IV.1.2.2. Analysis of the axonal composition of brachial nerves in Olig2-Cre;Npn1^{cond};Hb9::eGFP^{+} mice

Since *Hb9::GFP* is still expressed in postnatal motor neurons of *Olig2-Cre^{+};Npn1$^{cond-/-}$;Hb9::eGFP^{+}* mutants this line was used to investigate to which extent motor axons in the brachial nerves are affected. Therefore, I dissected the *N. radial* from the brachial plexus of these animals and analyzed the axonal composition. Motor and sensory axons in the brachial nerves of *Olig2-Cre;Npn1^{cond};Hb9::eGFP^{+}* mice were identified on cross sections of the nerve by immunohistochemical staining against GFP and neurofilament, respectively, and quantified by use of the Definens software. The results showed that in the *N. radial* the total number of motor and sensory axons was decreased (Figure 9A and B). Furthermore, in *Olig2-Cre^{+};Npn1$^{cond-/-}$;Hb9::eGFP^{+}* mutants a highly significant decrease of 53.6% for the size of the *N. radial* became evident (Figure 9C). For this reason, the normalization of the total number of axons with the nerve area was necessary, which revealed a significant reduction in the proportion of motor axons and an increase in the relative amount of sensory axons per μm^2 (Figure 9D).

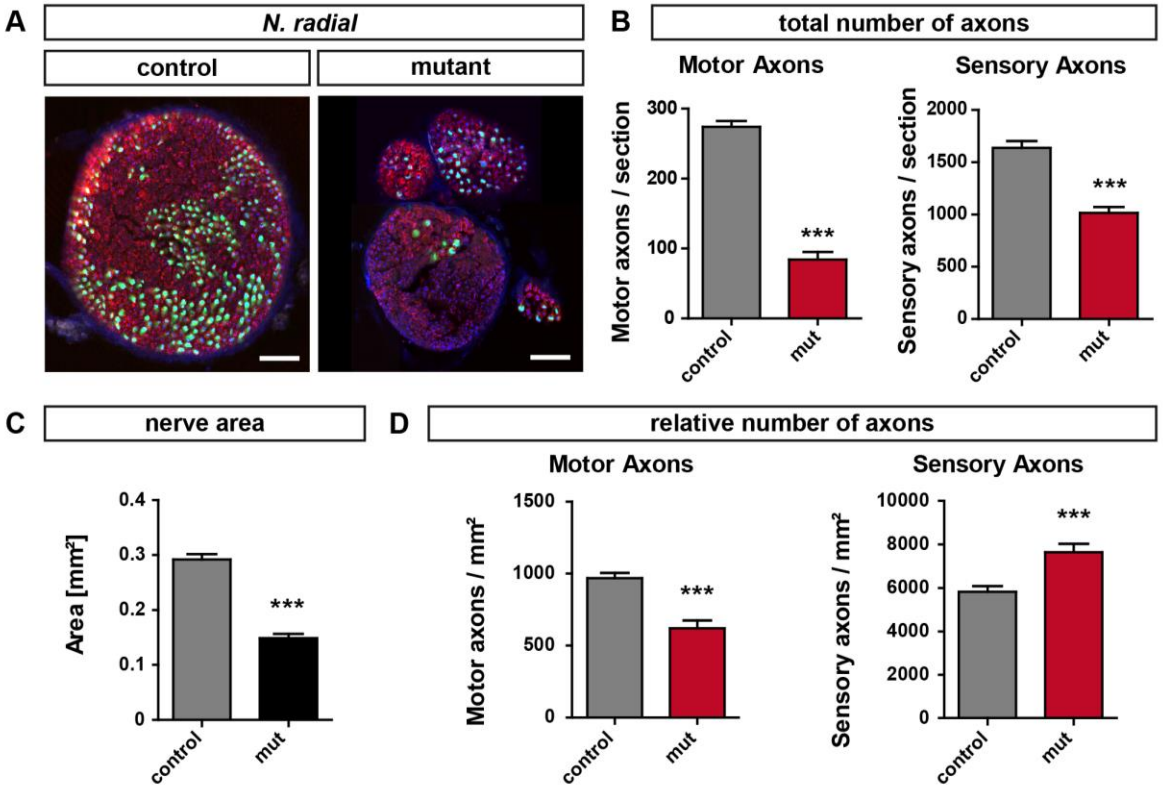

Figure 9: *N. radial* reveals alterations in nerve composition in *Olig2-Cre;Npn1^{cond}* mice

(A) Cross section of the radial nerve from *Olig2-Cre;Npn1^{cond};Hb9::eGFP*$^{+}$ animals after immunohistological staining against myelin basic protein (red), neurofilament (blue) and GFP (green). **(B)** Total numbers of motor (274.1 ± 8.3, n = 47 vs. 81.50 ± 7.580, n = 42; $p < 0.001$) and sensory axons (1638 ± 65.5, n = 47 vs. 1044 ± 46.49, n = 42, $p < 0.001$) are reduced in *Olig2-Cre*$^{+}$*;Npn1^{cond}* mutants when compared to controls. **(C)** Analysis of the *N. radial* of *Olig2-Cre;Npn1^{cond};Hb9::eGFP*$^{+}$ animals reveals a significant reduction in the size of the radial nerve in mutants compared to their littermate controls (0.292 ± 0.01 mm², n = 47 vs. 0.153 ± 0.012 mm², n = 42, $p < 0.001$). **(D)** The relative number of GFP^{+} motor axons in the radial nerve of mutants is decreased compared to their littermate controls (967.5 ± 36.42 1/mm², n = 47 vs. 565.7 ± 52.88 1/mm², n = 42, $p < 0.001$). In these nerves the relative number of sensory axons is significantly increased (5817 ± 259.6 1/mm²,, n = 47 vs. 7501 ± 394.8 1/mm², n = 42, $p < 0.001$). Scale bars: 50 μm.

Since in *Olig2-Cre*$^{+}$*;Npn1^{cond}* mutants only the dorsal side of the forelimb is affected, it was interesting to investigate if the *N. median*, which innervates the forelimb flexors, is affected in the same way (Figure 10A). Indeed, analysis of the *N. median* revealed that also in this nerve the total number of motor and sensory axons was significantly reduced (Figure 10B). Furthermore, also in this nerve the cross-sectional area was reduced by 33.8% in *Olig2-Cre*$^{+}$*;Npn1$^{cond-/-}$;Hb9::eGFP*$^{+}$ mutants when compared to control littermates (Figure 10C). However, in contrast to the *N. radial*, the relative composition of the *N. median* after normalization with the nerve area was not altered (Figure 10D).

These results show that both nerves, *N. median* and *N. radial,* have a reduced cross-sectional area. In contrast, the relative axonal composition of the *N. median* is unchanged, while the *N. radial* reveals a decreased proportion of motor axons and an increase in the relative number of sensory axons. These data are consistent with the previous ultra-structural analysis (Soellner, 2012; Helmbrecht *et al.*, 2015a) and suggest that the reduction of large diameter axons in the *N. radial* of *Olig2-Cre*$^{+}$*;Npn1^{cond}* mutants is not caused by reduction in axon diameter, but by a loss of motor axons in this nerve.

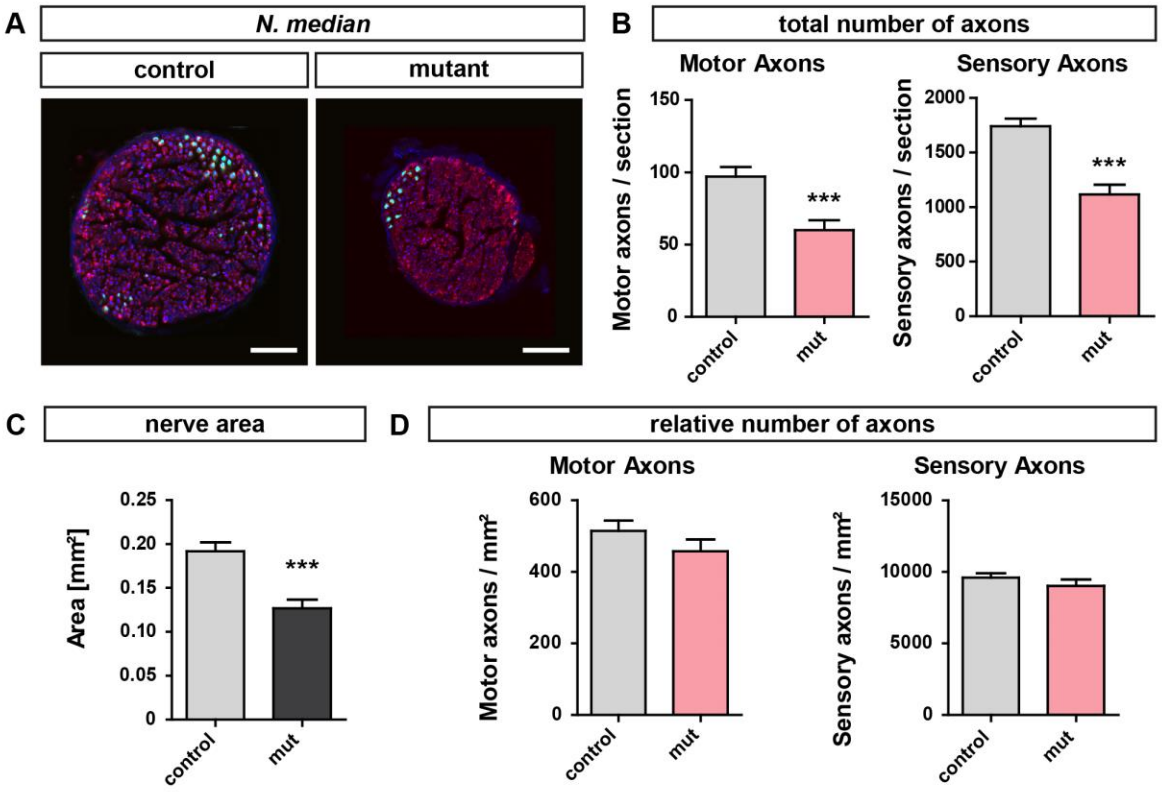

Figure 10: Composition of the *N. median* is not affected in *Olig2-Cre;Npn1^{cond}* mice

(A) Cross section of the *N. median* from *Olig2-Cre;Npn1^{cond};Hb9::eGFP^{+}* animals after immunohistological staining against myelin basic protein (red), neurofilament (blue) and GFP (green). **(B)** Quantification reveals a reduction in the total numbers of motor (97.1 ± 6.6, n = 44 vs. 57.43 ± 5.065, n = 42; $p < 0.001$) and sensory axons (1743 ± 68.2, n = 44 vs. 1156 ± 76.08, n = 42, $p < 0.001$) in *Olig2-Cre^{+};Npn1^{cond}* mutants when compared to controls. **(C)** Also the cross-sectional area of the nerve is reduced in *Olig2-Cre^{+};Npn1^{cond}* mutants (0.192 ± 0.01 mm², n = 44 vs. 0.124 ± 0.007 mm², n = 42, $p < 0.001$). **(D)** However, normalization of axon number with the nerve area shows that the relative number of axons in the median nerve is unchanged (motor axons: 514.9 ± 28.42 1/mm², n = 44 vs. 451.4 ± 31.64 1/mm², n = 42, $p = 0.14$; sensory axons: 9599 ± 301.5 1/mm², n = 44 vs. 9654 ± 398.0 1/mm², n = 42, $p = 0.68$). Scale bars: 50 μm.

IV.1.2.2a) Flexors of the forepaw are unaffected in Olig2-Cre^{+};Npn1^{cond} mutants

Analysis of the *N. median* in *Olig2-Cre;Npn1^{cond}* mice revealed a significant reduction of the nerve size for mutants when compared to control littermates (Figure 10C). This was a surprising result, since the forelimb flexors are not affected in *Olig2-Cre^{+};Npn1$^{cond-/-}$;Hb9::eGFP^{+}* mutants. Therefore, I used immunohistochemical stainings against myosin and neurofilament

in P0 animals to investigate if a defect in more distal flexor muscles is responsible for the described difference in the nerve size (Figure 11A).

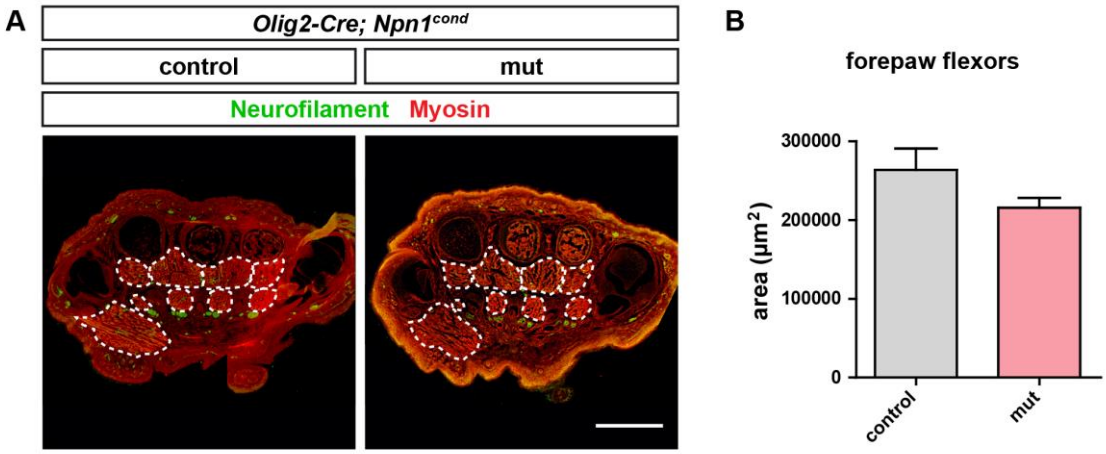

Figure 11: Forepaw flexors are not degenerated in *Olig2-Cre⁺;Npn1cond* mutants

(A) Immunohistochemical staining for myosin (red) and neurofilament (green) in 20 µm sections of the forepaws. **(B)** In *Olig2-Cre⁺;Npn1cond* mutants the total size of the forepaw flexors is not significantly reduced when compared to control littermates (264000 ± 27040 µm², n = 4 vs. 215800 ± 12430 µm², n = 6; p = 0.106). Scale bar: 50 µm.

In *Olig2-Cre⁺;Npn1cond* mutants, the overall size of the forepaw flexor musculature was not significantly affected when compared to paws of control littermates (Figure 11B). This suggests that the clear reduction in size of the *N. median* is not caused by muscular atrophy of the forelimb flexors.

IV.1.2.2b) Reduction of sensory axons in the N. radial of Olig2-Cre⁺;Npn1cond mutants is not caused by a loss of sensory neurons

Investigation of the axon composition in the *N. radial* revealed that the number of motor axons was decreased in *Olig2-Cre⁺;Npn1cond* mutants which correlates with the described posturing deficits in affected limbs. Intriguingly, also the total number of sensory axons was significantly reduced (Figure 12A and Figure 9B). Therefore, we asked if this effect is caused by a specific loss of proprioceptive sensory neurons due to the atrophy of extensor muscles,

or if the effect is a result from the overall reduction of nerve size in those mutants. In order to answer this question I investigated if the composition of sensory neurons in DRG at the brachial level of the spinal cord was affected (Figure 12B).

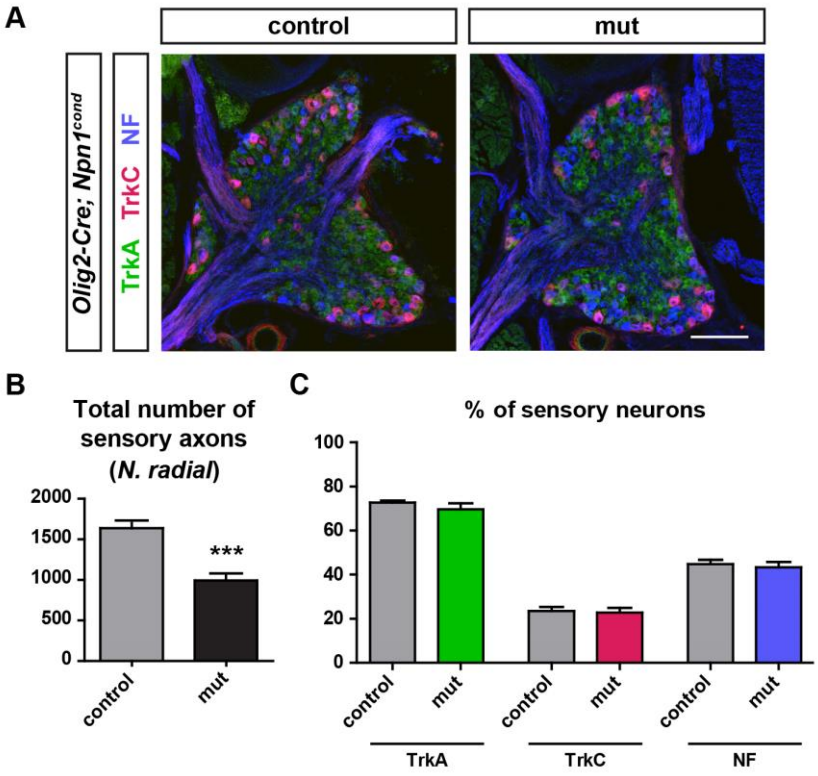

Figure 12: Composition of sensory neurons in the brachial DRGs of *Olig2-Cre⁺;Npn1^{cond}* mutants

(A) Immunohistological staining of sensory neurons in the DRGs of *Olig2-Cre;Npn1^{cond}* mice. **(B)** At P0, the total number of sensory axons is significantly reduced in the *N. radial* of *Olig2-Cre⁺;Npn1^{cond}* mutants (1638 ± 65.5, n = 7, vs. 992.6 ± 57.3, n = 5, $p < 0.001$) **(C)** The proportion of TrkA⁺ (72.63 ± 1.03% vs. 69.59 ± 2.75%, $p = 0.359$, n = 3), TrkC⁺ (23.51 ± 1.85% vs. 22.76 ± 2.14%, $p = 0.804$, n = 3) and NF⁺ (44.82 ± 1.86, $p = 0.654$, n = 3) sensory neurons are not significantly altered in *Olig2-Cre⁺;Npn1^{cond}* mutants compared to their littermate controls. Scale bar: 100 µm.

The proportion of sensory neuron types in the DRG of *Olig2-Cre⁺;Npn1^{cond}* mutants was not significantly altered in comparison to control littermates (Figure 12C). This result suggests that the reduction in the total number of sensory axons in the *N. radial* is not caused by functional deficits in sensory innervation.

IV.1.2.3. Correlation of N. radial composition with the severity of posturing deficits

In *Olig2-Cre*$^{+}$*;Npn1*^{cond} mutants the severity of the forelimb posturing deficits is very variable between individual animals and also within the same animal both forelimbs may be affected to different extents. This raised the question whether the composition of the *N. radial* correlates with the severity of the posturing phenotype in *Olig2-Cre*$^{+}$*;Npn1*^{cond} mutants. Therefore, we investigated the composition of the *N. radial* from mutant limbs that did not exhibit an obvious limb posture phenotype (mut (0)) and compared the data to the previously described results from mutants with a strong posturing deficit and their control littermates.

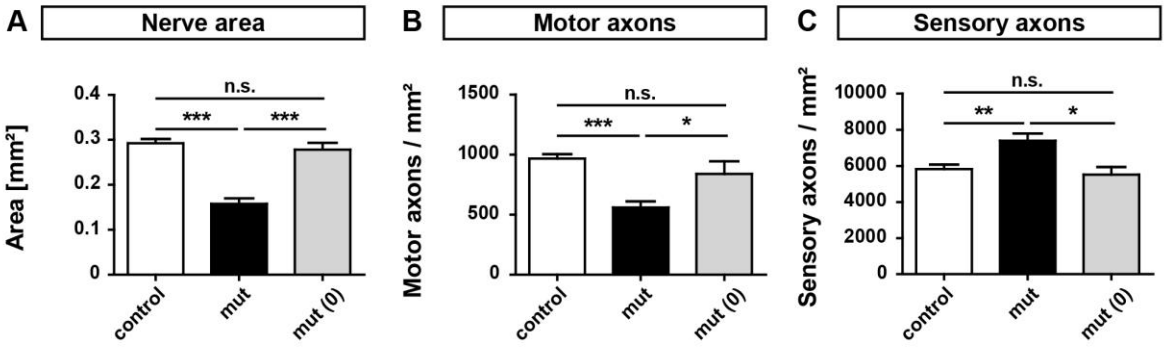

Figure 13: Nerve composition of the *N. radial* in *Olig2-Cre;Npn1*^{cond} mice correlates with the severity of the posturing phenotype

(A) The area of the *N. radial* correlates directly with the severity of the forelimb posturing deficits. Nerves of unaffected limbs (mut(0)) and control nerves are comparable in size (0.292 ± 0.010 mm², n = 47 (control) vs. 0.278 ± 0.015 mm², n = 8 (mut(0)); p = 0.66). In contrast, affected limbs show a significantly smaller nerve area (0.153 ± 0.012 mm², n = 42; mut vs. control: p < 0.0001; mut vs. mut(0): p < 0.0001). **(B)** The relative number of motor axons in nerves of affected limbs is significantly lower than in nerves of control littermates (967.5 ± 36.42 1/mm², n = 47 vs. 565.7 ± 52.88 1/mm², n = 42; p < 0.0001) or animals with no obvious limb posturing deficit 841.1 ± 104.7 1/mm², n = 8, p = 0.040). Between unaffected limbs and controls no difference in the proportion of motor axons was found for the *N. radial* (p = 0.19). **(C)** Correspondingly, the normalized number of sensory axons shows a similar picture with no differences between the nerves of unaffected limbs and controls (5817 ± 259.6 1/mm², n = 47 vs. 5517 ± 418.7 1/mm², n = 8, p = 0.41) and significantly increased numbers in affected limbs (7501 ± 394.8 1/mm², n = 42; mut vs. control: p = 0.007; mut vs. mut(0): p = 0.035).

Interestingly, our data reveal that while affected limbs show a reduced size of the *N. radial*, in unaffected limbs the area of the *N. radial* is not reduced when compared to nerves of control littermates (Figure 13A). Furthermore, we found that in unaffected forelimbs the relative number of motor axons in the *N. radial* is at comparable levels as in controls and significantly higher when compared to limbs in which posturing deficits are evident. (Figure 13B). Correspondingly, also the relative number of sensory axons in the *N. radial* in unaffected limbs shows no significant difference when compared to controls. In contrast, the relative number of sensory axons in affected limbs of *Olig2-Cre*$^{+}$*;Npn1*^{cond} mutants is significantly higher (Figure 13C). Thus, our results suggest that the composition of the *N. radial* correlates with the degree of the posturing deficit in *Olig2-Cre*$^{+}$*;Npn1*^{cond} mutants.

IV.1.3. Composition of the brachial nerves in *Npn1*$^{Sema-}$ mutants is unchanged

Our data demonstrate that defects in embryonic axon pathfinding caused by removal of Npn1 from motor neurons may have functional consequences even in adulthood. But also in *Npn1*$^{Sema-}$ mutants axon pathfinding is affected in the embryonic stage. Here, mutants show dorsal-ventral pathfinding deficits of motor axons, defasciculation of both motor and sensory axons in the brachial plexus, and precocious ingrowth of axons into the limb (Huber *et al.*, 2005). Nevertheless, after birth the innervation of forelimb extensors is not affected in the same way as it was shown for *Olig2-Cre*$^{+}$*;Npn1*^{cond} mutants and *Npn1*$^{Sema-}$ mutants do not exhibit a wrist drop phenotype (Soellner, 2012; Helmbrecht *et al.*, 2015a). For this reason, I investigated if the described disparities can be explained by differences in the nerve composition of the *N. radial* (Figure 14A). Indeed, in contrast to *Olig2-Cre*$^{+}$*;Npn1*^{cond}*;Hb9::eGFP*$^{+}$ mutants, the size of the *N. radial* was not affected in *Npn1*$^{Sema-}$*;Hb9::eGFP*$^{+}$ mutants and also the composition of motor and sensory axons was comparable between mutants and their control littermates (Figure 14B).

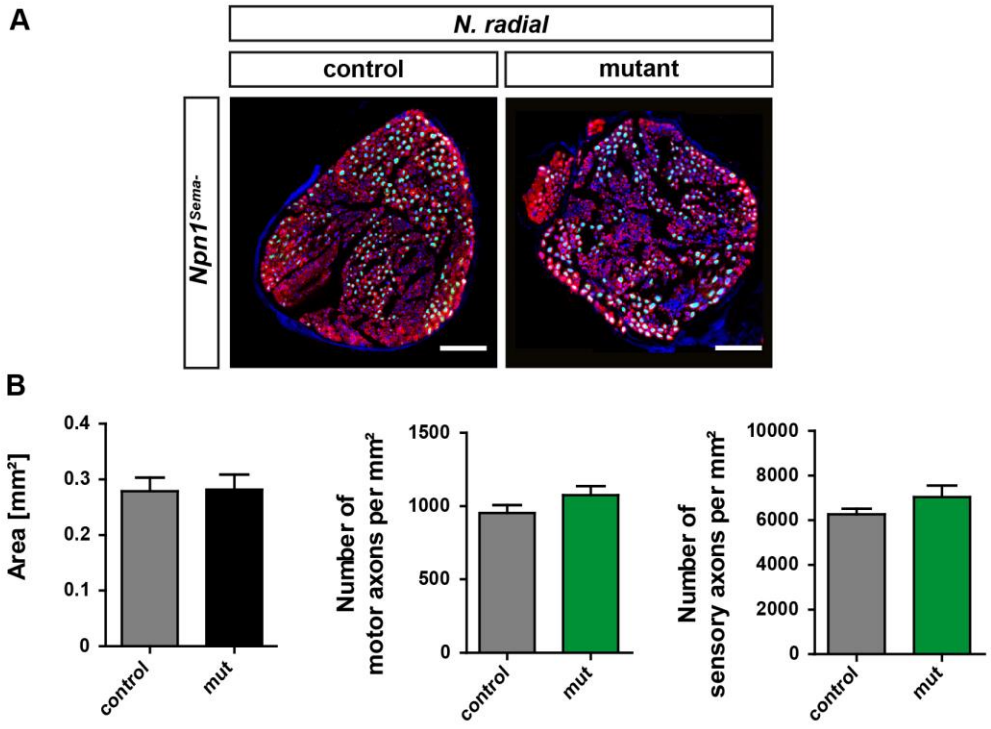

Figure 14: Composition of the *N. radial* of *Npn1*$^{Sema-}$ animals

(A) Immunohistochemical staining against myelin basic protein (red), neurofilament (blue) and GFP (green) on cross section of the *N. radial* from *Npn1*$^{Sema-}$*;Hb9::eGFP*$^{+}$ animals. **(B)** In *Npn1*$^{Sema-}$ mutants the size of the radial nerve shows no significant difference when compared to controls (0.279 ± 0.024 mm², n = 10 vs. 0.281 ± 0.027 mm², n = 11, p = 0.92). Also, the relative numbers of motor axons (919.6 ± 54.28 1/mm², n = 10 vs. 1074 ± 62.61 1/mm², n = 11, p = 0.07) and sensory axons (6270 ± 244.5 1/mm², n = 10 vs. 7033 ± 522.0 1/mm², n = 11, p = 0.28) remain unchanged when compared to littermate controls. Scale bars: 50 μm.

These data indicate that the axonal integrity of the *N. radial* might be important for the functional innervation of the forelimb extensor muscles and alterations in the nerve composition might explain the differences in forelimb posture between mutants of the lines *Olig2-Cre*$^{+}$*;Npn1*^{cond} and *Npn1*$^{Sema-}$.

IV.1.4. Retrograde tracings corroborate the results from nerve analyses in *Olig2-Cre^{+};Npn1^{cond}* and *Npn1^{Sema-}* mutants

Analysis of the brachial nerves in *Olig2-Cre;Npn1^{cond}* and *Npn1^{Sema-}* mice revealed a connection between the axonal composition of the brachial nerves and the limb posturing phenotype. However, these results depend on the expression of the genetic marker *Hb9::eGFP* which is known to be expressed during embryonic development. Even though the expression pattern of this marker seems to be not affected in postnatal animals, we used an additional, *Hb9::eGFP*-independent, approach to confirm that the number of axons projecting to the forelimb extensors is reduced in *Olig2-Cre^{+};Npn1^{cond}* mutants. For this purpose, I injected the retrograde tracer CTB-Ax555 directly into the *N. radial* and *N. median* at the brachial plexus and determined the number of retrogradely labeled motor neurons 3 days later (Figure 15A). After injection into the *N. radial*, the number of retrogradely labeled motor neurons was decreased by 24% in *Olig2-Cre^{+};Npn1^{cond}* mutants when compared to control littermates. In contrast, after injections into the *N. median* the number of traced motor neurons was not significantly reduced (Figure 15B). No significant differences were observed in *Npn1^{Sema-}* mutants (Figure 15C), thereby fully corroborating our results of the nerve composition analyses.

Hence, our results show that in affected limbs of *Olig2-Cre^{+};Npn1^{cond}* mutants the number of motor axons innervating the forelimb extensors is significantly reduced while in the *N. median* or in nerves from unaffected limbs no changes in motor innervation are observed. Analysis of *Npn1^{Sema-}* mutants corroborates these results, since these animals do not show the wrist drop phenotype and no differences in the axonal composition are evident. These results indicate that the development of a claw-paw phenotype in animals which lack the axon guidance receptor Npn1 in all somatic motor neurons, correlates inversely with the axonal integrity of their brachial nerves.

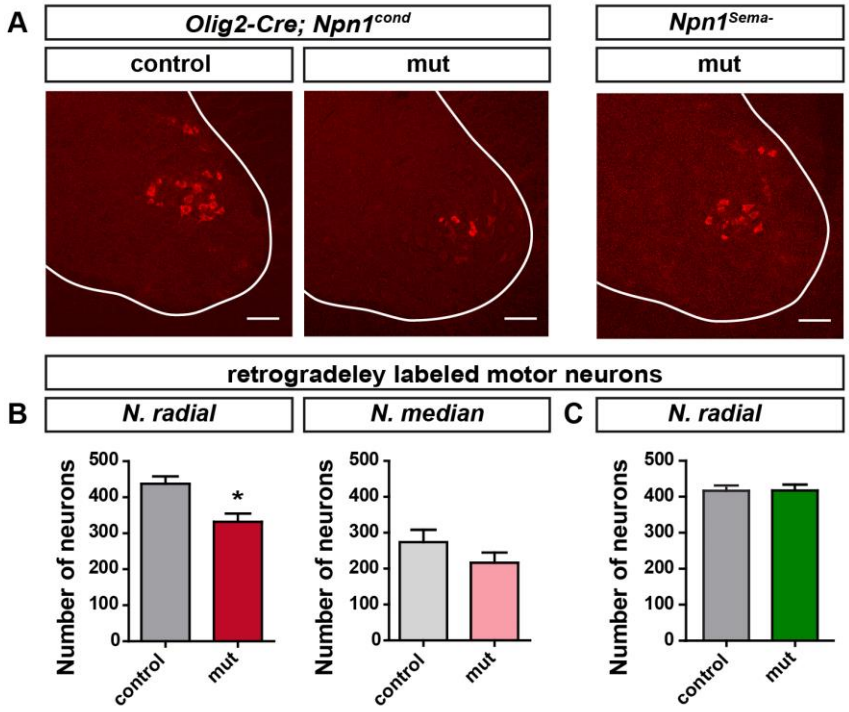

Figure 15: Retrograde labeling of motor neurons reveals alterations in the number of motor neurons innervating the dorsal forelimb of *Olig2-Cre^{+};Npn1^{cond}* mutants

(A) Retrogradely labeled motor neurons after injection of CTB-Ax555 into the radial nerve of *Olig2-Cre;Npn1^{cond}* and *Npn1^{Sema-}* animals at the age of 6 weeks. **(B)** The number of retrogradely traced motor neurons from the radial nerve is significantly lower than in littermate controls (437.3 ± 20.85 vs. 331.3 ± 23.62, n = 3, $p < 0.05$), while no significant changes are evident after retrograde tracing from the median nerve (280.7 ± 34.07 vs. 217.0 ± 21.57, n = 3, $p = 0.19$). **(C)** Tracer injection into the radial nerve of *Npn1^{Sema-}* mutants does not reveal any changes of the number of retrogradely labeled motor neurons in comparison to their littermate controls (416.5 ± 7.64, n = 4 vs. 417.3 ± 16.15, n = 3; $p = 0.96$). Scale bars: 100 μm.

In conclusion, we showed that the loss of Npn1 from motor neurons causes severe deficits in forepaw posture that is caused by alterations in the composition of the *N. radial* and cause deficits in the innervation of the forelimb extensors. Furthermore, we found that the sensory system of the forelimb is not affected since the composition of the brachial DRG is unchanged and the reduced size of the *N. median* is a consequence of muscle atrophy in the forearm flexors. These deficits are, however, not exclusively caused by the loss of Sema3A-Npn1 signaling, since *Npn1^{Sema-}* mutants are not affected to the same extent.

IV.2. A critical period for postnatal plasticity in a model of embryonic axon miswiring

After birth, neuronal circuits are generally considered as "hard-wired", because injury or degeneration cannot be compensated and result in permanent damage. However, since the early work of Hubel and Wiesel there is evidence for activity-dependent plastic rearrangements in the central nervous system that are caused by external stimulation (Wiesel & Hubel, 1963a). Indeed, we also found evidence for adaptive plasticity that is induced by enriched environment housing in the spinal cord of *Sema3F* knock-out mice which display severe axon wiring defects of ventrally projecting motor axons in the brachial spinal cord (Soellner, 2012; Helmbrecht *et al.*, 2015b (accepted)). Intriguingly, it has already been shown for many different neuronal circuits that adaptive plasticity is restricted to specific critical periods during early postnatal development (Berardi *et al.*, 2003; Hensch, 2004; Barkat *et al.*, 2011). Therefore, we investigated if such a critical period also exists for plastic rearrangements in the spinal motor system of *Sema3F* mutants.

IV.2.1. Impairments in motor coordination can be corrected by housing in enriched environments during a critical period after birth

A former study in our lab already showed that despite the dorsal-ventral pathfinding errors during embryonic development *Sema3F* mutants do not show any obvious deficits in gross locomotor behavior. However, forelimb-hindlimb coordination and skilled locomotion are affected, as assessed in the ladder rung test. Interestingly, *Sema3F* mutants can compensate for these deficits after enriched environment housing starting at birth, suggesting adaptive plasticity during postnatal development (Soellner, 2012; Helmbrecht *et al.*, 2015b (accepted)). In order to investigate whether the observed plastic rearrangements are restricted to a critical period we analyzed if delayed enriched environment housing is able to evoke the same effects. To that end, we tested the effects on motor coordination and skilled locomotor behavior of animals that were housed in an enriched environment starting at 4 weeks after birth in the ladder rung test. In this test, the latency for crossing the ladder is measured, however, to obtain a second, time-independent value that describes the motor performance of the animals, additionally also the number of slips is counted by the experimenter blinded to the genotype of the animals. To exclude that the results of this test might be affected by a change of the person that performs the experiment we decided to replicate this behavioral test for mice that were housed in normal and enriched environment conditions starting at birth.

IV.2.1.1. Replication of behavioral data after normal and enriched environment housing starting at birth

First, animals that were housed in normal conditions were tested. At 4 weeks of age, normally housed *Sema3F* mutants needed significantly more time to cross the ladder when compared to their wildtype littermates (Figure 16A). In addition, mutant animals revealed deficits in fine motor control since they showed a significantly increased number of slips during this task (Figure 16B). Over the time course of 8 weeks, these animals were able to improve their performance on the ladder, however they never reached the wildtype levels.

In contrast, *Sema3F* mutants that were housed under enriched environment conditions starting at birth were able to improve their performance over time. Hence, already at the age of 4 weeks these mutants needed significantly less time to cross the ladder when compared to mutants that were housed in normal housing conditions (Figure 17). Nevertheless, at this time point mutants still performed significantly worse than their wildtype littermates (Figure 16C and D). However, at 8 weeks of age, these motor deficits were compensated completely and no significant differences in latency or number of slips between the performance of wildtype and mutant animals were detectable anymore.

Thus, I reproduced the previous results from our lab (Soellner, 2012; Helmbrecht *et al.*, 2015b (accepted)), suggesting that enriched environment housing induces plastic changes that allow for the compensation of deficits in motor coordination in *Sema3F* mutants.

IV.2.1.2. Improvement of motor behavior by housing in an enriched environment is only possible during a critical period after birth

It has been shown in many different model systems that plastic rearrangements are usually restricted to critical periods (Hensch, 2004). If such a critical period also existed for the observed adaptive plasticity in the nervous system of *Sema3F* mutants, a delayed start of enriched environment hosing should not induce the same changes. Therefore, we next investigated mice that were only housed under enriched environment conditions starting at 4 weeks of age. Indeed, the ladder rung test revealed that these mice show a similar performance as animals housed in normal conditions (Figure 17). *Sema3F* mutants improved their performance over the time course of 8 weeks, but at each time point tested (4, 8 and 12 weeks

after birth) mutant animals performed significantly worse than their wildtype littermates (Figure 16E and F).

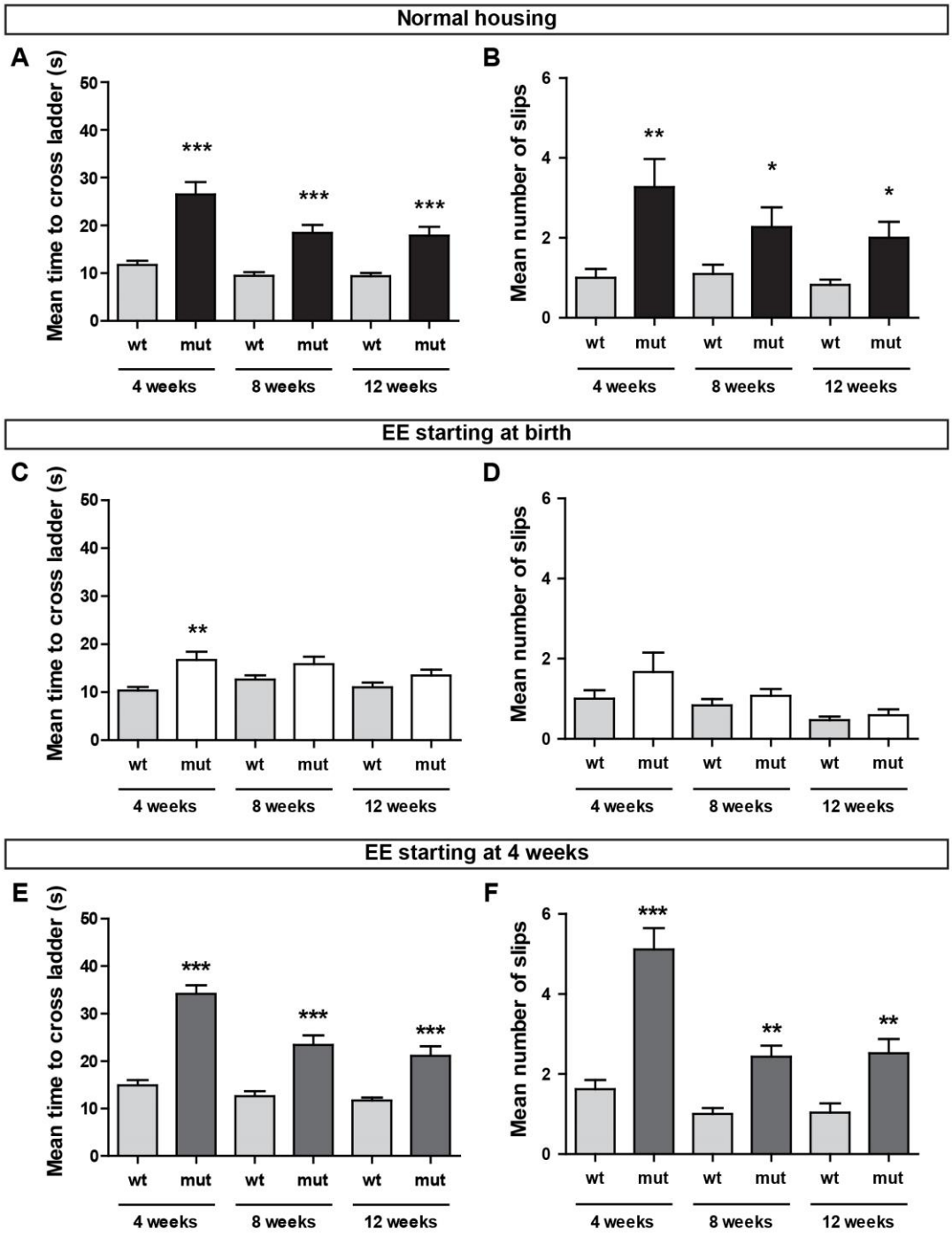

Figure 16: Motor coordination of *Sema3F* mice after housing in different environmental conditions

Deficits in motor coordination were analyzed using the ladder rung test. **(A)** Under normal housing conditions, *Sema3F* mutants need significantly more time to cross the ladder with irregular bars than

their littermate controls at each time point tested (4 weeks: 11.74 ± 0.86 s, n = 14 vs. 26.61 ± 2.60 s, n = 11, p < 0.001; 8 weeks: 9.48 ± 0.75 s, n = 14 vs. 18.48 ± 1.74 s, n = 11, p < 0.001; 12 weeks: 9.41 ± 0.67 s, n = 13 vs. 17.97 ± 2.04 s, n = 11, p < 0.001, Improvement mut 4-12 weeks: p = 0.006). **(B)** They also show a significantly increased number of slips from the ladder (4 weeks: 1.00 ± 0.22, n = 14 vs. 3.27 ± 0.70, n = 11, p = 0.006; 8 weeks: 1.10 ± 0.23, n = 14 vs. 2.27 ± 0.49, n = 11, p = 0.034; 12 weeks: 0.82 ± 0.14, n = 13 vs. 2.00 ± 0.40, n = 11, p = 0.023). **(C)** After enriched environment housing starting at birth the motor performance of *Sema3F* mutants reaches wildtype levels at 8 weeks after birth (4 weeks: 10.37 ± 0.76 s, n = 10 vs. 16.74 ± 1.71 s, n = 9, p < 0.005; 8 weeks: 12.63 ± 0.90 s, n = 10 vs. 15.85 ± 1.54 s, n = 9, p = 0.14; 12 weeks: 11.00 ± 0.98 s, n = 10 vs. 13.48 ± 1.19 s, n = 9, p = 0.07). **(D)** These animals show never a significant difference in the number of slips compared to wildtype littermates (4 weeks: 1.00 ± 0.21, n = 10 vs. 1.67 ± 0.49, n = 9, p = 0.36; 8 weeks: 0.83 ± 0.16, n = 10 vs. 1.07 ± 0.17, n = 9, p = 0.31; 12 weeks: 0.47 ± 0.09, n = 10 vs. 0.59 ± 0.15, n = 9, p = 0.50). **(E)** Enriched environment housing starting at 4 weeks after birth does not improve the motor performance of *Sema3F* mutants. They need significantly longer to cross the ladder throughout the tested period of time (4 weeks: 13.88 ± 1.66 s, n = 11 vs. 33.13 ± 2.073 s, n = 10, p < 0.001; 8 weeks: 12.88 ± 1.32 s, n = 11 vs. 23.17 ± 2.25 s, n = 10, p = 0.002; 12 weeks: 11.60 ± 0.62 s, n = 10 vs. 20.73 ± 2.29 s, n = 10, p = 0.0019). **(F)** Also the number of slips from the ladder is significantly increased at each time point after enriched environment housing starting at 4 weeks (4 weeks: 1.97 ± 0.40, n = 11 vs. 4.93 ± 0.51, n = 10, p < 0.001; 8 weeks: 1.21 ± 0.18, n = 11 vs. 2.43 ± 0.28, n = 10, p = 0.0041; 12 weeks: 0.80 ± 0.35, n = 10 vs. 2.20 ± 0.27, n = 10, p = 0.0055).

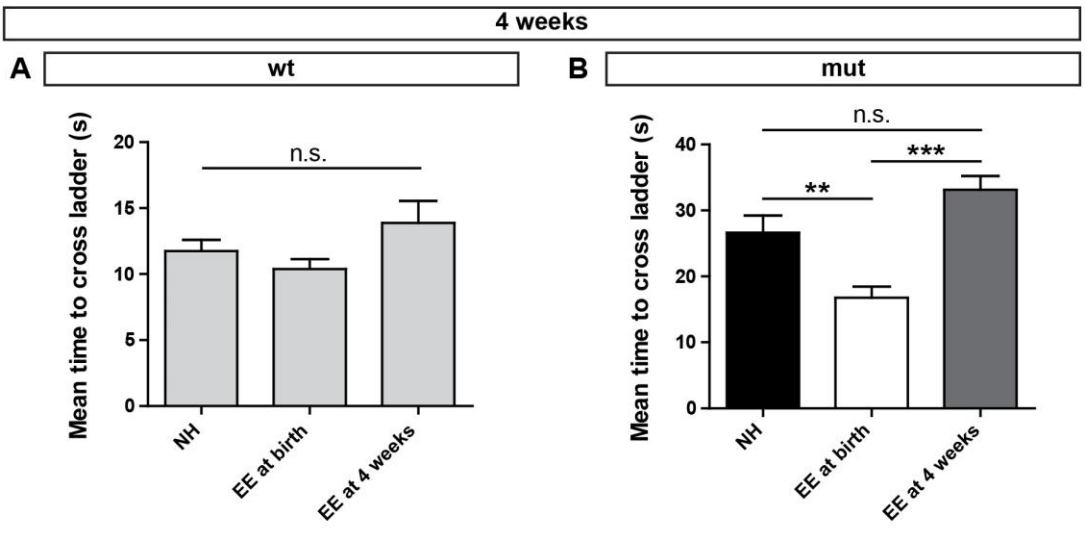

Figure 17: Already 4 weeks after birth, *Sema3F* mutants show improved motor skills due to enriched environment housing starting at birth

(A) Since *Sema3F* wildtypes already perform at a very high level housing conditions have no effect on the time that is needed to cross the ladder (NH: 11.74 ± 0.86 s, n = 14, EE: 10.37 ± 0.76 s, n = 10,

EE4: 13.88 ± 1.66 s, n = 11; p = 0.13 (ANOVA)). **(B)** In contrast, *Sema3F* mutants can improve their performance already at the age of 4 weeks, after enriched environment housing starting at birth (NH: 26.61 ± 2.60 s, n = 11, EE: 16.74 ± 1.71, n = 9, EE4: 33.13 ± 2.073 s, n = 10. P-Values: NH vs. EE: p = 0.0075; NH vs. EE4: p = 0.068, EE vs EE4: p < 0.001 (Student's t-test)).

These data suggest that *Sema3F* mutant mice can compensate their motor deficits due to experience-induced changes that take place within a critical period during the first 4 postnatal weeks.

IV.2.2. Housing conditions do not have an influence on the PNS of *Sema3F* mice

During embryonic development, *Sema3F* mutants show axon wiring deficits that cause an aberrant targeting of LMCm neurons to the dorsal side of the limb (Huber *et al.*, 2005). In order to assess whether the effects on motor behavior are not caused by a compensation of the wiring defects during the period of motor neuron death and axon pruning, we analyzed the innervation of the forelimb musculature by electrophysiological stimulation of the *N. musculocutaneous*. This nerve is projecting exclusively to the ventral side of the limb innervating mainly the *biceps brachii*. Accordingly, upon stimulation of the nerve in wildtype animals that were housed in an enriched environment starting at 4 weeks, signals were detected only in the *biceps brachii*, while the antagonistic *triceps brachii* muscle in the dorsal forelimb was not activated. In contrast, in *Sema3F* mutants I found signals in both muscles (Figure 18). This result is corroborated by earlier data from our lab that revealed misinnervation in the forelimb of *Sema3F* mutants in normal and enriched housing conditions starting at birth (Soellner, 2012; Helmbrecht *et al.*, 2015b (accepted)).

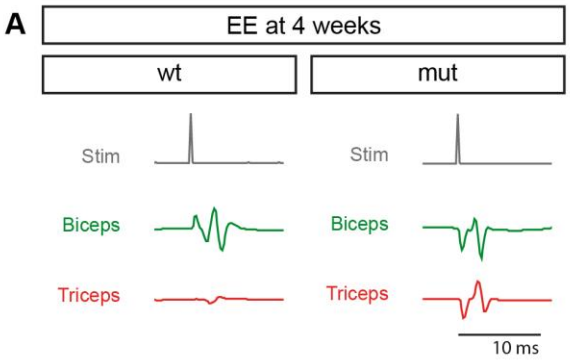

B

EE at 4 weeks	n	Biceps	Triceps
wt	6	6	0
mut	3	3	3

Figure 18: Electrophysiological stimulations reveal misinnervation of the *triceps brachii* in *Sema3F* mutants

(A) After stimulation of the *N. musculocutaneous* wildtype animals show a signal in the *biceps brachii* (green) while in the *triceps brachii* (red) only the stimulation artefact is visible. In *Sema3F* mutants, however, the stimulation of the same nerve leads to the activation of *biceps brachii* and *triceps brachii* muscles at the same time. **(B)** Quantification of activation signals. The table displays the total number of tested animals and the number of animals showing a signal in the respective muscle after activation of the *N. musculocutaneous*.

Since the innervation of forelimb musculature does not reveal any alterations between the different housing conditions this result shows that the peripheral nervous system remains hard-wired during postnatal development in all environmental conditions. This suggests that plastic changes in *Sema3F* mutants take place within the central nervous system of these animals. However, in order to convincingly exclude that changes in the PNS are involved in the behavioral improvement of *Sema3F* mutants after EE housing starting at birth it was necessary to investigate the neuromuscular junctions (NMJs) in their ventral forelimbs as well. Consequently, we analyzed the size of at least 100 NMJs per animal and found no difference between mice that were housed in normal or enriched housing conditions starting at birth (Figure 19).

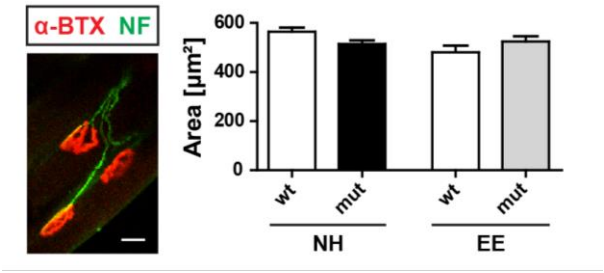

Figure 19: *Sema3F* mice show a comparable size of NMJs after normal and enriched environment housing

In *Sema3F* animals the surface area of NMJs in the ventral forelimb reveals no difference between animals that were housed in normal and enriched environment conditions starting at birth (NH: 564.4 ± 16.6 µm² vs. 514.5 ± 14.3 µm², N = 3; EE: 480.4 ± 27.0 µm² vs. 524.6 ± 22.0 µm², N = 3; p = 0.11, one-way ANOVA). Scale bar 20 µm.

IV.2.3. Neuroanatomical rearrangements corroborate a critical period for adaptive plasticity in the spinal cord of *Sema3F* mutants

Behavioral tests and the analysis of the PNS in *Sema3F* mice suggest that during a critical period in postnatal development adaptive plasticity in the CNS is responsible for the improved performance of *Sema3F* mutants after enriched environment housing. Thus, we investigated if this critical period can be detected at a neuroanatomical level in the spinal cord. For this purpose, Alexa Fluor-conjugated CTBs were injected into the dorsal and ventral musculature of the lower forelimb in order to retrogradely label their respective motor pools in the ventral horn of the spinal cord.

IV.2.3.1. Neuroanatomical data are comparable between different examiners

In order to compare the results to previous data from our lab it was necessary to demonstrate that the results from these tracings were not affected by the examiner. For this reason, I first compared the quality of the tracing experiments by quantifying the number of retrogradely traced motor neurons in the brachial spinal cord. The numbers of each motor pool revealed no significant differences between wildtypes and mutants or between animals of the three different housing conditions (Figure 20), showing that these results are independent from the experimenter. Furthermore, these results indicate that neuronal survival is not affected by

enriched environment housing and can therefore not be responsible for any changes in neuroanatomy.

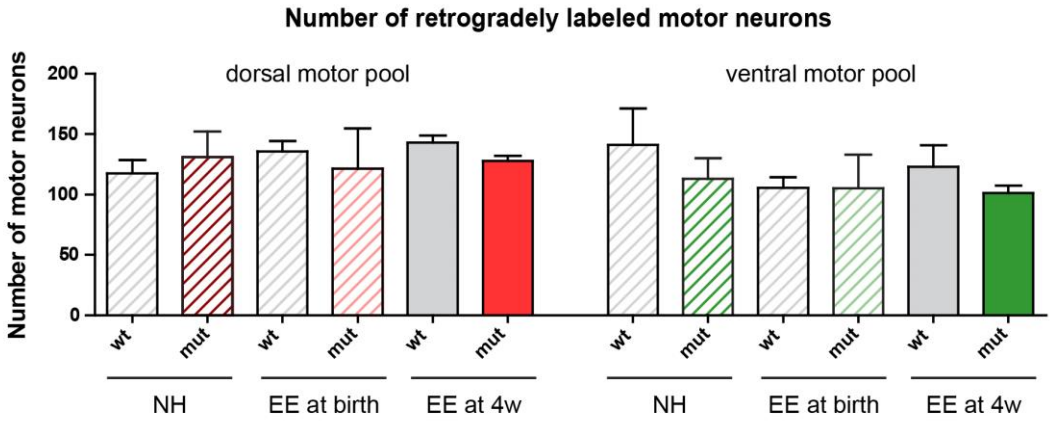

Figure 20: Retrograde tracings are comparable between all three housing groups

The number of retrogradely traced motor neurons in the respective motor pool was comparable in wildtypes and mutants of all housing conditions. Dorsal pool: NH (wt: 117.7 ±10.9, n = 3; mut: 131.0 ± 21.1, n = 3), EE at birth (wt: 135.7 ± 8.5, n = 7; mut: 121.3 ± 33.3, n = 4), EE at 4w (wt: 143.0 ± 5.7, n = 6; mut: 127.8 ± 4.2, n = 5); p = 0.83; one-way ANOVA. Ventral pool: NH (wt: 141.0 ± 30.3, n = 3; mut: 113.0 ±17.2, n = 3), EE at birth (wt: 105.6 ± 8.8, n = 7; mut: 105.0 ± 28.2, n = 4), EE at 4w (wt: 123.2 ± 17.6, n = 6; mut: 101.2 ± 6.4, n = 5); p = 0.68; one-way ANOVA. Data for NH and EE at birth were kindly provided by Heidi Söllner.

IV.2.3.2.A critical period for neuroanatomical rearrangement of spinal motor neuron pools

For a more detailed neuroanatomical analysis, we investigated the localization of motor neurons within their muscle specific pools. Previously done reconstruction of the ventrally projecting motor pools of normally housed *Sema3F* mutants showed an increased spreading in the dorsal-ventral direction, while in animals that were housed under enriched environment conditions the motor pools did not reveal any alterations between *Sema3F* mutants and their wildtype littermates (Soellner, 2012; Helmbrecht *et al.*, 2015b (accepted)).

After analysis of animals that were housed in an enriched environment starting at 4 weeks, I found that motor neurons innervating the ventral side of the limb appeared to be less organized in *Sema3F* mutants and spread into the dorsally projecting motor pool (Figure 21A).

In order to quantify this finding the scatter index was calculated, which characterizes the spreading of each motor pool within the spinal cord. The results show that in *Sema3F* mutants the pool of ventrally projecting motor neurons occupies a larger area than in their wildtype littermates. In contrast, the dorsal pool showed no significant alterations in size or scattering (Figure 21B). This finding is particularly interesting since it is supported by the observations during embryonic development, where only the ventrally projecting motor axons undergo guidance errors (Huber *et al.*, 2005). A closer investigation of the ventrally projecting motor pool revealed that the spreading of the motor neurons is specifically scattered in the dorsal-ventral axis, while the medial-lateral expansion of the pool was not affected (Figure 21C).

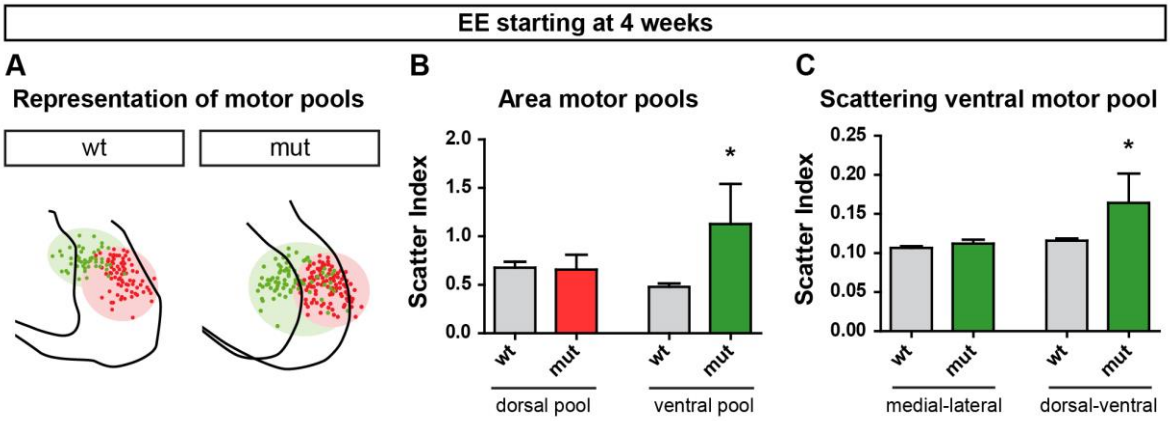

Figure 21: Specific disorganization of the ventrally projecting motor pool in *Sema3F* mutants

(A) Motor pools were reconstructed from labeled motor neurons of the brachial spinal cord. **(B)** After enriched environment housing starting at 4 weeks, the ventral motor pool of adult animals is significantly larger in *Sema3F* mutants compared to their wildtype littermates. In contrast, the dorsal motor pool remains unchanged (dorsal: 0.65 ± 0.060, n = 8 vs. 0.66 ± 0.15, n = 3, p = 0.94; ventral: 0.45 ± 0.04, n = 8 vs. 1.13 ± 0.41, n = 3, p < 0.02; Student's t-test). **(C)** Upon closer investigation of the ventral motor pool a specific scattering of the pool becomes evident in a dorsal-ventral direction, while the medial-lateral dimensions of the pool are not affected (dorsal-ventral: 0.12 ± 0.003, n = 8 vs. 0.16 ± 0.038, n = 3, p < 0.05; medial-lateral: 0.0.11 ± 0.002, n = 8 vs. 0.11 ± 0.005, n = 3, p = 0.26; Student's t-test)

Thus, also on a neuroanatomical level my results from animals that received a delayed enriched environment housing starting at 4 weeks show a similar effect as found for animals that were housed in normal conditions. Thereby, these findings corroborate the previous

results from behavioral and electrophysiological experiments and suggest a critical period for adaptive plasticity in the motor system of the brachial spinal cord.

IV.2.4. Perineuronal nets play no major role in the regulation of plasticity in *Sema3F* mutants

Since our results reveal evidence for the existence of a critical period for postnatal plasticity, we were interested in the underlying mechanisms that determine this critical period in the motor system of *Sema3F* mutants. The closure of critical periods for plasticity in the nervous system has been closely related to the development of perineuronal nets (PNNs) for several areas of the nervous system (Bavelier *et al.*, 2010; Foscarin *et al.*, 2011; Kwok *et al.*, 2011). These structures of extracellular matrix form around cell bodies as a tight meshwork and display a physical barrier for plastic changes, since they prevent the formation of new synapses (Pizzorusso *et al.*, 2002; Wang & Fawcett, 2012). In several cases it was shown that enriched environment housing can influence the formation of PNNs and thereby extend the period for adaptive plasticity (Bavelier *et al.*, 2010; Foscarin *et al.*, 2011). Therefore, we investigated if PNNs play a role in the adaptive plasticity that is induced by environmental enrichment in *Sema3F* mutants and analyzed the formation of PNNs on ventrally projecting motor neurons of the brachial spinal cord during the first 4 weeks of postnatal development.

Interestingly, we found that the formation of PNNs around motor neurons in the spinal cord is very heterogeneous (Figure 22A and B) and most motor neurons are not protected by PNNs. At 4 weeks, when the critical period is already closed, only about 35% of retrogradely labeled motor neurons are surrounded by PNNs and in less than 5% they form a very tight meshwork (Figure 22C). Furthermore, no significant difference in the composition of PNNs was found between the different housing groups. Additionally, we followed the development of PNNs in earlier stages and did not find any alterations between genotypes or housing groups from P7 until P21 (Figure 22D-F).

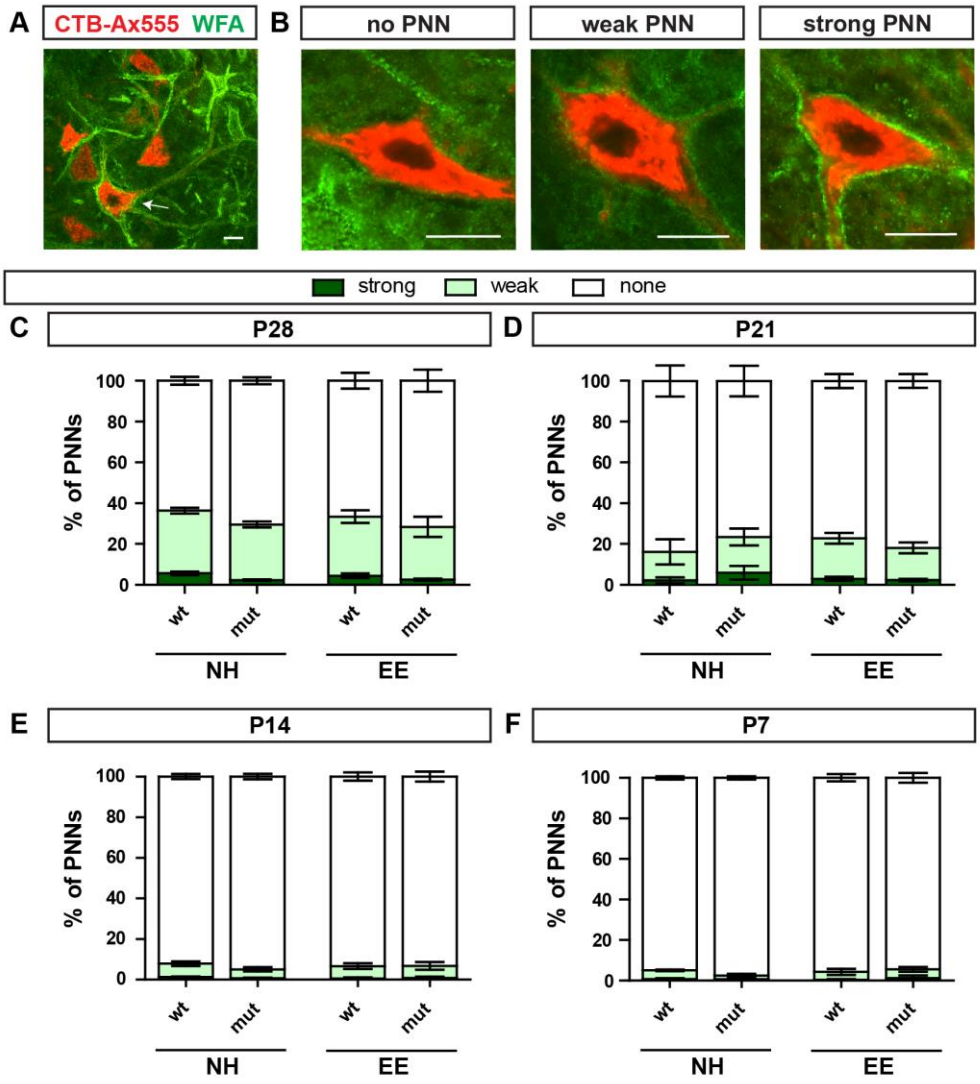

Figure 22: Enriched environment housing has no effect on the development of PNNs on spinal motor neurons

(A) In the adult spinal cord, only few retrogradely labeled motor neurons of the distal ventral forelimb show PNNs (arrow). **(B)** Examples of motor neurons with no, weak, or strong PNNs, respectively. **(C)** At 4 weeks of age, when the critical period for adaptive plasticity is closed, more than 65% of traced motor neurons are not covered by PNNs, regardless of the housing conditions (NH: wt: 63.6 ± 3.4%; mut: 70.4 ± 3.0%; EE: wt: 66.6 ± 6.8%, mut: 71.6 ± 9.4%; p = 0.43). Weak PNNs are found on less than 30% (NH: wt: 30.7 ± 2.5%; mut: 27.2 ± 2.5%; EE: wt: 29.0 ± 5.3%, mut: 25.9 ± 8.6%; p = 0.72) and less than 5% of motor neurons show strong PNNs (NH: wt: 5.7 ± 1.7%; mut: 2.4 ± 0.6%; EE: wt: 4.4 ± 2.0%, mut: 2.6 ± 0.8%; p = 0.06). Statistical analysis: n = 3 for each group, one-way ANOVA. **(D-F)** Also at earlier stages no significant differences in the formation of PNNs on retrogradely traced motor neurons was found at P21 (none: average 80.0%, p = 0.78; weak: average 16.9%, p = 0.78; strong: average 3.1%, p = 0.53), P14 (none: average 93.4%, p = 0.74; weak: average 5.8%, p = 0.73; strong: average 0.9%, p = 0.69) or P7 (none: average 95.72%, p = 0.56; weak: average

3.54%, p = 0.34; strong: average 0.73%, p = 0.82). Statistical analysis: n = 3 for each group, one-way ANOVA. Scale bars: 20 μm.

These results suggest that the formation of PNNs plays no important, if any, role in the regulation of adaptive plasticity in the spinal motor system of *Sema3F* mice.

IV.2.5. Enriched environment housing alters the balance of excitatory-inhibitory input on motor neurons

Ample research on brain plasticity has emerged during the last years and it is now generally accepted that neuronal circuits are initially plastic and can be modified by experience. After a specific sensitive period, these shaped networks have to be stabilized and therefore the capability for adaptive plasticity is limited. As mentioned above, this can be caused by structural changes in the extracellular matrix but also functional adaptations are known to influence the sensitive period for plasticity. Hence, there is emerging evidence that induction and closure of this critical period is linked to specific thresholds of inhibitory input on the respective neuronal circuits (Fagiolini & Hensch, 2000; Berardi *et al.*, 2003; Bavelier *et al.*, 2010). Furthermore, it has been shown that enriched environment housing can induce the formation of excitatory synapses and thereby influence the balance of excitatory-inhibitory within these circuits (van Praag *et al.*, 2000; Adkins *et al.*, 2006; Nithianantharajah & Hannan, 2006). In order to investigate if functional changes are also evident in the spinal motor circuits, we next analyzed the number of synapses on motor neurons that innervate the lower ventral forelimb. For the analysis of the synapses on each motor neuron the number of stained particles on the cell body was counted using the ImageJ software (Figure 23A). Between motor neurons of mutant and wildtype animals no changes in synaptic inputs were found. Also, the number of inhibitory synapses was comparable between *Sema3F* mice, regardless of their housing conditions (Figure 23B). This is particularly interesting, since the formation of inhibitory synapses has been shown to affect the closure of critical periods (Bavelier *et al.*, 2010). In contrast, the number of excitatory synapses was significantly increased after enriched environment housing starting at birth, while enriched environment housing starting at 4 weeks does not induce the same effect (Figure 23C).

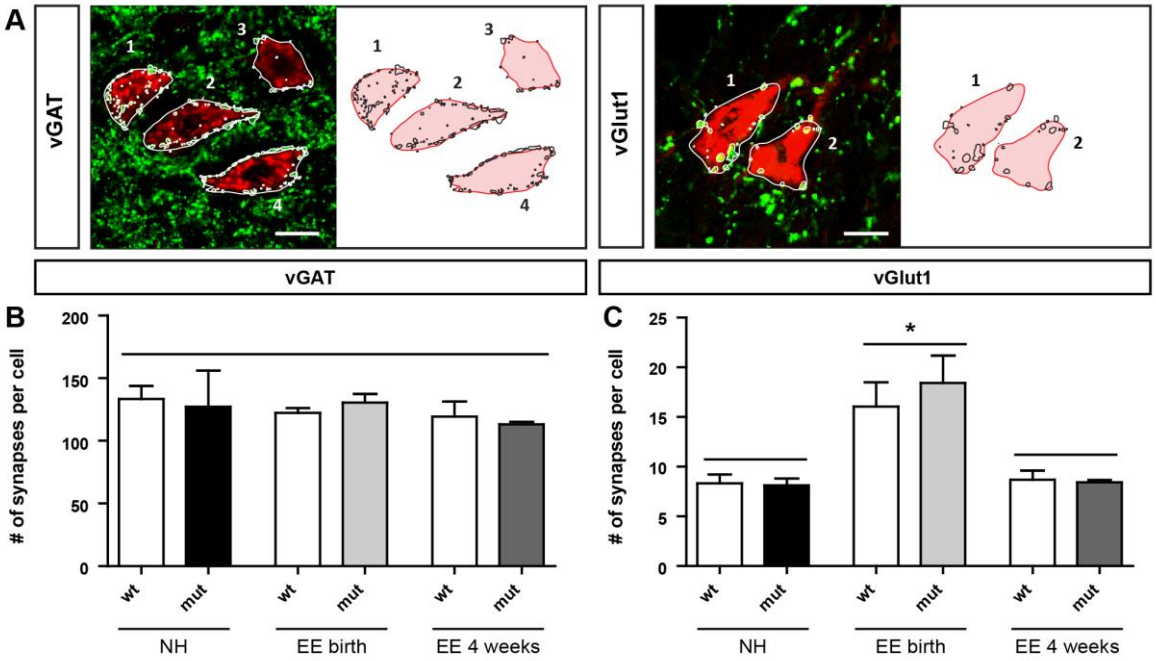

Figure 23: Excitatory-inhibitory balance of synaptic input is shifted by enriched environment housing

(A) Example of inhibitory (vGAT) and excitatory (vGlut1) synapses on retrogradely labeled motor neurons, respectively. **(B)** At the age of 12 weeks, the number of inhibitory synapses on traced motor neurons remains unchanged between wildtypes and mutants of both housing conditions (normal housing (wt: 133.5 ± 10.52, mut: 127.3 ± 28.76), enriched environment starting at birth (wt: 122.5 ± 3.85, mut: 125.0 ± 6.63), and enriched environment starting at 4 weeks (wt: 119.4 ± 12.0, mut: 113.2 ± 2.15); (n = 3 for each group, p = 0.91, one-way ANOVA). **(C)** Between *Sema3F* wildtypes and mutants, the number of excitatory synapses is not significantly altered (NH: wt: 8.32 ± 0.90, mut: 8.13 ± 0.67, p = 0.87; EEbirth: wt: 15.99 ± 2.51, mut: 16.81 ± 3.88, p = 0.75; EE4: wt: 8.70 ± 0.93, mut: 8.43 ± 0.24; n = 3 for each group, Students t-test), however, after enriched environment housing starting at birth the number of excitatory synapses were significantly increased when compared to normal housing conditions or enriched environment starting at 4 weeks (NH vs. EEbirth: wt: p = 0.04 , mut: p = 0.022; EEbirth vs. EE4: wt: p = 0.047, mut: p = 0.023; n = 3 for each group, Students t-test).

In conclusion, our results show that within a critical period in the first 4 weeks of postnatal development, enriched environment housing is inducing adaptive plasticity in the spinal motor system by the formation of additional excitatory synapses on affected motor neurons and rearrangement of motor pools in the ventral spinal cord. Furthermore, *Sema3F* mutants that

were housed in an enriched environment from birth can compensate for their behavioral deficits since they show a significant improvement of their skilled motor function and forelimb-hindlimb coordination. However, compensational mechanisms are only found in animals that received enriched housing conditions already at birth, which further corroborates the existence of a critical period for adaptive plasticity. Moreover, we show that the housing conditions are not affecting the timing of the critical period since the development of PNNs is unchanged and the number of inhibitory synapses is not affected.

V. DISCUSSION

V.1. Emerging consequences of deficient Npn1 signaling during postnatal development

The importance of Npn1 for the development of the nervous system of mice has been revealed in various studies. During development of the central nervous system signaling of secreted class 3 semaphorins with the axon guidance receptor Npn1 plays an essential role in the guidance of descending axon tracts in the forebrain (Chauvet *et al.*, 2007). In addition, Sema3A-Npn1 signaling has been found to regulate the crossing of pioneering axons of the cingulate cortex during development of the corpus callosum (Piper *et al.*, 2009), and the branching of basket cell axons in the cerebellum (Cioni *et al.*, 2013).

Even more studies have addressed the function of this guidance receptor for the development of the peripheral nervous system. Here it was shown that Npn1 is essential for the migration of neural crest cells, gangliogenesis of dorsal root ganglia, and axon guidance of sympathetic neurons (Roffers-Agarwal & Gammill, 2009; Schwarz *et al.*, 2009; Maden *et al.*, 2012). Furthermore, the importance of Npn1 signaling for the development of a functional limb innervation has been addressed in previous studies of our lab. Hence, an impaired Sema3A-Npn1 signaling in $Npn1^{Sema-}$ mutants leads to a precocious ingrowth of motor projections into the limb and motor axons are severely defasciculated. Additionally, medial and lateral LMC motor axons display dorsal-ventral guidance errors that are maintained throughout development (Huber *et al.*, 2005; Haupt *et al.*, 2010). In contrast, loss of Npn1 from all somatic motor neurons leads to reduced distal advancements of motor projections. However, also in these mice motor axons are severely defasciculated and display errors in their dorsal-ventral guidance choice (Huettl *et al.*, 2011).

Accordingly, the deficits that are caused by a defective Sema3A-Npn1 signaling during development have been investigated thoroughly. But what does this mean for postnatal development of these animals? In previous studies from our lab we have found that *Olig2-*Cre^{+}*;*$Npn1^{cond}$ mutants suffer from abnormal forelimb posturing that is accompanied by dysfunctional innervation by the *N. radial* and an atrophy of the extensor muscles. These deficits were never found in $Npn1^{Sema-}$ animals. In order to investigate the underlying reasons for these differences we compared weight development and nerve composition in these

mouse lines and found that both show similar deficits in weight but only *Olig2-Cre*$^{+}$*;Npn1*^{cond} mutants displayed a significant reduction of the number of motor axons innervating the extensor muscles of the forearm. These results suggest that deficits in forelimb innervation are responsible for the striking posturing deficits in the forelimbs of *Olig2-Cre*$^{+}$*;Npn1*^{cond} mutants.

V.1.1. Possible causes for a wrist drop phenotype

The wrist drop phenotype that is observed in *Olig2-Cre*$^{+}$*;Npn1*$^{cond-/-}$ mutants is characterized by the flexion of one or both wrists of the forelimbs and the inability to extend the affected paws. This phenotype is reminiscent of the deficits observed after radial nerve palsy (Reid, 1988) and may be caused by conceptually different defects. First, *Olig2-Cre*$^{+}$*;Npn1*$^{cond-/-}$ mutants might be unable to extend their limbs due to malformations in their forelimb skeleton. Earlier analysis in our lab, however, found that a passive extension of the forelimbs is possible and that, at birth, when the wrist drop is already evident, bone and cartilage structure of these animals are not affected (Soellner, 2012; Helmbrecht *et al.*, 2015a). Consequently, bone malformations are not responsible for the described phenotype in *Olig2-Cre*$^{+}$*;Npn1*^{cond} mutants.

Another possible reason for defects in forelimb posturing is a dysfunction of distinct forelimb muscles. Interestingly, a specific atrophy of forelimb extensor muscles has been described in *Olig2-Cre*$^{+}$*;Npn1*^{cond} mutants already at birth, while their lower forelimb flexors never showed any deficits (Soellner, 2012; Helmbrecht *et al.*, 2015a). Furthermore, I found that even more distally located flexors of the paw were not significantly smaller in mutants than in their control littermates. Thus, *Olig2-Cre*$^{+}$*;Npn1*^{cond} mutants show a very specific loss of muscle volume in the forelimb extensor muscles that might explain the inability of the animals to extend their affected paws.

But why do specifically the extensor muscles atrophy in mutant animals, while flexor muscles are not affected? One of the main causes for muscular atrophy is a dysfunctional innervation (Kraft, 1990; Jackman & Kandarian, 2004) and accordingly many motor neuron diseases like progressive motor neuropathy or amyotrophic lateral sclerosis show muscle atrophy as a major symptom (Schmalbruch *et al.*, 1991; Gonzalez de Aguilar *et al.*, 2007). *Olig2-Cre*$^{+}$*;Npn1*^{cond} mutants display severe defects in the innervation of the forelimb extensors that have been shown in functional and anatomical approaches. As a consequence, electrophysiological stimulation of the *N. radial* did not result in an activation of extensor muscles in the forearm, while the innervation of the forelimb flexors did not show any abnormalities and resulted in

the expected flexion of the wrists (Soellner, 2012; Helmbrecht *et al.*, 2015a). Anatomically, it was previously shown that the forelimb innervation of *Olig2-Cre^{+};Npn1^{cond}* mutants is severely compromised during embryonic development, since they display defasciculation of their brachial axons and dorsal-ventral guidance defects (Huettl *et al.*, 2011). For this reason it is plausible that innervation deficits cause the observed atrophy of the forelimb extensor muscles, which is the underlying reason for the wrist drop phenotype in *Olig2-Cre^{+};Npn1^{cond}* mutants.

V.1.2. Loss of motor axons is responsible for the innervation deficits in *Olig2-Cre^{+};Npn1^{cond}* mutants

Malfunctioning innervation of the forelimbs has been described as the underlying cause for a wrist drop phenotype in mice that carry the claw paw mutation (*clp*) (Henry *et al.*, 1991; Bermingham *et al.*, 2006). In these animals the wrists are flexed towards the body in one or more joints while passive extension of the affected limbs is possible. Therefore, the forelimb posturing defect phenotypically resembles the forelimb posturing we have observed in *Olig2-Cre^{+};Npn1^{cond}* mutants. In *clp* mutants, the wrist drop is caused by a 225-bp insertion in exon 4 of the *Lgi4* gene that results in abnormal splicing of the mRNA and inhibits the secretion of the protein from the cell. Since the Lgi4 protein is expressed in Schwann cells, the *clp* mutation results in a dysfunctional innervation of the limbs due to deficits in axonal sorting and myelination of the peripheral nervous system. Hence, in these animals myelination starts later during development and the nerves are generally hypomyelinated. Furthermore, in adult mice until the age of 20 months, large diameter axons were found in a promyelinated state and the size of these axons was noticeably smaller when compared to their controls (Henry *et al.*, 1991; Koszowski *et al.*, 1998; Darbas *et al.*, 2004). In *Olig2-Cre^{+};Npn1$^{cond-/-}$* mice, however, no differences in the size of the myelin sheaths were found upon ultrastructural analysis of the nerves (Soellner, 2012; Helmbrecht *et al.*, 2015a). Thus, in contrast to *clp* mice, problems in myelination do not seem to be the underlying cause for the wrist drop phenotype in *Olig2-Cre^{+};Npn1^{cond}* mutants.

In contrast, the investigation of the nerve structure in *Olig2-Cre^{+};Npn1$^{cond-/-}$* mice revealed significant differences. The results show a reduced proportion of large diameter axons in the nerves of affected animals (Soellner, 2012; Helmbrecht *et al.*, 2015a) which is corroborated by the relative reduction of GFP^{+} axons in the in the *N. radial* of *Olig2-Cre^{+};Npn1$^{cond-/-}$; Hb9::eGFP*

mice. These results can be explained by a loss of motor axons, which is supported by the reduced number of motor neurons that were retrogradely traced from the radial nerve in the brachial plexus. But what causes this specific loss of motor axons in the *N. radial*? Results from previous studies in our lab might provide an explanation for the observed effects. Investigations during embryonic development suggest that axons of the *N. radial* do not reach their target muscles in the dorsal forelimb, since at this side the injection of rhodamin-coupled dextran never led to any motor neurons cell bodies that are labeled by the retrogradely transported tracer (Huettl *et al.*, 2011). For this reason, it is likely that these axons die later due to a lack of trophic support. In contrast, at the ventral side of the limb sufficient axons seem to reach their appropriate target, which might explain why the *N. median* is not affected to the same extent and flexor innervation is still intact in postnatal animals.

Interestingly, however, upon investigation of the nerve area a significant decrease in size of *N. radial* and *N. median* was found and additionally the total number of motor and sensory axons was reduced in both nerves. This overall reduction in nerve size and axon number is probably the result of the severe deficits in axon fasciculation during embryonic development (Huettl *et al.*, 2011). In *Olig2-Cre*$^{+}$*;Npn1*^{cond} mutants, all brachial nerves are severely defasciculated in the embryonic state and it is hardly possible to distinguish specific nerve branches. During later development these defasciculated axons might be pruned (Vanderhaeghen & Cheng, 2010), which might result in an overall reduction in axon number and consequently in a decreased nerve size in postnatal animals.

V.1.3. *Npn1*$^{Sema-}$ mutants can compensate for developmental axon miswiring

During embryonic development, axon pathfinding deficits and defasciculation have been described for both, *Npn1*$^{Sema-}$ and *Olig2-Cre*$^{+}$*;Npn1*^{cond} mutants. However, in postnatal animals striking differences in their anatomy and behavior become evident. Thus, while *Olig2-Cre*$^{+}$*;Npn1*^{cond} mutants show a wrist drop phenotype in one or both forelimbs, such deficits were never found in *Npn1*$^{Sema-}$ mutants. Furthermore, *Olig2-Cre*$^{+}$*;Npn1*$^{cond-/-}$ mice reveal deficits in skilled motor behavior that are observed at all time points tested. In contrast, motor coordination of *Npn1*$^{Sema-}$ mutants was only affected in young animals, steadily improved during postnatal development and reached wildtype level at the age of 12 weeks (Soellner, 2012; Helmbrecht *et al.*, 2015a). What are the underlying reasons that allow *Npn1*$^{Sema-}$ mutants

to compensate their developmental deficits, while postnatal *Olig2-Cre^{+};Npn1$^{cond-/-}$* mice display permanent anatomical and behavioral impairments?

An answer for this question can be found by a detailed comparison of their axon wiring defects during embryonic development. *Olig2-Cre^{+};Npn1$^{cond-/-}$* mice reveal motor axons that are defasciculated and an increased number of misguided axons in the ventral side of the forelimb after retrograde tracing with rhodamin-coupled dextran (Huettl *et al.*, 2011). These deficits are restricted to motor neurons of the brachial spinal cord, which may explain why the posturing defect was never observed in the hindlimbs of *Olig2-Cre^{+};Npn1^{cond}* mutants. Additionally, the most distal advancement of the motor axons growing into the developing limb is significantly reduced in these animals and the radial nerve does not seem to reach its target muscles at the dorsal side of the limb since retrograde tracing from the extensor muscles of the forelimbs was not possible (Huettl *et al.*, 2011). This explains why we found a reduction of the proportion of motor axons specifically in the radial nerve, which in turn causes the atrophy of the extensor muscles and thereby the wrist drop phenotype in *Olig2-Cre^{+};Npn1^{cond}* mutants.

In contrast to *Olig2-Cre^{+};Npn1$^{cond-/-}$* mice, motor axons of *Npn1^{Sema-}* mutants enter the limb prematurely and reveal longer projections than their wildtype littermates (Huber *et al.*, 2005). Therefore, despite their pathfinding errors and defasciculation, motor axons might still reach their appropriate targets in a sufficient number to assure a functional innervation of the muscles. Due to a reduced competition for trophic support these axons will later survive during the period of naturally occurring motor neuron death (Hollyday & Hamburger, 1976; Phelan & Hollyday, 1991; Sendtner *et al.*, 2000). Additionally, the pruning of aberrant motor projections during normal development (Vanderhaeghen & Cheng, 2010) might contribute to the compensatory mechanisms that prevent the development of strong functional deficits in *Npn1^{Sema-}* mutants.

V.1.4. Molecular mechanisms underlying the differential axon wiring deficits in *Olig2-Cre^{+};Npn1^{cond}* and *Npn1^{Sema-}* mutants

The knock-in of the CRE recombinase into exon 2 of the *Olig2* gene causes a disruption of the Olig2 protein function (Dessaud *et al.*, 2007). Accordingly, homozygous *Olig2-Cre* animals do not have a functional *Olig2* allele, which impedes the generation of motor neurons in the spinal cord. Furthermore, loss of *Olig2* causes perinatal lethality and affected animals retained their *in utero* posture due to a lack of muscular activity (Takebayashi *et al.*, 2002). Consequently,

in *Olig2-Cre*$^{+}$*;Npn1*^{cond} mutants, which are heterozygous for *Olig2-Cre,* the loss of motor neurons might be a dosage effect due to the partial loss of Olig2 expression. However, *Olig2-Cre*$^{+/-}$ animals never showed any anatomical phenotype and after retrograde tracing of motor neurons from the *N. radial*, no difference in the number of labeled motor neurons was found in the spinal cord of *Olig2-Cre*$^{+/-}$ animals when compared to wildtype littermates (data not shown). This is supported by the study of Takebayashi and colleagues, who also found no morphological differences between *Olig2*$^{+/-}$ mice and their wildtype littermates (Takebayashi *et al.*, 2002). Hence, in *Olig2-Cre*$^{+/-}$ animals the expression levels of Olig2 seem to be sufficient to ensure the proper generation of motor neurons in the spinal cord and it is highly unlikely that the loss of one *Olig2* allele has any effect on the posturing phenotype and the loss of motor axons in *Olig2-Cre*$^{+}$*;Npn1*^{cond} mutants.

In *Olig2-Cre*$^{+}$*;Npn1*$^{cond-/-}$ mice the extracellular axon guidance receptor Npn1 is specifically ablated from Olig2^{+} precursor cells. Within the spinal cord, these cells are located in pMN domain of the ventricular zone and give rise to motor neurons and later also to oligodendrocytes (Takebayashi *et al.*, 2002). Since Npn1 has been shown to be expressed in oligodendrocytes and their precursors in the brain (Ricard *et al.*, 2001; Spassky *et al.*, 2002; Cohen *et al.*, 2003), the loss of Npn1 from these progenitors might, therefore, also affect the development of myelinating oligodendrocytes in the spinal cord. However, preliminary results from our lab showed that Npn1 is not expressed in the ventricular zone at the embryonic day 13.5, when newly generated oligodendrocyte precursor cells (OPCs) start to migrate away from the pMN domain (Masahira *et al.*, 2006). Furthermore, in *Olig2-Cre*$^{+}$*;Npn1*$^{cond-/-}$ spinal cords the migration of OPCs did not reveal any differences when compared to control littermates (Soellner, 2012; Helmbrecht *et al.*, 2015a). Thus, the specific ablation of Npn1 from Olig2^{+} progenitors does not seem to have any influence on the development of oligodendrocytes in the brachial spinal cord.

Since neither the loss of one functional *Olig2* allele nor a dysfunctional generation of oligodendrocytes is responsible for the observed effects in *Olig2-Cre*$^{+}$*;Npn1*^{cond} mutants, we can conclude that the specific loss of the Npn1 receptor form motor neurons is the underlying reason for developmental axon miswiring and the resulting functional deficits in these animals.

Also *Npn1*$^{Sema-}$ mutants show a defective signaling of the Npn1 receptor, however, these mutants do not reveal the same deficits as *Olig2-Cre*$^{+}$*;Npn1*$^{cond-/-}$ mice. What causes the developmental differences that allow *Npn1*$^{Sema-}$ mutants to compensate for their developmental deficits? In *Npn1*$^{Sema-}$ mutants, Sema3A-Npn1 signaling is disrupted by a substitution of 7

amino acids in the semaphorin binding site of the receptor that inhibits the binding of the Sema3 family members while binding sites for other interaction partners are not affected. Indeed, the receptor Npn1 has been shown to interact with many alternative ligands like L1 cell adhesion molecules (e.g. L1 and CHL1) or VEGF (Castellani, 2002; Schwarz *et al.*, 2004; Tillo *et al.*, 2015). Since both ligands have already been reported to be involved in neuronal patterning and axon guidance this might explain the differential axon miswiring between *Olig2-Cre^{+};Npn1^{cond}* and *Npn1^{Sema-}* mutants, which allow the latter to compensate for their developmental deficits, while *Olig2-Cre^{+};Npn1^{cond}* mutants, which lack the complete Npn1 receptor in all motor neurons, show a severe postnatal phenotype. One way to consolidate this conclusion, would be to cross the *Npn1^{Sema-}* line to *Npn1^{Y297A}* mice, which have a deficient binding site for VEGF (Fantin *et al.*, 2014). This approach would allow for the investigation of axon wiring deficits due to a defective signaling of the Npn1 receptor with both ligands, and a comparison to the existing mouse lines would help to understand which mechanisms are involved in the compensation of embryonic axon miswiring in *Npn1^{Sema-}* mutants.

V.1.5. Conclusion

In conclusion, our data suggest that the loss of Npn1 from motor neurons causes a wrist drop in the forelimbs of *Olig2-Cre^{+};Npn1$^{cond-/-}$* mice due to a reduced number of dorsally projecting motor neurons and the resulting deficient innervation of extensor muscles. This phenotype is accompanied by muscle atrophy, bone malformation, and deficits in skilled motor behavior. The loss of Sema3A-Npn1 signaling in motor neurons is, however, not the only molecular cause for the described effects, since *Npn1^{Sema-}* mutants do not reveal the same deficits. Therefore, it is likely that Npn1 is able to interact with additional binding partners like VEGF, L1 or other yet unknown ligands to control sensory-motor circuit wiring and that this interaction initiates compensatory mechanisms that account for the minor disturbances in *Npn1^{Sema-}* mutants.

V.2. Axon miswiring in *Sema3F* mutants as an injury-independent model for the investigation of postnatal plasticity in the spinal cord

During the last decades, a variety of studies have focused on the investigation of adaptive plasticity in the CNS. However, the underlying mechanisms are still not completely understood (Takesian & Hensch, 2013). Most of these studies have investigated changes in neuronal circuits of the brain since investigations in the spinal cord depend on plastic adaptations after injury which is accompanied by many disadvantages like a poor reproducibility even within the same laboratory and secondary damage that is caused by inflammation, changes in vascularization or scar formation (Maier & Schwab, 2006). To address these challenges, we used the genetically encoded axon miswiring of *Sema3F* mutants as a non-injury based model to investigate adaptive plasticity during postnatal development of the spinal motor system.

V.2.1. A critical period for adaptive plasticity in the brachial spinal cord

In the developing spinal circuit, the lack of the secreted axon guidance molecule Sema3F causes a very specific guidance defect on axons deriving from the medial aspect of the lateral motor column (LMCm). These axons express the guidance receptor Neuropilin 2 (Npn2) and are repelled by the ligand Sema3F that is expressed in the dorsal half of the limb mesenchyme. Due to the missing chemorepulsive effect in *Sema3F* mutants, LMCm axons are no longer pushed towards a ventral trajectory, which causes errors in the dorsal-ventral choice (Huber *et al.*, 2005). Interestingly, these wiring defects are not completely eliminated during the phase of axon pruning and naturally occurring motor neuron death in the late embryonic and early postnatal period, as shown by electromyographic recordings in adult mutants, which reveal an aberrant innervation of the *triceps brachii* by the *musculocutaneous* nerve (Figure 12). Consequently, *Sema3F* mutants have impairments in skilled motor functions like forelimb-hindlimb coordination that are accompanied by alterations in the organization of the LMCm (Figure 10 and Soellner, 2012; Helmbrecht *et al.*, 2015b (accepted)). However, housing of *Sema3F* mutants in an enriched environment starting at birth counteracts these adverse effects as motor coordination is improved to wildtype levels and normal neuroanatomy of the ventral motor pool is restored (Figure 10 and Soellner, 2012; Helmbrecht *et al.*, 2015b (accepted)). These results are corroborated by several studies that found that enriched environment can

alter the organization and connectivity of neuronal circuits in the cortex (Bengoetxea *et al.*, 2012). Hence, it has been shown that environmental enrichment induces changes in the forepaw representation of the somatosensory cortex (Coq & Xerri, 1998), alters the dendritic morphology in the auditory cortex (Bose *et al.*, 2010) and promotes physiological maturation of the neuronal circuits in the visual cortex of dark-reared rats (Bartoletti *et al.*, 2004). In the spinal cord, it has been reported that treadmill training has a beneficial effect on locomotor capabilities after spinal cord injury (Edgerton *et al.*, 2004), and enriched environment has been shown to induce plasticity after contusive spinal cord injury, which is demonstrated by alterations in cell survival and significant improvements in sensory function and motor performance (Berrocal *et al.*, 2007).

Furthermore, there is substantial evidence that such plastic rearrangements are restricted to critical periods during development in which the neuronal circuits are sensitive for activity-dependent changes (Hensch, 2004). Also in the nervous system of *Sema3F* mutants our results suggest the existence of a critical period for adaptive plasticity: animals that were housed in an enriched environment starting at 4 weeks do not show any behavioral or neuroanatomical alterations when compared to mice that were housed in normal conditions (Figures 10 and 15, and Soellner, 2012; Helmbrecht *et al.*, 2015b (accepted)). Changes in these parameters are already evident at 4 weeks of age (Figure 11 and Soellner, 2012; Helmbrecht *et al.*, 2015b (accepted)). Thus, our data suggest a critical period for plasticity in the postnatal spinal motor system within the first 4 postnatal weeks.

V.2.2. Early postnatal influences on adaptive plasticity

While behavioral and neuroanatomical experiments provide evidence for postnatal plasticity in the spinal cords of *Sema3F* mutants, it was unclear when these plastic rearrangements start. The comparable numbers of retrogradely traced motor neurons in the spinal cord (Figure 14) exclude that the rearranged motor pools are a secondary effect due to the loss of dislocated motor neurons during the period of naturally occurring cell death in late embryonic or early postnatal stage (Hollyday & Hamburger, 1976; Sendtner *et al.*, 2000). After birth, newborn pups begin to walk during postnatal day 12-21 (Heyser, 2004) and an active use of objects like the running wheel or the mini step ladder is not adequately possible before that phase. In our experimental settings, this would only leave a period of one week in which the described plastic changes have to take place. However, several studies have already described the

influence of enriched environment housing on maternal care behavior. It was shown that mothers that are housed in an enriched environment provide more physical contact to their pups as well as enhanced licking and grooming activities, and that these alterations in maternal care behavior can induce brain plasticity (Liu *et al.*, 2000; Sale *et al.*, 2004). Interestingly, mimicking the described increase in tactile stimulation by specifically developed massage protocols can induce the same plastic changes as enriched housing (Guzzetta *et al.*, 2009). Thus, already in neonatal pups enriched environment housing can indirectly induce activity-dependent mechanisms that cause plasticity in neuronal circuits.

In order to further narrow down the critical period in which the ventrally projecting motor pool of *Sema3F* mutants are rearranged it is therefore necessary to investigate the postnatal development of the motor neurons in more detail. Hence, it would be interesting to see the resulting effects of an enriched environment housing that starts at one, two or three weeks after birth in order to constrict the time frame of the critical period. Additionally, the early postnatal development of the Npn2 expressing LMCm motor pool might be analyzed by lineage tracing. For this purpose crossing the Npn2 reporter line (Takashima *et al.*, 2002) with *Sema3F* mice would allow for LacZ staining of the Npn2 expressing LMCm neurons. This approach is independent from a muscle specific tracing and thereby allows for comparability between all *Sema3F* mutants. Thus, it would be possible to investigate the rearrangements in the pool during postnatal development and follow the changes in motor neuron positioning that will be reflected by a continuous reduction of the scatter index.

V.2.3. The closure of the critical period in the spinal motor system of *Sema3F* mutants is not affected by enriched environment housing

Neuroanatomical and behavioral studies have provided evidence for the existence of a critical period for adaptive plasticity in the motor system of *Sema3F* mutants. However, the results did not grant insights into the underlying mechanisms that govern those sensitive periods. It has been shown that the closure of critical periods depends on two different factors: (1) the formation of structural barriers that limit the establishment of new synaptic connections, and (2) the ratio of excitatory-inhibitory synapses that is determined by a specific threshold of inhibitory synaptic input (Bavelier *et al.*, 2010). Therefore, we analyzed those factors in the developing spinal cord of *Sema3F* mutants.

V.2.3.1. Perineuronal nets are unlikely to play a role in the regulation of plasticity in Sema3F mutants

Structural brakes in the shape of perineuronal nets (PNNs) have been shown to limit plasticity in various neuronal circuits (Pizzorusso *et al.*, 2002; Kwok *et al.*, 2011; Wang & Fawcett, 2012). Furthermore, enriched environment housing has been shown to have an enhancing (Simonetti *et al.*, 2009) or suppressing (Bartoletti *et al.*, 2004; Foscarin *et al.*, 2011) effect on the formation of PNNs and consequently to influence the timing of the critical period in those model systems. Surprisingly, however, in the spinal motor system of *Sema3F* mutants we found that after closure of the critical period at the age of 4 weeks, about 65% of all labeled motor neurons were not covered by PNNs and only about 5% revealed strong nets of this specialized form of extracellular matrix. This picture is corroborated by a study that examined the distribution of extracellular matrix components within the adult spinal cord of rats and found that only about 30% of the motor neurons in the ventral horn exhibit PNNs (Galtrey *et al.*, 2008). This indicates that the formation of PNNs is very unlikely to play an important role in the regulation of adaptive plasticity in the spinal motor system of *Sema3F* mutants. Moreover, our data reveal no significant difference in the development of PNNs between the different housing groups (Figure 16), suggesting that their formation in the spinal cord is not affected by activity-dependent mechanisms and enriched environment housing does not influence the timing of the critical period by manipulating the formation of structural barriers.

Nevertheless, 35% of the analyzed motor neurons in the ventral horn do form PNNs. So, even if enriched environment housing does not affect the closure of the critical period, it remains unclear to which extent the formation of those nets per se is involved in critical period regulation in the spinal motor system of *Sema3F* mutants. In order to investigate this interesting question it might be suitable to destroy the PNNs in the spinal cord of adult animals by bilateral injection of the enzyme ChondroitinaseABC into the ventral horn (Bradbury *et al.*, 2002; Galtrey *et al.*, 2007). If PNNs are involved in the control of the critical period in *Sema3F* spinal cords this should open a new window of opportunity and subsequent enriched environment housing should be able to induce an improvement in motor coordination and neuroanatomical changes in their ventrally projecting motor pools.

V.2.3.2. The formation of excitatory but not inhibitory synapses is induced by enriched environment housing in Sema3F mutants

As mentioned above, also the balance of excitatory and inhibitory synaptic input has been shown to affect the critical period in the nervous system (Murphy *et al.*, 2005; Bavelier *et al.*, 2010). During development, first, excitation dominates the activity of neuronal circuits, which is later regulated by the formation of inhibitory synapses. Accordingly, the maturation and consequently also the plastic capability of a neuron is controlled by the generation of inhibitory synaptic input. Additionally, it has been shown that specific inhibitory thresholds exist that regulate the opening and closure of the critical period for adaptive plasticity (Fagiolini & Hensch, 2000; Berardi *et al.*, 2003). Interestingly, we found no change in the number of excitatory and inhibitory synapses between *Sema3F* mutants and their wildtype littermates, indicating that synapse formation is not affected in the spinal motor system of these animals. Furthermore, our results show no difference in the number of inhibitory synapses on ventrally projecting motor neurons of *Sema3F* mice after normal or enriched housing starting at birth. Due to the described link between inhibitory thresholds and the timing of critical periods, it is therefore unlikely that enriched environment housing has an influence on the regulation of the critical period in the motor system of *Sema3F* mutants, which further corroborates the findings after analysis of PNN formation under different housing conditions.

Nevertheless, enriched environment housing caused a shift of the excitatory-inhibitory synaptic balance in the medial LMC pool. This shift is caused by the formation of additional excitatory synapses due to an increased activity of the animals. The result is supported by various studies, which show that neuronal circuits are shaped by experience during postnatal development (Nithianantharajah & Hannan, 2006; Carulli *et al.*, 2011; Bengoetxea *et al.*, 2012). Analysis of the influence of activity-dependent mechanisms on synaptic connections suggests that enriched environment housing can modify the excitatory synaptic density in cerebellum and cortex (van Praag *et al.*, 2000; Lonetti *et al.*, 2010). Furthermore, motor training has been shown to alter motor neuron excitability and induce synaptogenesis in the spinal cord. Interestingly, also here only the number of excitatory synapses was increased, while inhibitory synapses were not affected (Adkins *et al.*, 2006), which corroborates the effects of enriched environment housing in *Sema3F* mice.

In summary, these results show that environmental enrichment does not influence critical period regulation in the spinal motor system of *Sema3F* mutants, however, it induces activity-dependent plastic changes that are evident by the formation of excitatory synapses on ventrally projecting motor neurons.

V.2.4. Regulation of activity-dependent plastic adaptations

Investigation of environmental factors that can affect the development of neuronal circuits and behavior has started decades ago (Rosenzweig *et al.*, 1978). Since then the influence of activity-based mechanisms on neuronal plasticity has been proven for numerous systems, such as the hippocampus or different cortical areas (van Praag *et al.*, 2000; Nithianantharajah & Hannan, 2006), but the mechanisms that govern these plastic changes are still not completely understood. On the molecular level, neurotrophic factors and N-methyl-D-aspartate (NMDA) receptors are the most promising candidates to cause these manipulations (Berardi *et al.*, 2003). In order to gain further insights in the mechanisms regulating adaptive plasticity in the motor system of *Sema3F* mutants it might, therefore, be interesting to specifically investigate the involvement of these factors.

V.2.4.1. BDNF and spinal cord plasticity

Among the neurotrophins, brain-derived neurotrophic factor (BDNF) has been in the focus of many studies, which investigated the regulation of adaptive plasticity. Indeed, BDNF levels in motor neurons of the lumbar spinal cord are increased by treadmill training (Joseph *et al.*, 2012) and in the visual cortex BDNF has been shown to influence adaptive plasticity during the critical period (Berardi *et al.*, 2003). However, a study in transgenic mice that overexpress BDNF reveals an accelerated maturation of inhibitory synapses. Consequently, the increased BDNF levels in the visual cortex of these mice lead to a faster termination of the critical period for cortical plasticity (Huang *et al.*, 1999). This makes it unlikely that BDNF is involved in the plastic rearrangements of spinal motor neurons in *Sema3F* mice, since our experiments showed that inhibitory synapses are unchanged and the timing of the critical period is not affected.

V.2.4.2. Effects of glutamatergic synaptic transmission

NMDA receptors have been connected to activity-dependent plasticity in the nervous system ever since their discovery (Berardi *et al.*, 2003; Hensch, 2004; Tahayori & Koceja, 2012). Interestingly, the receptor is transiently expressed in the ventral horn of the spinal cord with a high expression level at postnatal day 7 that gets reduced in the following weeks (Kalb *et al.*, 1992). Since we found a critical period for adaptive plasticity in the spinal motor system within the first 4 postnatal weeks this similar time course might suggest an involvement of NMDA receptors in the observed plastic rearrangements in *Sema3F* mutants. In addition, the same research group also showed that blocking NMDA receptors during the second and third postnatal week with the antagonist MK-801 resulted in morphological changes of spinal motor neurons (Kalb, 1994). For this reason, it might be interesting to investigate if the effects of enriched environment housing starting at birth can be prevented by blocking the NMDA receptors during this time. I have started an experiment addressing this question, however, the systemic application of MK-801 by i.p. injection as described (Kalb, 1994) resulted in an substantial increase in postnatal mortality, thereby prohibiting subsequent neuroanatomical and behavioral experiments. Consequently, it might be more suitable to apply the NMDA receptor antagonist directly to the ventral horn. Unfortunately, however, the lack of adequate anesthesia protocols for early postnatal mice makes it technically very challenging to perform surgeries with animals this young and therefore a prolonged spatially restricted administration of the antagonist, for example by implantation of an osmotic minipump (Gomez-Pinilla *et al.*, 1989) or of a silastic tube for multiple postoperative injections into the spinal cord (Bradbury *et al.*, 2002), is not feasible. Thus, i.p. injections using lower MK-801 concentrations or only every second day might help to decrease the mortality of *Sema3F* mutant pups and allow for the analysis of enriched environment induced effects after NMDA receptor blocking.

V.2.5. Relevance of plasticity within the sensory-motor cortex of *Sema3F* mutants

In our study we show that enriched environment housing starting at birth causes a structural rearrangement of the ventrally projecting spinal motor pool in *Sema3F* mutants that correlates with an improvement of motor coordination. However, since also normally housed mutants show a significant improvement of their motor performance between 4 and 12 weeks of age motor learning might also be involved and contribute to the compensation of their behavioral impairments (Parker, 2000; Sanes & Donoghue, 2000). However, since animals that were

tested only at a single time point at the age of 8 or 12 weeks show the same age-matched results as animals that were tested at all time points, it is unlikely that the improved motor performance was caused by task specific motor learning (Soellner, 2012; Helmbrecht *et al.*, 2015b (accepted)). Furthermore, we showed that the critical period for adaptive plasticity is closed at 4 weeks of age and that the rearrangement of the ventrally projecting motor pool in normally housed *Sema3F* mutants is equally evident at the age of 4 and 12 weeks (Soellner, 2012; Helmbrecht *et al.*, 2015b (accepted)). This suggests that the observed behavioral amelioration is not caused by structural adaptations within the spinal cord.

Since motor learning is not restricted to a critical period during early postnatal development (Donoghue, 1995) it is plausible that changes in the cerebral cortex are possible between the postnatal weeks 4 and 12 and that these changes might allow *Sema3F* mutants to compensate for their neuroanatomical impairments. Hence, it would be interesting to investigate if plastic changes in the cortical motor areas are the underlying reason for the improved motor coordination in *Sema3F* mutants. This could be accomplished by muscle specific transsynaptic retrograde tracing of motor areas using the rabies virus (Kelly & Strick, 2000). However, working with the wild virus (SVC-11) requires strict biosafety and animal care protocols. Furthermore, due to the unlimited distribution of the virus through the nervous system, the determination of direct and indirect connectivity depends on the uncertain parameter of "time after injection" (Arber, 2012). In order to overcome these problems attenuated virus variants lacking the glycoprotein (Gly), which is essential for transsynaptic spreading, were generated and monosynaptic spread of the virus was established by genetic or viral introduction of Gly expression in selected cells (Wickersham *et al.*, 2007; Callaway, 2008). Unfortunately, using the attenuated rabies virus successful muscle specific tracings have only been described in the early postnatal stage (P0-P10) and also extensive trials in our lab did not allow for successful tracings in older animals (Stepien *et al.*, 2010). However, even though this elegant approach cannot be applied in order to investigate the respective cortical motor areas in adult mice, other methods might help for an approximation of this issue. In this respect, the use of genetically encoded GCaMP calcium indicators might allow for the investigation of neural activity in the cerebral cortex of moving mice (Tian *et al.*, 2009). With this approach the muscle specificity will be lost, however, it might allow for a more detailed analysis of the cortical activity in *Sema3F* animals during treadmill walking and thereby contribute to the understanding of mechanisms underlying the behavioral differences of *Sema3F* mutants after normal or enriched environment housing.

V.2.6. Conclusion

In conclusion, our data reveal a critical period for adaptive plasticity in the spinal motor system of *Sema3F* mutants. Thus, within the first four postnatal weeks, enriched environment housing is able to induce rearrangements of the ventrally projecting motor pool and improvements in motor coordination. After this critical phase, the window of opportunity has closed and enriched environment housing does no longer affect motor skills or neuroanatomical organization in the brachial spinal cord. Additionally, we showed that within the critical period activity-dependent mechanisms induce synaptogenesis on LMCm neurons, which causes a significant increase in the number of excitatory synapses. How these changes in synaptic connectivity are related to the observed improvements in motor coordination and which mechanisms cause the reorganization of the ventrally projecting motor pool remains to be clarified. However, an influence on the timing of the critical period can be excluded, since inhibitory synapses and perineuronal nets, which have been shown to be involved in critical period regulation, are not altered by changes in the housing conditions.

VI. REFERENCES

(1999) Unified nomenclature for the semaphorins/collapsins. Semaphorin Nomenclature Committee. *Cell*, **97**, 551-552.

Adkins, D.L., Boychuk, J., Remple, M.S. & Kleim, J.A. (2006) Motor training induces experience-specific patterns of plasticity across motor cortex and spinal cord. *Journal of applied physiology*, **101**, 1776-1782.

Arber, S. (2012) Motor circuits in action: specification, connectivity, and function. *Neuron*, **74**, 975-989.

Baehrecke, E.H. (2002) How death shapes life during development. *Nature reviews. Molecular cell biology*, **3**, 779-787.

Barbeau, H. & Rossignol, S. (1987) Recovery of locomotion after chronic spinalization in the adult cat. *Brain research*, **412**, 84-95.

Barkat, T.R., Polley, D.B. & Hensch, T.K. (2011) A critical period for auditory thalamocortical connectivity. *Nat Neurosci*, **14**, 1189-1194.

Bartoletti, A., Medini, P., Berardi, N. & Maffei, L. (2004) Environmental enrichment prevents effects of dark-rearing in the rat visual cortex. *Nat Neurosci*, **7**, 215-216.

Bavelier, D., Levi, D.M., Li, R.W., Dan, Y. & Hensch, T.K. (2010) Removing brakes on adult brain plasticity: from molecular to behavioral interventions. *J Neurosci*, **30**, 14964-14971.

Bear, M.F. (1996) NMDA-receptor-dependent synaptic plasticity in the visual cortex. *Progress in brain research*, **108**, 205-218.

Bengoetxea, H., Ortuzar, N., Bulnes, S., Rico-Barrio, I., Lafuente, J.V. & Argandona, E.G. (2012) Enriched and deprived sensory experience induces structural changes and rewires connectivity during the postnatal development of the brain. *Neural plasticity*, **2012**, 305693.

Berardi, N., Pizzorusso, T., Ratto, G.M. & Maffei, L. (2003) Molecular basis of plasticity in the visual cortex. *Trends in neurosciences*, **26**, 369-378.

Bermingham, J.R., Jr., Shearin, H., Pennington, J., O'Moore, J., Jaegle, M., Driegen, S., van Zon, A., Darbas, A., Ozkaynak, E., Ryu, E.J., Milbrandt, J. & Meijer, D. (2006) The claw paw mutation reveals a role for Lgi4 in peripheral nerve development. *Nat Neurosci*, **9**, 76-84.

Bernstein, M. & Lichtman, J.W. (1999) Axonal atrophy: the retraction reaction. *Curr Opin Neurobiol*, **9**, 364-370.

Berrocal, Y., Pearse, D.D., Singh, A., Andrade, C.M., McBroom, J.S., Puentes, R. & Eaton, M.J. (2007) Social and environmental enrichment improves sensory and motor recovery after severe contusive spinal cord injury in the rat. *Journal of neurotrauma*, **24**, 1761-1772.

Bjursten, L.M., Norrsell, K. & Norrsell, U. (1976) Behavioural repertory of cats without cerebral cortex from infancy. *Experimental brain research. Experimentelle Hirnforschung. Experimentation cerebrale*, **25**, 115-130.

Bonanomi, D. & Pfaff, S.L. (2010) Motor axon pathfinding. *Cold Spring Harbor perspectives in biology*, **2**, a001735.

Bose, M., Munoz-Llancao, P., Roychowdhury, S., Nichols, J.A., Jakkamsetti, V., Porter, B., Byrapureddy, R., Salgado, H., Kilgard, M.P., Aboitiz, F., Dagnino-Subiabre, A. & Atzori, M. (2010) Effect of the environment on the dendritic morphology of the rat auditory cortex. *Synapse*, **64**, 97-110.

Bradbury, E.J., Moon, L.D., Popat, R.J., King, V.R., Bennett, G.S., Patel, P.N., Fawcett, J.W. & McMahon, S.B. (2002) Chondroitinase ABC promotes functional recovery after spinal cord injury. *Nature*, **416**, 636-640.

Brose, K., Bland, K.S., Wang, K.H., Arnott, D., Henzel, W., Goodman, C.S., Tessier-Lavigne, M. & Kidd, T. (1999) Slit proteins bind Robo receptors and have an evolutionarily conserved role in repulsive axon guidance. *Cell*, **96**, 795-806.

Brown, T.G. (1914) On the nature of the fundamental activity of the nervous centres; together with an analysis of the conditioning of rhythmic activity in progression, and a theory of the evolution of function in the nervous system. *The Journal of physiology*, **48**, 18-46.

Callaway, E.M. (2008) Transneuronal circuit tracing with neurotropic viruses. *Curr Opin Neurobiol*, **18**, 617-623.

Carulli, D., Foscarin, S. & Rossi, F. (2011) Activity-dependent plasticity and gene expression modifications in the adult CNS. *Frontiers in molecular neuroscience*, **4**, 50.

Castellani, V. (2002) The function of neuropilin/L1 complex. *Advances in experimental medicine and biology*, **515**, 91-102.

Chauvet, S., Cohen, S., Yoshida, Y., Fekrane, L., Livet, J., Gayet, O., Segu, L., Buhot, M.C., Jessell, T.M., Henderson, C.E. & Mann, F. (2007) Gating of Sema3E/PlexinD1 signaling by neuropilin-1 switches axonal repulsion to attraction during brain development. *Neuron*, **56**, 807-822.

Chen, H.H., Hippenmeyer, S., Arber, S. & Frank, E. (2003) Development of the monosynaptic stretch reflex circuit. *Curr Opin Neurobiol*, **13**, 96-102.

Cioni, J.M., Telley, L., Saywell, V., Cadilhac, C., Jourdan, C., Huber, A.B., Huang, J.Z., Jahannault-Talignani, C. & Ango, F. (2013) SEMA3A signaling controls layer-specific interneuron branching in the cerebellum. *Current biology : CB*, **23**, 850-861.

Claudepierre, T., Koncina, E., Pfrieger, F.W., Bagnard, D., Aunis, D. & Reber, M. (2008) Implication of neuropilin 2/semaphorin 3F in retinocollicular map formation. *Dev Dyn*, **237**, 3394-3403.

Cloutier, J.F., Sahay, A., Chang, E.C., Tessier-Lavigne, M., Dulac, C., Kolodkin, A.L. & Ginty, D.D. (2004) Differential requirements for semaphorin 3F and Slit-1 in axonal targeting, fasciculation, and segregation of olfactory sensory neuron projections. *J Neurosci*, **24**, 9087-9096.

Cohen, R.I., Rottkamp, D.M., Maric, D., Barker, J.L. & Hudson, L.D. (2003) A role for semaphorins and neuropilins in oligodendrocyte guidance. *Journal of neurochemistry*, **85**, 1262-1278.

Cohen, S. & Levi-Montalcini, R. (1956) A Nerve Growth-Stimulating Factor Isolated from Snake Venom. *Proc Natl Acad Sci U S A*, **42**, 571-574.

Coq, J.O. & Xerri, C. (1998) Environmental enrichment alters organizational features of the forepaw representation in the primary somatosensory cortex of adult rats. *Experimental brain research. Experimentelle Hirnforschung. Experimentation cerebrale*, **121**, 191-204.

Darbas, A., Jaegle, M., Walbeehm, E., van den Burg, H., Driegen, S., Broos, L., Uyl, M., Visser, P., Grosveld, F. & Meijer, D. (2004) Cell autonomy of the mouse claw paw mutation. *Dev Biol*, **272**, 470-482.

Dessaud, E., Yang, L.L., Hill, K., Cox, B., Ulloa, F., Ribeiro, A., Mynett, A., Novitch, B.G. & Briscoe, J. (2007) Interpretation of the sonic hedgehog morphogen gradient by a temporal adaptation mechanism. *Nature*, **450**, 717-720.

Donoghue, J.P. (1995) Plasticity of adult sensorimotor representations. *Curr Opin Neurobiol*, **5**, 749-754.

Edgerton, V.R., Tillakaratne, N.J., Bigbee, A.J., de Leon, R.D. & Roy, R.R. (2004) Plasticity of the spinal neural circuitry after injury. *Annual review of neuroscience*, **27**, 145-167.

Eisen, J.S. (1999) Patterning motoneurons in the vertebrate nervous system. *Trends in neurosciences*, **22**, 321-326.

Epstein, J.A., Aghajanian, H. & Singh, M.K. (2015) Semaphorin Signaling in Cardiovascular Development. *Cell Metab*, **21**, 163-173.

Fagiolini, M. & Hensch, T.K. (2000) Inhibitory threshold for critical-period activation in primary visual cortex. *Nature*, **404**, 183-186.

Fantin, A., Herzog, B., Mahmoud, M., Yamaji, M., Plein, A., Denti, L., Ruhrberg, C. & Zachary, I. (2014) Neuropilin 1 (NRP1) hypomorphism combined with defective VEGF-A binding reveals novel roles for NRP1 in developmental and pathological angiogenesis. *Development*, **141**, 556-562.

Fiala, J.C. (2005) Reconstruct: a free editor for serial section microscopy. *Journal of microscopy*, **218**, 52-61.

Foscarin, S., Ponchione, D., Pajaj, E., Leto, K., Gawlak, M., Wilczynski, G.M., Rossi, F. & Carulli, D. (2011) Experience-dependent plasticity and modulation of growth regulatory molecules at central synapses. *PLoS One*, **6**, e16666.

Galtrey, C.M., Asher, R.A., Nothias, F. & Fawcett, J.W. (2007) Promoting plasticity in the spinal cord with chondroitinase improves functional recovery after peripheral nerve repair. *Brain : a journal of neurology*, **130**, 926-939.

Galtrey, C.M., Kwok, J.C., Carulli, D., Rhodes, K.E. & Fawcett, J.W. (2008) Distribution and synthesis of extracellular matrix proteoglycans, hyaluronan, link proteins and tenascin-R in the rat spinal cord. *Eur J Neurosci*, **27**, 1373-1390.

Gherardi, E., Love, C.A., Esnouf, R.M. & Jones, E.Y. (2004) The sema domain. *Curr Opin Struct Biol*, **14**, 669-678.

Glinka, Y. & Prud'homme, G.J. (2008) Neuropilin-1 is a receptor for transforming growth factor beta-1, activates its latent form, and promotes regulatory T cell activity. *Journal of leukocyte biology*, **84**, 302-310.

Gomez-Pinilla, F., Tram, H., Cotman, C.W. & Nieto-Sampedro, M. (1989) Neuroprotective effect of MK-801 and U-50488H after contusive spinal cord injury. *Experimental neurology*, **104**, 118-124.

Gonzalez de Aguilar, J.L., Echaniz-Laguna, A., Fergani, A., Rene, F., Meininger, V., Loeffler, J.P. & Dupuis, L. (2007) Amyotrophic lateral sclerosis: all roads lead to Rome. *Journal of neurochemistry*, **101**, 1153-1160.

Gould, T.W. & Enomoto, H. (2009) Neurotrophic modulation of motor neuron development. *The Neuroscientist : a review journal bringing neurobiology, neurology and psychiatry*, **15**, 105-116.

Graybiel, A.M., Aosaki, T., Flaherty, A.W. & Kimura, M. (1994) The basal ganglia and adaptive motor control. *Science*, **265**, 1826-1831.

Grillner, S., Hellgren, J., Menard, A., Saitoh, K. & Wikstrom, M.A. (2005) Mechanisms for selection of basic motor programs--roles for the striatum and pallidum. *Trends in neurosciences*, **28**, 364-370.

Gu, C., Rodriguez, E.R., Reimert, D.V., Shu, T., Fritzsch, B., Richards, L.J., Kolodkin, A.L. & Ginty, D.D. (2003) Neuropilin-1 conveys semaphorin and VEGF signaling during neural and cardiovascular development. *Dev Cell*, **5**, 45-57.

Guzzetta, A., Baldini, S., Bancale, A., Baroncelli, L., Ciucci, F., Ghirri, P., Putignano, E., Sale, A., Viegi, A., Berardi, N., Boldrini, A., Cioni, G. & Maffei, L. (2009) Massage accelerates brain development and the maturation of visual function. *J Neurosci*, **29**, 6042-6051.

Hamburger, V. (1958) Regression versus peripheral control of differentiation in motor hypoplasia. *The American journal of anatomy*, **102**, 365-409.

Hamburger, V. (1975) Cell death in the development of the lateral motor column of the chick embryo. *The Journal of comparative neurology*, **160**, 535-546.

Hamburger, V. & Levi-Montalcini, R. (1949) Proliferation, differentiation and degeneration in the spinal ganglia of the chick embryo under normal and experimental conditions. *The Journal of experimental zoology*, **111**, 457-501.

Haupt, C., Kloos, K., Faus-Kessler, T. & Huber, A.B. (2010) Semaphorin 3A-Neuropilin-1 signaling regulates peripheral axon fasciculation and pathfinding but not developmental cell death patterns. *Eur J Neurosci*, **31**, 1164-1172.

Heffner, R.S. & Masterton, R.B. (1983) The role of the corticospinal tract in the evolution of human digital dexterity. *Brain, behavior and evolution*, **23**, 165-183.

Helmbrecht, M.S., Soellner, H., Truckenbrodt, A.M., Sundermeier, J., Cohrs, C., Hans, W., de Angelis, M.H., Feuchtinger, A., Aichler, M., Fouad, K. & Huber, A.B. (2015a) Loss of Npn1 from motor neurons causes postnatal deficits independent from Sema3A signaling. *Dev Biol*, **399**, 2-14.

Helmbrecht, M.S., Soellner H., Castiblanco-Urbina M. A., Winzeck S., Sundermeier J., Theis F.J., Fouad K. & A.B., H. (2015b) A critical period for postnatal adaptive plasticity in a model of motor axon miswiring. *PLoS One*,(accepted).

Henry, E.W., Eicher, E.M. & Sidman, R.L. (1991) The mouse mutation claw paw: forelimb deformity and delayed myelination throughout the peripheral nervous system. *The Journal of heredity*, **82**, 287-294.

Hensch, T.K. (2004) Critical period regulation. *Annual review of neuroscience*, **27**, 549-579.

Heyser, C.J. (2004) Assessment of developmental milestones in rodents. *Current protocols in neuroscience / editorial board, Jacqueline N. Crawley ... [et al.]*, **Chapter 8**, Unit 8 18.

Hollyday, M. & Hamburger, V. (1976) Reduction of the naturally occurring motor neuron loss by enlargement of the periphery. *The Journal of comparative neurology*, **170**, 311-320.

Huang, Z.J., Kirkwood, A., Pizzorusso, T., Porciatti, V., Morales, B., Bear, M.F., Maffei, L. & Tonegawa, S. (1999) BDNF regulates the maturation of inhibition and the critical period of plasticity in mouse visual cortex. *Cell*, **98**, 739-755.

Hubel, D.H. & Wiesel, T.N. (1970) The period of susceptibility to the physiological effects of unilateral eye closure in kittens. *The Journal of physiology*, **206**, 419-436.

Huber, A.B., Kania, A., Tran, T.S., Gu, C., De Marco Garcia, N., Lieberam, I., Johnson, D., Jessell, T.M., Ginty, D.D. & Kolodkin, A.L. (2005) Distinct roles for secreted semaphorin signaling in spinal motor axon guidance. *Neuron*, **48**, 949-964.

Huber, A.B., Kolodkin, A.L., Ginty, D.D. & Cloutier, J.F. (2003) Signaling at the growth cone: ligand-receptor complexes and the control of axon growth and guidance. *Annual review of neuroscience*, **26**, 509-563.

Huettl, R.E., Soellner, H., Bianchi, E., Novitch, B.G. & Huber, A.B. (2011) Npn-1 contributes to axon-axon interactions that differentially control sensory and motor innervation of the limb. *PLoS biology*, **9**, e1001020.

Jackman, R.W. & Kandarian, S.C. (2004) The molecular basis of skeletal muscle atrophy. *American journal of physiology. Cell physiology*, **287**, C834-843.

Jessell, T.M. (2000) Neuronal specification in the spinal cord: inductive signals and transcriptional codes. *Nature reviews. Genetics*, **1**, 20-29.

Joseph, M.S., Tillakaratne, N.J. & de Leon, R.D. (2012) Treadmill training stimulates brain-derived neurotrophic factor mRNA expression in motor neurons of the lumbar spinal cord in spinally transected rats. *Neuroscience*, **224**, 135-144.

Kalb, R.G. (1994) Regulation of motor neuron dendrite growth by NMDA receptor activation. *Development*, **120**, 3063-3071.

Kalb, R.G., Lidow, M.S., Halsted, M.J. & Hockfield, S. (1992) N-methyl-D-aspartate receptors are transiently expressed in the developing spinal cord ventral horn. *Proc Natl Acad Sci U S A*, **89**, 8502-8506.

Kao, T.J., Law, C. & Kania, A. (2012) Eph and ephrin signaling: lessons learned from spinal motor neurons. *Seminars in cell & developmental biology*, **23**, 83-91.

Kawasaki, T., Kitsukawa, T., Bekku, Y., Matsuda, Y., Sanbo, M., Yagi, T. & Fujisawa, H. (1999) A requirement for neuropilin-1 in embryonic vessel formation. *Development*, **126**, 4895-4902.

Keino-Masu, K., Masu, M., Hinck, L., Leonardo, E.D., Chan, S.S., Culotti, J.G. & Tessier-Lavigne, M. (1996) Deleted in Colorectal Cancer (DCC) encodes a netrin receptor. *Cell*, **87**, 175-185.

Kelly, R.M. & Strick, P.L. (2000) Rabies as a transneuronal tracer of circuits in the central nervous system. *Journal of neuroscience methods*, **103**, 63-71.

Kitsukawa, T., Shimizu, M., Sanbo, M., Hirata, T., Taniguchi, M., Bekku, Y., Yagi, T. & Fujisawa, H. (1997) Neuropilin-semaphorin III/D-mediated chemorepulsive signals play a crucial role in peripheral nerve projection in mice. *Neuron*, **19**, 995-1005.

Kolodkin, A.L., Levengood, D.V., Rowe, E.G., Tai, Y.T., Giger, R.J. & Ginty, D.D. (1997) Neuropilin is a semaphorin III receptor. *Cell*, **90**, 753-762.

Kolodkin, A.L., Matthes, D.J., O'Connor, T.P., Patel, N.H., Admon, A., Bentley, D. & Goodman, C.S. (1992) Fasciclin IV: sequence, expression, and function during growth cone guidance in the grasshopper embryo. *Neuron*, **9**, 831-845.

Kolodkin, A.L. & Tessier-Lavigne, M. (2011) Mechanisms and molecules of neuronal wiring: a primer. *Cold Spring Harbor perspectives in biology*, **3**.

Koszowski, A.G., Owens, G.C. & Levinson, S.R. (1998) The effect of the mouse mutation claw paw on myelination and nodal frequency in sciatic nerves. *J Neurosci*, **18**, 5859-5868.

Kraft, G.H. (1990) Fibrillation potential amplitude and muscle atrophy following peripheral nerve injury. *Muscle & nerve*, **13**, 814-821.

Kuchler, M., Fouad, K., Weinmann, O., Schwab, M.E. & Raineteau, O. (2002) Red nucleus projections to distinct motor neuron pools in the rat spinal cord. *The Journal of comparative neurology*, **448**, 349-359.

Kwok, J.C., Dick, G., Wang, D. & Fawcett, J.W. (2011) Extracellular matrix and perineuronal nets in CNS repair. *Developmental neurobiology*, **71**, 1073-1089.

Landmesser, L.T. (2001) The acquisition of motoneuron subtype identity and motor circuit formation. *International journal of developmental neuroscience : the official journal of the International Society for Developmental Neuroscience*, **19**, 175-182.

Lee, S.K. & Pfaff, S.L. (2001) Transcriptional networks regulating neuronal identity in the developing spinal cord. *Nat Neurosci*, **4 Suppl**, 1183-1191.

Lemon, R.N. (2008) Descending pathways in motor control. *Annual review of neuroscience*, **31**, 195-218.

Liu, D., Diorio, J., Day, J.C., Francis, D.D. & Meaney, M.J. (2000) Maternal care, hippocampal synaptogenesis and cognitive development in rats. *Nat Neurosci*, **3**, 799-806.

Lonetti, G., Angelucci, A., Morando, L., Boggio, E.M., Giustetto, M. & Pizzorusso, T. (2010) Early environmental enrichment moderates the behavioral and synaptic phenotype of MeCP2 null mice. *Biological psychiatry*, **67**, 657-665.

Luo, L. & O'Leary, D.D. (2005) Axon retraction and degeneration in development and disease. *Annual review of neuroscience*, **28**, 127-156.

Luo, Y., Raible, D. & Raper, J.A. (1993) Collapsin: a protein in brain that induces the collapse and paralysis of neuronal growth cones. *Cell*, **75**, 217-227.

Maden, C.H., Gomes, J., Schwarz, Q., Davidson, K., Tinker, A. & Ruhrberg, C. (2012) NRP1 and NRP2 cooperate to regulate gangliogenesis, axon guidance and target innervation in the sympathetic nervous system. *Dev Biol*, **369**, 277-285.

Maier, I.C. & Schwab, M.E. (2006) Sprouting, regeneration and circuit formation in the injured spinal cord: factors and activity. *Philosophical transactions of the Royal Society of London. Series B, Biological sciences*, **361**, 1611-1634.

Marder, E. & Bucher, D. (2001) Central pattern generators and the control of rhythmic movements. *Current biology : CB*, **11**, R986-996.

Masahira, N., Takebayashi, H., Ono, K., Watanabe, K., Ding, L., Furusho, M., Ogawa, Y., Nabeshima, Y., Alvarez-Buylla, A., Shimizu, K. & Ikenaka, K. (2006) Olig2-positive progenitors in the embryonic spinal cord give rise not only to motoneurons and oligodendrocytes, but also to a subset of astrocytes and ependymal cells. *Dev Biol*, **293**, 358-369.

Miller, M.W. (1987) The origin of corticospinal projection neurons in rat. *Experimental brain research. Experimentelle Hirnforschung. Experimentation cerebrale*, **67**, 339-351.

Murphy, K.M., Beston, B.R., Boley, P.M. & Jones, D.G. (2005) Development of human visual cortex: a balance between excitatory and inhibitory plasticity mechanisms. *Developmental psychobiology*, **46**, 209-221.

Naka, F., Narita, N., Okado, N. & Narita, M. (2005) Modification of AMPA receptor properties following environmental enrichment. *Brain & development*, **27**, 275-278.

Nasarre, P., Gemmill, R.M. & Drabkin, H.A. (2014) The emerging role of class-3 semaphorins and their neuropilin receptors in oncology. *Onco Targets Ther*, **7**, 1663-1687.

Nelson, P.G., Fields, R.D., Yu, C. & Neale, E.A. (1990) Mechanisms involved in activity-dependent synapse formation in mammalian central nervous system cell cultures. *Journal of neurobiology*, **21**, 138-156.

Neufeld, G. & Kessler, O. (2008) The semaphorins: versatile regulators of tumour progression and tumour angiogenesis. *Nature reviews. Cancer*, **8**, 632-645.

Nithianantharajah, J. & Hannan, A.J. (2006) Enriched environments, experience-dependent plasticity and disorders of the nervous system. *Nature reviews. Neuroscience*, **7**, 697-709.

O'Malley, A.M., Shanley, D.K., Kelly, A.T. & Barry, D.S. (2014) Towards an understanding of semaphorin signalling in the spinal cord. *Gene*, **553**, 69-74.

Parker, D. (2000) Spinal-Cord plasticity: independent and interactive effects of neuromodulator and activity-dependent plasticity. *Molecular neurobiology*, **22**, 55-80.

Pearson, K.G., Acharya, H. & Fouad, K. (2005) A new electrode configuration for recording electromyographic activity in behaving mice. *Journal of neuroscience methods*, **148**, 36-42.

Perrot, R., Berges, R., Bocquet, A. & Eyer, J. (2008) Review of the multiple aspects of neurofilament functions, and their possible contribution to neurodegeneration. *Molecular neurobiology*, **38**, 27-65.

Peterson, B.W., Pitts, N.G. & Fukushima, K. (1979) Reticulospinal connections with limb and axial motoneurons. *Experimental brain research. Experimentelle Hirnforschung. Experimentation cerebrale*, **36**, 1-20.

Pham, T.M., Winblad, B., Granholm, A.C. & Mohammed, A.H. (2002) Environmental influences on brain neurotrophins in rats. *Pharmacology, biochemistry, and behavior*, **73**, 167-175.

Phelan, K.A. & Hollyday, M. (1991) Embryonic development and survival of brachial motoneurons projecting to muscleless chick wings. *The Journal of comparative neurology*, **311**, 313-320.

Piper, M., Plachez, C., Zalucki, O., Fothergill, T., Goudreau, G., Erzurumlu, R., Gu, C. & Richards, L.J. (2009) Neuropilin 1-Sema signaling regulates crossing of cingulate pioneering axons during development of the corpus callosum. *Cereb Cortex*, **19 Suppl 1**, i11-21.

Pizzorusso, T., Medini, P., Berardi, N., Chierzi, S., Fawcett, J.W. & Maffei, L. (2002) Reactivation of ocular dominance plasticity in the adult visual cortex. *Science*, **298**, 1248-1251.

Plumier, J.C., Hopkins, D.A., Robertson, H.A. & Currie, R.W. (1997) Constitutive expression of the 27-kDa heat shock protein (Hsp27) in sensory and motor neurons of the rat nervous system. *The Journal of comparative neurology*, **384**, 409-428.

Purves, D., Snider, W.D. & Voyvodic, J.T. (1988) Trophic regulation of nerve cell morphology and innervation in the autonomic nervous system. *Nature*, **336**, 123-128.

Reid, R.L. (1988) Radial nerve palsy. *Hand clinics*, **4**, 179-185.

Ricard, D., Rogemond, V., Charrier, E., Aguera, M., Bagnard, D., Belin, M.F., Thomasset, N. & Honnorat, J. (2001) Isolation and expression pattern of human Unc-33-like phosphoprotein 6/collapsin response mediator protein 5 (Ulip6/CRMP5): coexistence with Ulip2/CRMP2 in Sema3a- sensitive oligodendrocytes. *J Neurosci*, **21**, 7203-7214.

Roffers-Agarwal, J. & Gammill, L.S. (2009) Neuropilin receptors guide distinct phases of sensory and motor neuronal segmentation. *Development*, **136**, 1879-1888.

Rosenzweig, M.R., Bennett, E.L., Hebert, M. & Morimoto, H. (1978) Social grouping cannot account for cerebral effects of enriched environments. *Brain research*, **153**, 563-576.

Sahay, A., Molliver, M.E., Ginty, D.D. & Kolodkin, A.L. (2003) Semaphorin 3F is critical for development of limbic system circuitry and is required in neurons for selective CNS axon guidance events. *J Neurosci*, **23**, 6671-6680.

Sale, A., Putignano, E., Cancedda, L., Landi, S., Cirulli, F., Berardi, N. & Maffei, L. (2004) Enriched environment and acceleration of visual system development. *Neuropharmacology*, **47**, 649-660.

Sanes, J.N. & Donoghue, J.P. (2000) Plasticity and primary motor cortex. *Annual review of neuroscience*, **23**, 393-415.

Schmalbruch, H., Jensen, H.J., Bjaerg, M., Kamieniecka, Z. & Kurland, L. (1991) A new mouse mutant with progressive motor neuronopathy. *Journal of neuropathology and experimental neurology*, **50**, 192-204.

Schwarz, Q., Gu, C., Fujisawa, H., Sabelko, K., Gertsenstein, M., Nagy, A., Taniguchi, M., Kolodkin, A.L., Ginty, D.D., Shima, D.T. & Ruhrberg, C. (2004) Vascular endothelial growth factor controls neuronal migration and cooperates with Sema3A to pattern distinct compartments of the facial nerve. *Genes & development*, **18**, 2822-2834.

Schwarz, Q., Maden, C.H., Davidson, K. & Ruhrberg, C. (2009) Neuropilin-mediated neural crest cell guidance is essential to organise sensory neurons into segmented dorsal root ganglia. *Development*, **136**, 1785-1789.

Sendtner, M., Pei, G., Beck, M., Schweizer, U. & Wiese, S. (2000) Developmental motoneuron cell death and neurotrophic factors. *Cell and tissue research*, **301**, 71-84.

Simonetti, T., Lee, H., Bourke, M., Leamey, C.A. & Sawatari, A. (2009) Enrichment from birth accelerates the functional and cellular development of a motor control area in the mouse. *PLoS One*, **4**, e6780.

Soellner, H. (2012) Developmental wiring and adaptive plasticity of peripheral sensorimotor circuitry (Dissertation) *Helmholtz Zentrum München - German Research Center for Environmental Health; Institute of Developmental Genetics*. Technical University Munich, pp. 160.

Spassky, N., de Castro, F., Le Bras, B., Heydon, K., Queraud-LeSaux, F., Bloch-Gallego, E., Chedotal, A., Zalc, B. & Thomas, J.L. (2002) Directional guidance of oligodendroglial migration by class 3 semaphorins and netrin-1. *J Neurosci*, **22**, 5992-6004.

Stepien, A.E., Tripodi, M. & Arber, S. (2010) Monosynaptic rabies virus reveals premotor network organization and synaptic specificity of cholinergic partition cells. *Neuron*, **68**, 456-472.

Tahayori, B. & Koceja, D.M. (2012) Activity-dependent plasticity of spinal circuits in the developing and mature spinal cord. *Neural plasticity*, **2012**, 964843.

Takashima, S., Kitakaze, M., Asakura, M., Asanuma, H., Sanada, S., Tashiro, F., Niwa, H., Miyazaki Ji, J., Hirota, S., Kitamura, Y., Kitsukawa, T., Fujisawa, H., Klagsbrun, M. & Hori, M. (2002) Targeting of both mouse neuropilin-1 and neuropilin-2 genes severely impairs developmental yolk sac and embryonic angiogenesis. *Proc Natl Acad Sci U S A*, **99**, 3657-3662.

Takebayashi, H., Nabeshima, Y., Yoshida, S., Chisaka, O., Ikenaka, K. & Nabeshima, Y. (2002) The basic helix-loop-helix factor olig2 is essential for the development of motoneuron and oligodendrocyte lineages. *Current biology : CB*, **12**, 1157-1163.

Takesian, A.E. & Hensch, T.K. (2013) Balancing plasticity/stability across brain development. *Progress in brain research*, **207**, 3-34.

Tamagnone, L., Artigiani, S., Chen, H., He, Z., Ming, G.I., Song, H., Chedotal, A., Winberg, M.L., Goodman, C.S., Poo, M., Tessier-Lavigne, M. & Comoglio, P.M. (1999) Plexins are a large family of receptors for transmembrane, secreted, and GPI-anchored semaphorins in vertebrates. *Cell*, **99**, 71-80.

ten Donkelaar, H.J. (1988) Evolution of the red nucleus and rubrospinal tract. *Behav Brain Res*, **28**, 9-20.

Tian, L., Hires, S.A., Mao, T., Huber, D., Chiappe, M.E., Chalasani, S.H., Petreanu, L., Akerboom, J., McKinney, S.A., Schreiter, E.R., Bargmann, C.I., Jayaraman, V., Svoboda, K. & Looger, L.L. (2009) Imaging neural activity in worms, flies and mice with improved GCaMP calcium indicators. *Nature methods*, **6**, 875-881.

Tillo, M., Erskine, L., Cariboni, A., Fantin, A., Joyce, A., Denti, L. & Ruhrberg, C. (2015) VEGF189 binds NRP1 and is sufficient for VEGF/NRP1-dependent neuronal patterning in the developing brain. *Development*, **142**, 314-319.

Tsuchida, T., Ensini, M., Morton, S.B., Baldassare, M., Edlund, T., Jessell, T.M. & Pfaff, S.L. (1994) Topographic organization of embryonic motor neurons defined by expression of LIM homeobox genes. *Cell*, **79**, 957-970.

Vadasz, Z. & Toubi, E. (2014) Semaphorins: their dual role in regulating immune-mediated diseases. *Clin Rev Allergy Immunol*, **47**, 17-25.

van Praag, H., Kempermann, G. & Gage, F.H. (2000) Neural consequences of environmental enrichment. *Nature reviews. Neuroscience*, **1**, 191-198.

Vanderhaeghen, P. & Cheng, H.J. (2010) Guidance molecules in axon pruning and cell death. *Cold Spring Harbor perspectives in biology*, **2**, a001859.

Walsh, M.K. & Lichtman, J.W. (2003) In vivo time-lapse imaging of synaptic takeover associated with naturally occurring synapse elimination. *Neuron*, **37**, 67-73.

Wang, D. & Fawcett, J. (2012) The perineuronal net and the control of CNS plasticity. *Cell and tissue research*, **349**, 147-160.

Whishaw, I.Q., Pellis, S.M., Gorny, B.P. & Pellis, V.C. (1991) The impairments in reaching and the movements of compensation in rats with motor cortex lesions: an endpoint, videorecording, and movement notation analysis. *Behav Brain Res*, **42**, 77-91.

Wichterle, H., Lieberam, I., Porter, J.A. & Jessell, T.M. (2002) Directed differentiation of embryonic stem cells into motor neurons. *Cell*, **110**, 385-397.

Wickersham, I.R., Lyon, D.C., Barnard, R.J., Mori, T., Finke, S., Conzelmann, K.K., Young, J.A. & Callaway, E.M. (2007) Monosynaptic restriction of transsynaptic tracing from single, genetically targeted neurons. *Neuron*, **53**, 639-647.

Wiesel, T.N. & Hubel, D.H. (1963a) Effects of Visual Deprivation on Morphology and Physiology of Cells in the Cats Lateral Geniculate Body. *Journal of neurophysiology*, **26**, 978-993.

Wiesel, T.N. & Hubel, D.H. (1963b) Single-Cell Responses in Striate Cortex of Kittens Deprived of Vision in One Eye. *Journal of neurophysiology*, **26**, 1003-1017.

VII. APPENDIX

VI.1. Abbreviations

%	Percent
°C	Degree Celsius
µl	Microliter
µs	Microsecond(s)
A	Adenine (Purine base)
ALS	Amyotrophic lateral sclerosis
Ax	Alexa Fluor
BDNF	Brain-derived neurotrophic factor
bp	base pair
BSA	Bovine serum albumine
C	Cytosine (Pyrimidine base)
Ca^{2+}	Calcium ion
CHL1	Close homolog of L1
clp	Claw paw
cm	Centimeter
CNS	Central nervous system
cond	Conditional knockout
CPG	Central pattern generator
Cre	Causes recombination
CST	Corticospinal tract
CTB	Cholera toxin B subunit
DNA	Desoxyribonucleic acid
dNTP	Desoxynucleotide
DRG	Dorsal root ganglion
E	Embryonic day

EDTA	Ethylendiaminintetraacetic acid
EE	Enriched environment
eGFP	Enhanced GFP
EMG	Electromyogram
EtOH	Ethanol
g	Gram
G	Guanine (Purine base)
GABA	Gamma-Aminobutyric acid
GCaMP	Green Fluorescent-calmodulin protein (calcium indicator)
GFP	Green fluorescent protein
Gly	Glycoprotein
Hb9	Homeobox gene Hb9
HCl	Hydrochloride
HMGU	Helmholtz-Zentrum München für Gesundheit und Umwelt
Hsp-27	27-kDa heat shock protein
i.p.	Intraperitoneal
IVC	Individually ventilated cage
kDa	Kilo Dalton
l	Liter
LMC	Lateral motor column
LMCm	Medial division of the LMC
M	Molar (mol/l)
mA	Milliampere
MBP	Myelin basic protein
mg	Milligram
MilliQ-H_2O	Ultrapure water, purified by a Milli-Q Water Purification System
min	Minute
ml	Milliliter
mm	Millimeter
MN	Motor neuron

mRNA	Messenger RNA
mut	Mutant
n	Sample size
N.	Nerve
NaCl	Sodium chloride
NaOH	Sodium hydroxid
NF	Neurofilament
NGF	Nerve growth factor
NH	Normal housing
NMDA	N-methyl-D-aspartate
NMJ	Neuromuscular junction
Npn	Neuropilin
OPC	Oligodendrocyte precursor cell
P	Postnatal day
PBS	Phosphate buffered saline
PCR	Polymerase chain reaction
PFA	Paraformaldehyde
PNN	Perineuronal net
PNS	Peripheral nervous system
RNA	Ribonucleic acid
rpm	Rounds per minute
RT	Room temperature
s	Second(s)
SDS	Sodium dodecylsulfate
SEM	Standard error of the mean
Sema	Semaphorin
Shh	Sonic hedgehog
SI	Scatter index
T	Thymine (Pyrimidine base)
	Temperature

TE	Tris/EDTA buffer
TGF-β1	Transforming growth factor beta1
T_m	Melting temperature
Tris	Tris-Hydroxy-Methyl-Amino-Methan
TrK	Tyrosine receptor kinase
VEGF	Vesicular endothelial growth factor
vGAT	Vesicular GABA Transporter
vGlut	Vesicular glutamate transporter
vs.	Versus
WFA	*Wisteria Floribuda* Agglutinin
wt	wildtype
µ	Micro

VI.2. Table of figures

VI.3. Danksagung

An dieser Stelle möchte ich die Gelegenheit nutzen mich bei den Menschen zu bedanken, die mich während meiner Doktorandenzeit unterstützt haben und so direkt oder indirekt zum Erfolg meiner Arbeit beigetragen haben. Insbesondere möchte ich folgenden Personen danken:

Prof. Dr. Wolfgang Wurst, der mir die Möglichkeit gegeben hat an seinem Institut zu arbeiten. Ich möchte ihm außerdem für seine fortwährende Unterstützung und sein Interesse an meiner Arbeit danken.

Dr. Andrea Huber Brösamle möchte ich einen besonderen Dank aussprechen, dafür, dass sie mich für die Neurobiologie begeistert hat und ich an gleich mehreren faszinierenden Forschungsprojekten arbeiten durfte. Insbesondere möchte ich ihr auch dafür danken, dass sie mich von Freiburg aus weiterhin betreut hat und mir immer mit Rat und Tat zur Seite stand.

Dr. Daniela Vogt-Weisenhorn, die uns AHBlern in ihrer Gruppe ein neues Zuhause gegeben hat und mir dadurch ermöglichte meine Doktorarbeit normal fortzusetzen. Danke für deine Hilfsbereitschaft und Unterstützung in den letzten 1,5 Jahren!

Den weiteren Mitgliedern meines Thesis Committees, **Prof. Dr. Harald Luksch** und **Dr. Sabine Hölter-Koch**, für die wissenschaftlichen Diskussionen und neuen Ideen während unserer Meetings. Besonders möchte ich mich auch Prof. Luksch dafür bedanken, dass er sich dazu bereit erklärt hat als mein Zweitprüfer zu fungieren. Außerdem möchte ich **Prof. Dr. Erwin Grill** dafür danken, dass er den Vorsitz meines Prüfungsausschusses übernommen hat.

Prof. Dr. Karim Fouad, für seine fachliche Unterstützung in allen Fragen zu Elektrophysiologie und EMG Rekordings, **Prof. Dr. Fabian Theis**, für seine bioinformatische Expertise und die Hilfe bei der Berechnung des Scatter Index und **Dr. Annette Feuchtinger** für ihre Unterstützung bei der Bildanalyse mit Hilfe der Definiens Software.

Ein besonders großer Dank geht an **Dr. Heidi Soellner**, die meine Projekte während ihrer Doktorarbeit startete. Ich möchte ihr vor allem dafür danken, dass sie mich so geduldig eingearbeitet hat und dass sie mich auch später noch in ihrer Freitzeit weiterhin unterstützt hat. Das ist nicht selbstverständlich – VIELEN DANK!

Stefan Winzeck möchte ich besonders für seine Hilfe bei der Rekonstruktion und Berechnung der spinalen Motorneuronen Pools danken.

Außerdem möchte ich mich sehr herzlich bei den ehemaligen und aktuellen Postdocs unseres Labors, **Dr. Georg Luxenhofer**, **Dr. Corinna Haupt** und **Dr. Rosa-Eva Hüttl**, bedanken. Vielen Dank für eure Unterstützung bei Experimenten, die großartigen wissenschaftlichen Diskussionen und vor allem die tolle Atmosphäre in unserem Büro. Rosa, dir danke ich auch besonders fürs Korrekturlesen und die aufmunternden Worte während diverser Schreibblockaden.

Ein großer Dank auch an meine Doktoranden-Kollegen **Maximilian Saller** und **Maria Angelica Castiblanco Urbina**. Max, danke dass du es mit uns Mädls so gut ausgehalten hast und für deine immer gute Laune. Maria, thank you for everything! Not only for your help in the Sema3F project but especially for being so much more than a colleague!!!

Auch außerhalb des Labors haben mir viele Menschen während meiner Promotion in besonderer Weise beigestanden. Daher möchte ich auch einige meiner besten Freunde hier namentlich erwähnen. Als erstes **Martina** und **Helena**, meine ältesten Freundinnen, die mich schon seit Ewigkeiten kennen immer genau wussten wie sich mich am besten von den Arbeitsproblemen ablenken konnten (wenn es nötig war). Außerdem, meine Mädls aus Garching, **Anja** und **Kathi**, die seit Anfang des Studiums mit mir durch Dick und Dünn gegangen sind. Und natürlich meine **Lena** und meine **Tini**, die mir in den letzten Jahren eine besondere Stütze waren. Danke, dass ihr immer für mich da seid!!!

Ein riesiges Dankeschön geht an meinen Partner **Tobi**. Danke für dein Verständnis, deine aufmunternden Worte und deinen Humor! Ich bin so froh, dass ich dich hab!

Außerdem möchte ich meinem Bruder **Thomas** danken, der während meiner Doktorarbeit auch mein Mitbewohner war. Du musstest eine Menge mit mir durchmachen. Danke dafür!

Zum Schluss möchte ich noch **meinen Eltern** danken. Nicht nur dafür, dass ihr mich auf meiner schulischen und akademischen Laufbahn immer unterstützt habt, sondern ganz besonders auch dafür, dass ihr immer für mich da wart. Ich weiß, dass ich immer auf euch zählen kann und das ist mir unglaublich viel wert! Ich hab euch lieb!